

# FPGA-BASED SOFT VECTOR PROCESSORS

by

Peter Yiannacouras

A thesis submitted in conformity with the requirements  
for the degree of Doctor of Philosophy  
Graduate Department of Electrical and Computer Engineering  
University of Toronto

Copyright © 2009 by Peter Yiannacouras

# Abstract

FPGA-Based Soft Vector Processors

Peter Yiannacouras

Doctor of Philosophy

Graduate Department of Electrical and Computer Engineering

University of Toronto

2009

FPGAs are increasingly used to implement embedded digital systems because of their low time-to-market and low costs compared to integrated circuit design, as well as their superior performance and area over a general purpose microprocessor. However, the hardware design necessary to achieve this superior performance and area is very difficult to perform causing long design times and preventing wide-spread adoption of FPGA technology. The amount of hardware design can be reduced by employing a microprocessor for less-critical computation in the system. Often this microprocessor is implemented using the FPGA reprogrammable fabric as a *soft processor* which can preserve the benefits of a single-chip FPGA solution without specializing the device with dedicated hard processors. Current soft processors have simple architectures that provide performance adequate for only the least-critical computations.

Our goal is to improve soft processors by scaling their performance and expanding their suitability to more critical computation. To this end we focus on the data parallelism found in many embedded applications and propose that soft processors be augmented with vector extensions to exploit this parallelism. We support this proposal through experimentation with a parameterized soft vector processor called VESPA (Vector Extended Soft Processor Architecture) which is designed, implemented, and evaluated on real FPGA hardware.

The scalability of VESPA combined with several other architectural parameters can be used to finely span a large design space and derive a custom architecture for exactly matching the

needs of an application. Such customization is a key advantage for soft processors since their architectures can be easily reconfigured by the end-user. Specifically, customizations can be made to the pipeline, functional units, and memory system within VESPA. In addition, general purpose overheads can be automatically eliminated from VESPA.

Comparing VESPA to manual hardware design, we observe a 13x speed advantage for hardware over our fastest VESPA, though this is significantly less than the 500x speed advantage over scalar soft processors. The performance-per-area of VESPA is also observed to be significantly higher than a scalar soft processor suggesting that the addition of vector extensions makes more efficient use of silicon area for data parallel workloads.

## Acknowledgements

I would like to thank my advisors Professor Greg Steffan and Professor Jonathan Rose for all their guidance throughout the years. Our weekly meetings were key in directing and executing this research. Also countless writing edits and many dry runs helped improve my written and oral communication. Thank you for all of that, your advice and insights along the way, and also thank you for the opportunity to teach some classes.

My committee including Professor Moshovos and Professor Abdelrahman, as well as Professor Enright Jerger provided useful suggestions and commentary for filling out this work.

Many thanks to Professor Christos Kozyrakis for corresponding with me and sending me the hand-vectorized benchmarks used throughout this work. I would also like to acknowledge the useful input received from Vaughn Betz, David Lewis, and James Ball which helped guide our research direction.

Throughout my six years in LP392 and in the PaCRaT group, it was certainly a pleasure interacting with all my colleagues, thanks for technical breadth, good fun, and stimulating discussions.

Thank you to my parents and brothers for raising me, taking care of me, and looking out for me throughout my life.

To my wife Melinda, thank you for all your love and support, I'm glad to have had you by my side for every step of the way.

*for Meli*

# Contents

<b>List of Tables</b>	<b>xi</b>
-----------------------	-----------

<b>List of Figures</b>	<b>xiii</b>
------------------------	-------------

<b>1 Introduction</b>	<b>1</b>
1.1 Research Goals . . . . .	4
1.2 Organization . . . . .	5
<b>2 Background</b>	<b>6</b>
2.1 Microprocessor Background . . . . .	6
2.2 Vector Processors . . . . .	7
2.2.1 Vector Instructions . . . . .	8
2.2.2 Vector Architecture . . . . .	9
2.2.3 Vector Lanes . . . . .	10
2.2.4 Vector Chaining . . . . .	11
2.2.5 The T0 Vector Processor . . . . .	12
2.2.6 The VIRAM Vector Processor . . . . .	12
2.2.7 SIMD Extensions . . . . .	15
2.3 Field-Programmable Gate Arrays (FPGAs) . . . . .	15
2.3.1 Block RAMs . . . . .	16
2.3.2 Multiply-Accumulate blocks . . . . .	16
2.3.3 Microprocessor Cores . . . . .	17
2.4 FPGA Design . . . . .	17

2.4.1	Behavioural Synthesis . . . . .	18
2.4.2	Extensible Processors . . . . .	20
2.5	Soft Processors and Related Work . . . . .	21
2.5.1	Soft Single-Issue In-Order Pipelines . . . . .	22
2.5.2	Soft Multi-Issue Pipelines . . . . .	22
2.5.3	Soft Multi-Threaded Pipelines . . . . .	23
2.5.4	Soft Multiprocessors . . . . .	25
2.5.5	Soft Vector Processors . . . . .	25
<b>3</b>	<b>Experimental Framework</b>	<b>27</b>
3.1	Overview . . . . .	27
3.2	Benchmarks . . . . .	28
3.3	Software Compilation Framework . . . . .	30
3.4	FPGA CAD Software . . . . .	30
3.4.1	Measuring Area . . . . .	31
3.4.2	Measuring Clock Frequency . . . . .	31
3.5	Hardware Platforms . . . . .	32
3.5.1	Transmogripher-4 . . . . .	32
3.5.2	Terasic DE3 . . . . .	33
3.5.3	Measuring Wall Clock Time . . . . .	33
3.6	Measurement Error . . . . .	34
3.7	Verification . . . . .	35
3.7.1	Instruction Set Simulation . . . . .	35
3.7.2	Register Transfer Level (RTL) Simulation . . . . .	36
3.7.3	In-Hardware Debugging . . . . .	37
3.8	Advantages of Hardware Execution . . . . .	37
3.9	Summary . . . . .	38
<b>4</b>	<b>Performance Bottlenecks of Scalar Soft Processors</b>	<b>39</b>
4.1	Integrating Scalar Soft Processors with Off-Chip Memory . . . . .	39

4.1.1	Scalar Soft Processor Area Breakdown . . . . .	41
4.1.2	Scalar Soft Processor Memory Latency . . . . .	42
4.2	Scaling Soft Processor Caches . . . . .	44
4.3	Soft vs Hard Processor Comparison . . . . .	46
4.4	Summary . . . . .	49
<b>5</b>	<b>The VESPA Soft Vector Processor</b>	<b>50</b>
5.1	Motivating Soft Vector Processors . . . . .	50
5.2	VESPA Design Goals . . . . .	51
5.3	VESPA . . . . .	53
5.3.1	MIPS-Based Scalar Processor . . . . .	54
5.3.2	VIRAM-Based Vector Instruction Set . . . . .	55
5.3.3	Vector Memory Architecture . . . . .	57
5.3.4	VESPA Pipelines . . . . .	59
5.4	Meeting the Design Goals . . . . .	60
5.4.1	VESPA Flexibility . . . . .	60
5.4.2	VESPA Portability . . . . .	62
5.5	FPGA Influences on VESPA Architecture . . . . .	63
5.6	Selecting a Maximum Vector Length (MVL) . . . . .	64
5.7	Summary . . . . .	68
<b>6</b>	<b>Scalability of the VESPA Soft Vector Processor</b>	<b>69</b>
6.1	Initial Scalability (L) . . . . .	69
6.1.1	Analyzing the Initial Design . . . . .	71
6.2	Improving the Memory System . . . . .	72
6.2.1	Cache Design Trade-Offs (DD and DW) . . . . .	72
6.2.2	Impact of Data Prefetching (DPK and DPV) . . . . .	77
6.2.3	Reduced Memory Bottleneck . . . . .	83
6.2.4	Impact of Instruction Cache (IW and ID) . . . . .	84
6.3	Decoupling Vector and Control Pipelines . . . . .	85

6.4	Improved VESPA Scalability . . . . .	87
6.4.1	Cycle Performance . . . . .	87
6.4.2	Clock Frequency . . . . .	89
6.4.3	Area . . . . .	90
6.5	Summary . . . . .	91
<b>7</b>	<b>Expanding and Exploring the VESPA Design Space</b>	<b>92</b>
7.1	Heterogeneous Lanes . . . . .	93
7.1.1	Supporting Heterogeneous Lanes . . . . .	93
7.1.2	Impact of Multiplier Lanes (X) . . . . .	94
7.1.3	Impact of Memory Crossbar (M) . . . . .	95
7.2	Vector Chaining in VESPA . . . . .	98
7.2.1	Supporting Vector Chaining . . . . .	99
7.2.2	Impact of Vector Chaining . . . . .	101
7.2.3	Vector Lanes and Powers of Two . . . . .	105
7.3	Exploring the VESPA Design Space . . . . .	105
7.3.1	Selecting and Pruning the Design Space . . . . .	105
7.3.2	Exploring the Pruned Design Space . . . . .	108
7.3.3	Per-Application Analysis . . . . .	112
7.4	Eliminating Functionality . . . . .	116
7.4.1	Hardware Elimination Opportunities . . . . .	116
7.4.2	Impact of Vector Datapath Width Reduction (W) . . . . .	118
7.4.3	Impact of Instruction Set Subsetting . . . . .	120
7.4.4	Impact of Combining Width Reduction and Instruction Set Subsetting . .	121
7.5	Summary . . . . .	123
<b>8</b>	<b>Soft Vector Processors vs Manual FPGA Hardware Design</b>	<b>125</b>
8.1	Designing Custom Hardware Circuits . . . . .	126
8.1.1	System-Level Design Constraints . . . . .	126
8.1.2	Simplifying Hardware Design Optimistically . . . . .	127

8.2	Evaluating Hardware Circuits . . . . .	130
8.2.1	Area Measurement . . . . .	131
8.2.2	Clock Frequency Measurement . . . . .	131
8.2.3	Cycle Count Measurement . . . . .	131
8.2.4	Area-Delay Product . . . . .	132
8.3	Implementing Hardware Circuits . . . . .	132
8.4	Comparing to Hardware . . . . .	133
8.4.1	Software vs Hardware: Area . . . . .	133
8.4.2	Software vs Hardware: Wall Clock Speed . . . . .	137
8.4.3	Software vs Hardware: Area-Delay . . . . .	142
8.5	Effect of Subsetting and Width Reduction . . . . .	143
8.6	Summary . . . . .	145
<b>9</b>	<b>Conclusions</b>	<b>146</b>
9.1	Contributions . . . . .	147
9.2	Future Work . . . . .	150
<b>A</b>	<b>Measured Model Parameters</b>	<b>152</b>
<b>B</b>	<b>Raw VESPA Data on DE3 Platform</b>	<b>155</b>
<b>C</b>	<b>Instruction Disabling Using Verilog</b>	<b>168</b>
	<b>Bibliography</b>	<b>171</b>

# List of Tables

3.1	Vectorized benchmark applications. . . . .	29
3.2	Benchmark execution speeds. . . . .	37
4.1	Memory latencies on soft and hard processor systems. . . . .	43
5.1	VIRAM instructions supported . . . . .	55
5.2	Configurable parameters for VESPA. . . . .	60
6.1	Clock frequency of different cache line sizes for a 16-lane VESPA. . . . .	74
6.2	Performance of VESPA varying lanes from 1 to 32. . . . .	88
7.1	Explored parameters in VESPA. . . . .	106
7.2	Pareto optimal VESPA configurations. . . . .	110
7.3	Configurations with best wall clock performance for each benchmark. . . . .	113
7.4	Configurations with best performance-per-area for each benchmark. . . . .	114
7.5	Hardware elimination opportunitites across all benchmarks. . . . .	117
7.6	Area after width reduction across benchmarks normalized to 32-bit width. . . . .	119
8.1	Hardware circuit area and performance. . . . .	133
8.2	Area advantage for hardware over various processors . . . . .	134
8.3	Speed advantage for hardware over various processors. . . . .	135
8.4	Hardware advantages over fastest VESPA. . . . .	140
A.1	Load frequency and miss rates across cache size for EEMBC benchmarks. . . . .	153
A.2	Store frequency and miss rates across cache size for EEMBC benchmarks. . . . .	154

B.1	Area of VESPA system without the vector coprocessor. . . . .	155
B.2	Area of VESPA system without the vector coprocessor. . . . .	155
B.3	System area of pareto optimal VESPA configurations. . . . .	156
B.4	Performance of pareto optimal VESPA configurations. . . . .	157
B.5	Performance of pareto optimal VESPA configurations (cont'd). . . . .	158
B.6	System area after customizing to AUTCOR. . . . .	159
B.7	System area after customizing to CONVEN. . . . .	160
B.8	System area after customizing to RGBCMYK. . . . .	161
B.9	System area after customizing to RGBYIQ. . . . .	162
B.10	System area after customizing to IP_CHECKSUM. . . . .	163
B.11	System area after customizing to IMGBLEND. . . . .	164
B.12	System area after customizing to FILT3X3. . . . .	165
B.13	System area after customizing to FBITAL. . . . .	166
B.14	System area after customizing to VITERB. . . . .	167

# List of Figures

2.1	Vector processing and vector chaining in space/time. . . . .	10
2.2	VIRAM processor state. . . . .	14
3.1	Overview of measurement infrastructure. . . . .	28
4.1	Area breakdown of scalar SPREE processor with off-chip memory system. . . . .	41
4.2	Memory latency breakdown on TM4. . . . .	42
4.3	Average speedup of various direct-mapped data cache sizes. . . . .	45
4.4	Performance of IBM PPC 750GX versus SPREE. . . . .	47
5.1	Application space targeted by VESPA. . . . .	52
5.2	VESPA processor system block diagram. . . . .	53
5.3	VESPA memory system diagram. . . . .	56
5.4	The VESPA memory unit. . . . .	57
5.5	The VESPA pipelines. . . . .	59
5.6	Area of the vector coprocessor across different MVL and lane configurations. . . . .	66
5.7	Cycle speedup measured when MVL is increased from 32 to 256. . . . .	67
6.1	Performance scalability of initial VESPA design. . . . .	70
6.2	Average wall clock speedup of various cache configurations. . . . .	73
6.3	Wall clock speedup of various cache configurations for VITERB. . . . .	74
6.4	System area of different cache configurations. . . . .	75
6.5	A wide cache assembled from multiple narrow block RAMs. . . . .	76

6.6	Average speedup for different prefetching triggers. . . . .	80
6.7	Speedup of prefetching fixed number of cache lines. . . . .	81
6.8	Speedup of vector length prefetcher. . . . .	82
6.9	Analysis of memory and miss cycles before/after cache and prefetcher. . . . .	83
6.10	Average cycle performance across various icache configurations. . . . .	84
6.11	Performance improvement after decoupling the vector control pipeline. . . . .	86
6.12	Performance scalability of improved VESPA. . . . .	87
6.13	Performance/area design space of 1-32 lane VESPA. . . . .	90
7.1	Performance impact of varying $X$ . . . . .	94
7.2	Cycle performance of various memory crossbar configurations. . . . .	96
7.3	Cycle performance versus area for various memory crossbar configurations. . . .	97
7.4	Wall clock performance of various memory crossbar configurations. . . . .	98
7.5	Element-partitioned vector register file banks shown for 2 banks. . . . .	100
7.6	Vector chaining support for a 1-lane VESPA processor with 2 banks. . . . .	100
7.7	Cycle performance of different banking configurations. . . . .	102
7.8	Average cycle performance for different chaining configurations. . . . .	103
7.9	Performance/area space of varying chaining and lane configurations. . . . .	104
7.10	Average normalized wall clock time and area VESPA design space. . . . .	107
7.11	Average normalized cycle count and area VESPA design space after pruning. . .	109
7.12	Average wall clock time and area of pruned VESPA design space. . . . .	111
7.13	Area of width-reduced VESPA processors. . . . .	119
7.14	Area of the vector coprocessor after instruction set subsetting. . . . .	120
7.15	Area of the vector coprocessor after subsetting and width reduction. . . . .	121
7.16	Normalized clock frequency of VESPA after subsetting and width reduction. . . .	122
8.1	Hardware circuit implemented for IP_CHECKSUM. . . . .	130
8.2	Area-performance design space of scalar and pareto-optimal VESPAs. . . . .	138
8.3	Area-delay product of VESPA versus hardware. . . . .	142
8.4	Area-performance design space after subsetting and width reduction. . . . .	144

8.5	Area-delay product versus hardware after subsetting and width reduction. . . .	144
-----	--	-----

# Chapter 1

## Introduction

Field-Programmable Gate Arrays (FPGAs) are commonly used to implement embedded systems because of their low cost and fast time-to-market relative to the creation of fully-fabricated VLSI chips. FPGAs also provide superior speed/area/power compared to a microprocessor, although the hardware design necessary to achieve this is cumbersome and requires specialized knowledge making it difficult for average programmers to adopt FPGAs. Specifically, the detailed cycle-to-cycle description necessary for design in a hardware description language (HDL) requires programmers to comprehend both their application and hardware substrate with very low-level detail. In addition, hardware design is accompanied with very limited-scope debugging and complexities such as circuit timing and clock domains. To enable rapid and easy access to this better-performing FPGA technology, we are motivated to simplify the design of FPGA-based systems by leveraging the high-level programming languages and single-step debugging features of software design.

Most FPGA-based systems include a microprocessor at the heart of the system, and approximately 25% contain a processor implemented using the FPGA reprogrammable fabric itself [3], such as the Altera Nios II [5] or Xilinx Microblaze [67]. These *soft processors* are inefficient compared to their hard counterparts but have some key advantages. Compared to using both an FPGA and a separate microprocessor chip, soft processors

preserve a single-chip solution and avoid the increased board real estate, latency, cost, and power of using a second chip. An alternative approach to addressing these issues is to embed hard microprocessors and FPGA fabric on a single device such as the Xilinx Virtex II Pro [68]. But this specializes the device resulting in multiple device families for meeting the needs of designers who may want varying numbers of processors or even specific architectural features. Maintaining these device families as well as the design and/or licensing of the processor core itself contribute to increasing the cost of FPGA devices. A soft processor avoids these increased costs while maintaining the benefits of a single-chip solution.

The software design environment provided by soft processors can be used for quickly implementing system components which do not require highly-optimized hardware implementations, and can instead be implemented with less effort in software executing on a soft processor. In this thesis, we leverage the inherent configurability of a soft processor to adapt its architecture and match the properties found in the application to achieve better performance and area. These improved soft processors can better compete with the efficiencies gained through hardware design and be used to implement non-critical computations in software rather than through laborious hardware design. As more computations within a digital system are implemented in software on a soft processor, the overall time required to implement the digital system is reduced hence achieving our goal of making FPGAs more easily programmable.

Simplifying hardware design is a goal analogous to that of behavioural synthesis which aims to automatically compile applications described in a high-level programming language to a custom hardware circuit. However pursuing this goal within a processor framework provides several advantages. First it provides a more fluid design methodology allowing designers to manually optimize the algorithm, code, compiler, assembly output, and architecture. Behavioural synthesis tools combine these into one black box tool which outputs a single result with few options for navigating the immense design space along each of these axes. Second, the intractable complexities in behavioural syn-

thesis can result in poor results that may be improved from the knowledge gained by customizing within a processor framework. Third, processors provide single-step debugging infrastructure making it far easier to diagnose problems within the system. Fourth, processors provide compiled libraries for easily sharing software and maintaining optimization effort. In contrast, the output from behavioural synthesis depends heavily on surrounding components making a given synthesized task questionably portable. Finally, a processor provides full support for ANSI C while behavioural synthesis typically do not. Overall, processors provide a fluid and portable framework that can be immediately leveraged by soft processors to simplify FPGA design.

The architecture of current commercial soft processors are based on simple single-issue pipelines with few variations, limiting their use to predominantly system control tasks. To support more compute-intensive tasks on soft processors, they must be able to scale up performance by using increased FPGA resources. While this problem has been thoroughly studied in traditional *hard processors* [28], an FPGA substrate leads to different trade-offs and conclusions. In addition, traditional processor architecture research favoured features that benefit a large application domain, while in a soft processor we can appreciate features which benefit only a few applications since each soft processor can be configured to exactly match the application it is executing. These key differences motivate new research into scaling the performance of existing soft processors while considering the configurability and internal architecture of FPGAs.

Recent research has considered several options for increasing soft processor performance. One option is to modify the amount and organization of the pipelining in existing single-issue soft processors [70, 71] which provide limited performance gains. A second option is to pursue VLIW [31] or superscalar [12] pipelines which are limited due to the few ports in FPGA block RAMs and the available instruction-level parallelism within an application. A third option is multi-threaded pipelines [16, 21, 38] and multiprocessors [55, 62] which exploit thread-level parallelism but require complicated parallelization of the software. In this thesis we propose and explore vector extensions for soft proces-

sors which can be relatively easily programmed to allow a single vector instruction to command multiple datapaths. An FPGA designer can then scale the number of these datapaths, referred to as *vector lanes*, in their design to convert the data parallelism in an application to increased performance.

## 1.1 Research Goals

The goal of this research is to simplify FPGA design by making soft processors more competitive with manual hardware design. This thesis proposes that soft vector processors are an effective means of doing so for data parallel workloads, which we aim to prove by setting the following goals:

1. To efficiently implement a soft vector processor on an FPGA.
2. To evaluate the performance gains achievable on real embedded applications. FPGAs are frequently used in the embedded domain so this application-class is well-suited for our purposes.
3. To provide a broad area/performance design space with fine-grain resolution allowing an FPGA designer to select a soft vector processor architecture that meets their needs.
4. To support automatic customization of soft vector processors to a specific application, by enabling the removal of general purpose area overheads.
5. To quantify the area and speed advantages of manual hardware design versus a soft vector processor and a scalar soft processor.

To satisfy the first goal we implement a full soft vector processor called *VESPA* (*Vector Extended Soft Processor Architecture*) and demonstrate its scalability in real hardware. For the second goal we execute industry-standard benchmarks on several VESPA configurations. For the third goal we extend VESPA with parameterizable architectural options

that can be used to further match an application’s data-level parallelism, memory access pattern, and instruction mix. For the fourth we enhance VESPA with the capability to remove hardware for unused instructions and datapath bit-widths. Finally for the last goal, we compare VESPA to manually designed hardware and show it can significantly reduce the performance gap over scalar soft processors, hence luring more designers into using soft processors and avoiding laborious hardware design.

## 1.2 Organization

This thesis is organized as follows: Chapter 2 provides necessary background and summarizes related work. Chapter 3 describes the infrastructure components used in this thesis. Chapter 4 analyzes bottlenecks in current scalar soft processor architectures and motivates the need for additional computational power. Chapter 5 describes the VESPA processor. Chapter 6 shows that with accompanying architectural improvements, VESPA can scale within a large performance/area design space. Chapter 7 explores the VESPA design space by implementing heterogeneous lanes, vector chaining, and automatic removal of unused hardware. Chapter 8 compares VESPA to a scalar soft processor and to manual hardware design, quantifying the area and performance gaps and demonstrating how significant strides are made towards the performance of manual hardware design over scalar soft processors. Finally, Chapter 9 concludes and suggests future avenues for research.

## Chapter 2

# Background

This chapter provides necessary background on microprocessors, vector processors, and FPGAs. It also describes soft processors and summarizes research related to this thesis.

### 2.1 Microprocessor Background

Microprocessors have radically changed the world we live in and are integral parts of the semiconductor industry. Compared to chip design, they provide a low cost path to silicon by serving multiple applications with a single general purpose device which can be easily programmed using a simple sequential programming model. Microprocessor improvements have been achieved by primarily two methods: (i) shrinking the minimum width of manufacturable transistors which increases the processor clock rate and reduces its size; and (ii) improving the architecture of microprocessors by adding structures for supporting faster execution. In this thesis we focus only on the latter approach.

Many architectural variants and enhancements have been thoroughly studied [28] in conventional microprocessors. Architectural improvements such as branch predictors alleviate pipeline inefficiencies, but scalable performance gains are achievable only by executing operations spatially rather than temporally over the processor datapath. The parallelism necessary for spatial computation comes in three forms:

- **Instruction Level Parallelism (ILP):** When an instruction produces a result not

used by a later instruction in the same instruction stream, those two instructions exhibit instruction level parallelism which allows them to be executed concurrently.

- **Data Level Parallelism (DLP):** When the same operation is performed over multiple data elements allowing all operations to be performed concurrently.
- **Thread Level Parallelism (TLP):** When multiple instruction streams exist they can be executed concurrently except for memory operations which may access data shared between both instruction streams.

ILP has been heavily leveraged in creating aggressive out-of-order superscalar microprocessors, until three factors combined to prevent further improvements using this approach: the complexity involved in exploiting this ILP, the growing performance gap between processors and memory (known as the *memory wall*) [66], and most recently, the limited power density that can be dissipated by semiconductor chips (known as the *power wall*) [20]. Since then the microprocessor industry has turned to solving the parallel programming problem in hopes of simplifying the extraction of TLP. With multiple threads an architect can build a more efficient *multithreaded* processor which time-multiplexes the different threads onto a single datapath. Additionally multiple processors, or *multiprocessors*, can be used to scale performance by simultaneously executing threads on dedicated processor cores. Presently all mainstream processors now provide 4 or 8 cores such as the Intel Core i7 family [29]. Exploiting either ILP and TLP can be used to scale performance in soft processors; later in this chapter we discuss related work in that area as well as its suitability to FPGA architectures. This thesis focuses primarily on exploiting the DLP found in many of the embedded applications in which FPGAs are employed.

## 2.2 Vector Processors

DLP has been historically exploited through a vector processor which is designed for efficient execution of DLP workloads [28]. Vector processors have existed in supercomputers

Listing 2.1: C code of array sum.

```
int a[16], b[16], c[16];  
...  
for (int i=0; i<16; i++)  
    c[i]=a[i]+b[i];
```

since the 1960s and were the highest-performing processors for decades. The fundamental concept behind vector processors is to accept and process *vector instructions* which communicate some variable number of homogeneous operations to be performed. This concept and its advantages are discussed below in the context of an example.

### 2.2.1 Vector Instructions

Vector processors provide direct instruction set support for operations on whole vectors—i.e., on multiple data elements rather than on a single scalar value. These instructions can be used to exploit the DLP in an application to essentially execute multiple loop iterations simultaneously. Listing 2.1 shows an example of a data parallel loop that sums two 16 element arrays. The assembly instructions necessary to execute this loop on a scalar processor is shown in Listing 2.2. Tracing through this code shows that a total of 148 machine instructions need to be executed, with 80 of them responsible for managing the loop and advancing pointers to the next element.

With support for vector instructions, a vector processor can execute the same loop with just the 8 instructions shown in Listing 2.3. After initializing the pointers, the current vector length is set to 16 since the loop operates on 16-element arrays. Following this, the vector instructions for loading, adding, and storing the resulting 16-element array back to memory are executed. Note that due to finite hardware resources, a vector processor exposes its internal maximum vector length MVL in a special readable register. In this code we assume MVL is greater than or equal to 16, otherwise the loop must be *strip-mined* into multiple iterations of MVL sized vectors. Nonetheless, the savings in executed instructions is dramatic due to: (i) the multiple operations encapsulated in a

Listing 2.2: Pseudo-MIPS assembly of array sum. Destination registers are on the left.

```

move    r1 , a
move    r2 , b
move    r3 , c
move    r7 , 0
loop_add :
load.w  r4 , ( r1 )
load.w  r5 , ( r2 )
add     r6 , r4 , r5
stor.w  r6 , ( r3 )
add     r7 , r7 , 1      # Loop overhead
add     r1 , r1 , r7     # Advance pointer
add     r2 , r2 , r7     # Advance pointer
add     r3 , r3 , r7     # Advance pointer
blt     r7 , 16 , loop_add # Loop overhead

```

Listing 2.3: Vectorized assembly of array sum. For simplicity it is assumed the maximum vector length is greater than or equal to 16.

```

move    vbase1 , a
move    vbase2 , b
move    vbase3 , c
move    vl , 16          #Set vector length to 16
vload.w vr4 , ( vbase1 )
vload.w vr5 , ( vbase2 )
vadd     vr6 , vr4 , vr5
vstor.w  vr6 , ( vbase3 )

```

single vector instruction; and (ii) the savings in loop overheads and pointer advancing.

Listing 2.3 shows the use of one possible vector instruction set. Many different vector instruction sets have been extensively researched, including in modern processors [24]. Simultaneous research into the architectures that supports these vector instructions was also thoroughly performed and is described next.

### 2.2.2 Vector Architecture

The vector architecture is responsible for accepting a stream of variable-lengthed vector instructions and completing their associated operations as quickly as possible. We now describe several architectural modifications that can be used to achieve this; a more comprehensive summary can be found in [28].

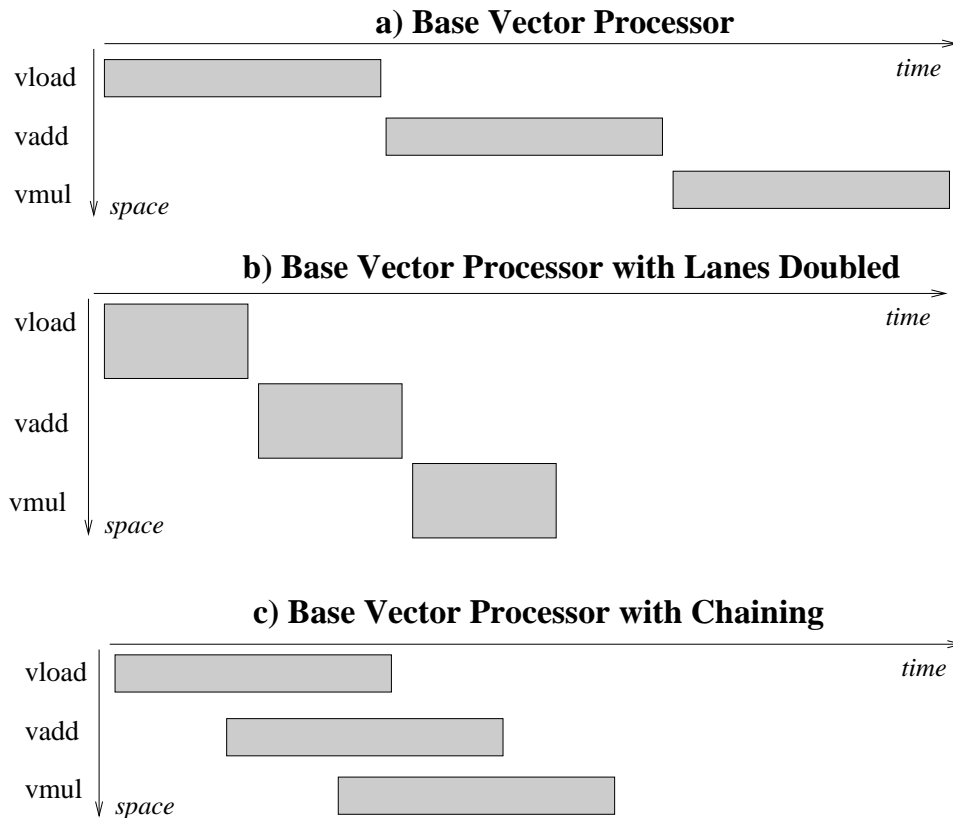


Figure 2.1: Comparing vector execution of doubling lanes (b) and chaining (c) against a base vector processor (a). The area of the boxes represents the amount of work for each instruction. The base vector processor in (a) waits for each vector instruction to complete before executing the next. In (b), doubling the number of lanes allows more of the work to be computed spatially on the additional lanes, this makes the instructions twice as tall in space and half as long in time. Chaining allows the work to be overlapped with the work of other instructions as seen in (c). The execution is staggered so that at any point in time each instruction is executing on different element groups.

### 2.2.3 Vector Lanes

The most important architectural feature of a vector processor is the number of vector datapaths or *vector lanes*. A single lane can operate on a single element of the vector at a time in a pipelined fashion; with more vector lanes a vector processor can perform more of the element operations in parallel hence increasing performance. For example, the `vadd` instruction in Listing 2.3 encodes 16 additions to be performed across 16 elements. A vector processor with 8 lanes can then execute 8 element operations at a time—we refer to this group of elements as an *element group*. After the first element group with

indices 0-7 is processed, the next element group with indices 8-15 is processed and the **vadd** instruction completes in two cycles.

Figure 2.1 shows a visual depiction of the effect of doubling lanes on vector instruction execution. Compared to (a), doubling the number of lanes in (b) results in twice as much spatial execution of the vector instructions, resulting in half as much execution time. The number of lanes is a powerful parameter for trading silicon area (used for spatial execution on the vector lanes) and performance (the time needed to complete the vector instruction). Note that the number of lanes is always a power of two, otherwise accessing an arbitrary element requires division and modulo operations to be performed.

#### 2.2.4 Vector Chaining

Vector chaining provides another axis of scaling performance in addition to increasing the number of lanes. Chaining allows multiple vector instructions to be executed simultaneously; the concept was first presented in the Cray-1 [56]. Using Listing 2.3 as an example, the first element group of the **vadd** instruction does not need to wait for the **vload** instruction preceding it to complete in its entirety. Rather, after the **vload** has loaded the first element group into **vr5**, the **vadd** can execute its first element group since its data is ready. Similarly the first element group for the **stor** can be stored as soon as the **vadd** completes that element group. With this concept the throughput of the vector processor can scale beyond the available number of lanes.

Figure 2.1 c) shows the effect of chaining compared to part a) of the same figure. After an initial set of element groups have been processed, the next instruction can execute alongside the previous. A continuous supply of vector instructions can lead to a steady-state of multiple vector instructions in flight. However successful vector chaining requires (i) available functional units, (ii) read/write access to multiple vector element groups, and (iii) vector lengths long enough to access multiple element groups. The first is achieved by replicating functional units, specifically the arithmetic and logic unit (ALU). The second can be achieved by implementing many read/write ports to the vector

register file or many register banks each with their own read/write ports. Historically vector supercomputers used the latter approach, while research in more modern single-chip implementations of vector architectures have resorted to the former [6] as discussed below. Finally the third requires applications with enough DLP to use vector lengths longer than the number of lanes.

### 2.2.5 The T0 Vector Processor

While traditional vector supercomputers spanned multiple processor and memory chips, Asanovic *et. al.* proposed harnessing advances in CMOS technologies to implement vector processors on a single chip with the aim of including them as add-ons to existing scalar microprocessors [6, 7]. The 8-lane T0 vector processor was implemented with up to 3-way chaining for a peak of 24 operations per cycle while issuing only one vector instruction per cycle. A key contribution was in the reduction of the large delays historically associated with starting and completing a vector instruction. These delays require a high-degree of data parallelism to be amortized, but with the shorter electrical delays of a single-chip design, the delays were greatly reduced enabling new application classes to exploit vector architectures. The T0 also first realized the area efficiency gains of using a many-ported vector register file to support chaining rather than a many-banked register file. Finally, while caches were not typically used in traditional vector supercomputers, they are further motivated in the T0 which connects to DRAM instead of SRAM.

### 2.2.6 The VIRAM Vector Processor

The IRAM project [1] investigated placing memory and microprocessors on the same chip, which lead to the design of a processor architecture that can best utilize the resulting high-bandwidth low-latency access to memory. The group selected a vector processor based on the T0, but optimized it for this memory system and for the embedded application domain creating VIRAM [32, 33, 34, 35, 60]. The VIRAM vector processor was shown to provide faster performance across several EEMBC industry-standard benchmarks compared to

superscalar and out-of-order processors while consuming less energy. The vector unit is attached as a coprocessor to a scalar MIPS processor with both connected to the on-chip DRAM. The complete system is manufactured in a 180nm CMOS process. The VIRAM vector processor has 4 lanes each 64-bits wide but can be reconfigured into as many as 16 16-bit vector lanes. The architecture is massively pipelined with 15 stages in each vector lane to tolerate the worst case on-chip memory latency. With this pipelining and the low-latency on-chip DRAM, no cache is used in VIRAM. The soft vector processor implemented in this thesis is based on the VIRAM instruction set which is described in more detail below.

### 2.2.6.1 VIRAM Instruction Set

VIRAM supports a full range of integer and floating-point vector operations including absolute value, and min/max instructions. Fixed-point operations are directly supported by the instruction set as well, providing automatic scaling and saturation hardware. VIRAM also supports predication, meaning each element operation in a vector instruction has a corresponding flag indicating whether the operation is to be performed or not. This allows loops with `if/else` constructs to be vectorized. Finally VIRAM has memory instructions for describing consecutive, strided, and indexed memory access patterns. The latter can be used to perform scatter/gather operations albeit with significantly less performance than consecutive accesses.

Figure 2.2 shows the vector state in VIRAM consisting of the 32 vector `vr` registers, the 32 flag `vf` registers, the 64 control `vc` registers, and the 32 `vs` scalar registers. The vector registers are used to store the vectors being operated on, while the flag registers store the masks used for predication. The control registers are each used for dedicated purposes throughout various parts of the vector pipeline. For example `vc0`, also referred to as `v1`, holds the vector length of the current vector instruction, while `vc24` or `mv1` is used to specify the maximum vector length of the processor (and hence this register is read-only). The `vc1` or `vpw` register stores the width of each element used to determine

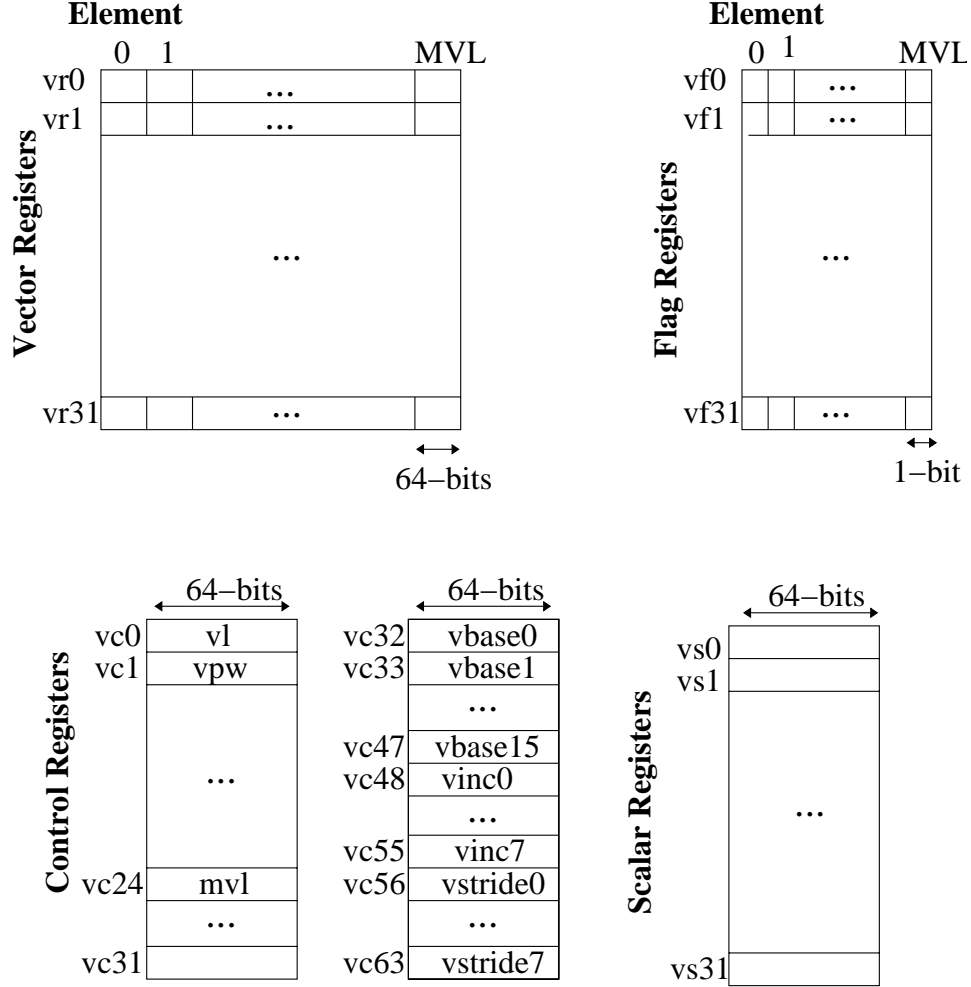


Figure 2.2: Processor state of VIRAM vector coprocessor consisting of vector registers, flag registers, control registers, and scalar registers. Our VESPA soft vector processor uses this same state though with widths of 32 bits instead of 64 bits.

the datapath width of the vector lanes. As seen in the figure, this is normally 64-bits, but can be modified to create narrower elements down to 16-bits which is automatically accompanied by a corresponding 4x increase to `mvl`.

The control registers also include dedicated registers for memory operations. The `vbase0-15` registers can store any base address which can be auto-incremented by the value stored in the `vinc0-7` registers. The `vstride0-7` registers can store different constant strides for specifying strided memory accesses. For example, if `vl` was 16 and the instruction `vld.w vr0,vbase1,vstride2,vinc5` was executed, the vector processor would load the 16 elements starting at `vbase1` each separated by `vstride2` words, store

them in `vr0`, and finally update `vbase1` by adding `vinc5` to it. More detailed information can be found in the VIRAM instruction set manual [60]. Note the implementation of VIRAM used in VESPA uses exactly the same vector state as in Figure 2.2 except that it is 32-bits instead of 64-bits, and without supporting the width reconfiguration using `vpw`.

### 2.2.7 SIMD Extensions

Modern microprocessors exploit data-level parallelism via SIMD (single-instruction, multiple-data) support, including IBM's AltiVec, AMD's 3DNow!, MIPS's MDMX, and Intel's MMX/SSE/AVX. SIMD support is very similar to vector support except that it is typically limited to a fixed and small number of elements which is exposed to the application programmer. In contrast, true vector processing abstracts from the software the actual number of hardware vector lanes, instead providing a machine-readable `MVL` parameter (discussed below) for limiting vector lengths. This is partly due to the longer vector lengths typically used in vector processing which are permitted to exceed the amount of hardware resources so that future vector architectures could add hardware resources to exploit the DLP without software modification. In addition, vector processors are typically equipped with a wider range of vector memory instructions that can explicitly describe different memory access patterns. These features make vector processing appealing for current microprocessors instead of the SIMD extensions used to date [24].

## 2.3 Field-Programmable Gate Arrays (FPGAs)

Field-Programmable Gate Arrays are prefabricated programmable logic devices often composed of lookup table based programmable logic blocks connected by a programmable routing network. Using these elements an FPGA can implement any digital logic circuit making them (originally) useful for implementing miscellaneous glue logic. As FPGAs have grown in capacity they have become capable of implementing complete embedded

systems. To augment their area efficiency and speed for certain operations, FPGA vendors have included dedicated circuits for better implementing certain operations that are typical in an embedded system. These dedicated circuits presently include flip flops, random access memory (RAM), multiply-accumulate logic, and microprocessor cores [36]. We describe these in more detail below since they are used extensively in soft processors, or in the case of the microprocessor cores, as an alternative to soft processors.

### 2.3.1 Block RAMs

The block RAMs in FPGAs provide efficient large storage structures which would otherwise require large amounts of lookup tables and flip flops to implement. While the capacity of a given block RAM is fixed, multiple block RAMs can be connected to form larger capacity RAM storage. Additional flexibility is available in the width and depth of the block RAMs allowing them to be configured as deep and narrow 1-bit memories, or shallow and wide 32-bit memories. A key limitation of block RAMs is they have only two access ports allowing just two simultaneous reads or writes to occur. This limitation inhibits soft processor architectures which require many-ported register files to sustain multiple instructions in flight. As a result most soft processor research has been on single-issue pipelines or multiprocessors.

### 2.3.2 Multiply-Accumulate blocks

The multiply-accumulate blocks, referred to also as *DSP blocks*, have dedicated circuitry for performing multiply and accumulate operations. The smallest such blocks are 9 or 18 bits wide and can be combined to perform multiply-accumulate for larger inputs. In this work we use the multiply-accumulate blocks to efficiently implement the multiplier functional units in a processor, which we also use to perform shift operations since barrel shifters are inefficient when built out of lookup tables.

### 2.3.3 Microprocessor Cores

Some FPGAs include one or two microprocessor cores implemented directly in silicon with the FPGA programmable fabric surrounding it [4, 68]. These *hard processors* provide superior performance relative to a soft processor but also have many disadvantages: (i) the number of hard processors on an FPGA may be insufficient or too many resulting in wasted silicon; (ii) the architecture is fixed making it difficult to satisfy all application domains; (iii) the cost of the FPGA is increased since vendors must design, build, and/or license a processor core; and (iv) the FPGA is specialized often producing multiple families of devices with/without processor cores which further increases design and inventory costs. As a result soft processors have seen significant uptake by both vendors and FPGA users, motivating research into improving soft processors.

## 2.4 FPGA Design

The typical FPGA design flow begins with an HDL language such as Verilog or VHDL which describes the desired circuit. FPGA vendors provide computer-aided design (CAD) tools for parsing this description and efficiently mapping the circuit onto the FPGA fabric. This design process is far more difficult than the software-based flows of microprocessors. An FPGA designer must specify the cycle-to-cycle behaviour of each component of the system, and the interaction between these components creates many opportunities for errors. Unlike the single-stepping debug infrastructure in a microprocessor, debugging a hardware design is very difficult. A logic analyzer can be used to capture a snapshot of a few signals at some event, but finding the erroneous event among its many symptoms can involve weeks of effort. In addition, an FPGA designer must respect the timing constraints of the system. Doing so requires pipelining, retiming, and other optimizations which can create more state and hence increased opportunities for errors. Overall, the biggest bottleneck of the FPGA design process is the design and verification of the desired system. Unlike an ASIC, fabrication is performed in minutes to days depending on the

circuit size and the compilation time of the FPGA CAD tools.

### 2.4.1 Behavioural Synthesis

Many efforts have been made to simplify the FPGA design flow. One option adopted by the FPGA vendors is to use processors (soft or hard) to implement less critical components and system control tasks—where errors can be very difficult to find if implemented in a hardware finite state machine (FSM). But another option which has been extensively researched in both FPGAs and ASICs is to automatically derive hardware implementations from a C-like sequential program. This is referred to as *behavioural synthesis* and its goal is aligned with our own goal of simplifying FPGA-design by using sequential programming for soft processors instead. Some examples of behavioural synthesis tools and languages include Handel-C [59], Catapult-C [43], Impulse C [52], and SystemC [51]. Altera has their own behavioural synthesis tool called C2H [40] which can convert C functions into hardware accelerators attached to a Nios II soft processor. Previous work has shown that soft vector processors can scale significantly better than C2H-generated accelerators even when manual code-restructuring is performed to aid C2H [75]. The state-of-the-art behavioural synthesis results in overheads due to the intractable nature of the problem including the pointer aliasing problem. These complexities have limited the quality of results available from behavioural synthesis tools.

We believe that customized processors will continue to be useful until and even after high-quality behavioural synthesis tools exist because of the following advantages.

1. **Fluid Design Methodology** – Processors have well-defined intermediate steps throughout the design flow. Each of these steps are taught to engineers at the undergraduate level providing them with the knowledge to manually optimize the algorithm, compiler, assembler output, and processor architecture. Behavioural synthesis tools aim to reap the efficiency gains from not having a fixed architecture structure or instruction set. As a result it is difficult for designers to manually navigate the vastly different hardware implementations possible.

2. **Libraries** – For a processor, compiled output can be packaged and shared very easily between software designers. This same idea has failed to gain traction in hardware design because of differing speed/area constraints and non-standardized interfaces. In contrast, software is decoupled from the hardware implementation allowing it to be designed primarily for speed. Moreover, libraries can preserve manual optimization of the compiled software.
3. **Debug Support** – Processors provide single-step debug capability. While this can be emulated to some degree by hardware simulators, the parallel nature of hardware can make it confusing. In addition, hardware simulators can not precisely model the behaviour of the hardware itself because of external stimuli and hardware imperfections. Inevitably this means some bugs will manifest only in the hardware implementation where they are difficult to find and fix.
4. **Intractable Complexities** – The complexities in deriving a high-quality hardware implementation of a system has made it a holy grail for many decades. Until high-quality behavioural synthesis exists, designers can instead utilize the customization opportunities in microprocessor systems. The knowledge gained through this research can also be used for improving behavioural synthesis tools.
5. **ANSI C Support** – Overcoming the complexities in behavioural synthesis most often leads to limited support for the full ANSI C standard or radically different programming models. Some examples of these are summarized below, however the willingness of FPGA designers to adopt new C variants or programming models casts doubt on the future adoption of behavioural synthesis. In contrast a processor can easily support full ANSI C which provides a familiar programming interface.

One of the largest hurdles to supporting full ANSI C in behavioural synthesis is the global memory model used in high-level programming languages. While arithmetic operations can be literally converted to hardware circuits, a literal conversion of this memory model would result in many processing elements being sequenced to preserve memory

consistency but at the same time competing over the single memory. The CHiMPS [54] project aims to support traditional memory models by providing caches for many processing elements. Compiler analysis determines regions of memory safe for caching by analyzing dependencies in scientific computing applications which rarely have complex memory aliasing. Additionally, traditional memory models can be preserved with multi-threaded and/or multi-processor systems but programming these systems requires facing the difficult parallel programming problem. The implementation of these systems onto FPGAs leads to soft processor research which is summarized in Section 2.5.3 and Section 2.5.4.

Most behavioural synthesis compilers modify or restrict the memory model to facilitate better quality hardware implementations. The SA-C [17] compiler prohibits the use of pointers and recursion and forces all variables to be single-assignment. While these restrictions impose difficulties on the programmer, the resulting application code can be more easily converted to hardware. The streaming programming paradigm has also been researched as a means of programming FPGAs. For example the Streams-C [25] language allows a programmer to express their computation in a consume-compute-produce model. Data and task level parallelism can be extracted and used to build parallel hardware for faster execution. Similar work was done using the Brook stream language [53] and also using regular C file I/O streams for the PACT behavioural synthesis tool [48] [30].

### 2.4.2 Extensible Processors

Behavioural synthesis aims to convert whole programs into hardware, but other approaches are premised on the common characteristic that a small computation is largely responsible for overall performance. The Warp [42] processing project derives on-the-fly hardware accelerators for a simplified FPGA fabric. This allows an application to be programmed in C and executed on a generic microprocessor which will automatically accelerate critical computations. The eMIPS [44] project converts blocks of binary MIPS instructions to hardware that can be dynamically configured onto an FPGA. The

instructions are then replaced with an invocation of the hardware accelerator. These dynamically extensible processors can be used to accelerate software and avoid custom hardware design similar to our own goals. However they are accompanied with significant overhead in synthesizing and configuring hardware accelerators and are hence critically dependent on correctly identifying computation to accelerate. This decision depends on how amenable the computation is to hardware acceleration and also depends on its overall contribution to system performance. As the system is improved and computation is more balanced across different kernels, it becomes increasingly difficult to select a computation which can amortize the dynamic configuration overheads.

## 2.5 Soft Processors and Related Work

Soft processors are processors designed for a reprogrammable fabric such as an FPGA. The two key attributes of soft processors are (i) the ease with which they can be customized and subsequently implemented in hardware, and (ii) that they are designed to target the fixed resources available on a reprogrammable fabric. This distinguishes soft processors from hard processors which are extremely difficult to customize due to the high cost and long design and fabrication times of full-custom VLSI design. Also, soft processors are distinct from parameterized processor cores which are pre-designed synthesizable RTL implementations not necessarily targeting efficient FPGA implementation.

The Actel Cortex-M1 [2], Altera Nios II [5], Lattice Micro32 [39], and Xilinx Microblaze [67] are widely used soft processors with scalar in-order single-issue architectures that are either unpipelined or have between 3 and 5 pipeline stages. While this is sufficient for system coordination tasks and least-critical computations, significant performance improvements are necessary for soft processors to replace the hardware designs of more important system components. Research in this direction is recent and ongoing, and summarized below.

### 2.5.1 Soft Single-Issue In-Order Pipelines

The SPREE (Soft Processor Rapid Exploration Environment) system was developed to explore the architectural space of current soft processors in our previous research [69, 70, 71]. SPREE can automatically generate a Verilog hardware implementation of a processor from a higher-level description of the datapath and instruction set. The tool was used to explore the implementation and latencies of functional units as well as the depth and organization of pipeline stages creating a thorough space of soft processor design points that were competitive with the slower and mid-range Altera Nios II commercial soft processors. We found diminishing returns with deeper pipelining which required more advanced architectural features to avoid pipeline stalls. While this work succeeded in exploring the space and finding processor configurations superior to a mid-speed commercial soft processor, it failed to extend the space, specifically with faster soft processors. In this thesis, we continue to use SPREE by choosing the best overall generated design and manually adding vector extensions to the architecture and compiler infrastructure.

Numerous other works created parameterized scalar soft processors aimed at customization. The LEON [23] is a parameterized VHDL description of a SPARC processor targetted for both FPGAs and ASICS with several customization options including cache configuration and functional unit support. LEON is heavily focussed on system-level features fully supporting exceptions, virtual memory, and multiprocessors. No scalable performance options exist other than multiprocessing which requires parallelized code. Similarly the XiRisc [41] is a parameterized core written in VHDL supporting 2-way VLIW, 16/32-bit datapaths, and optional shifter, multiplier, divider, and multiply-accumulate units. While these options provide some performance improvements it cannot scale to compete with manual hardware design. Other VLIW processors are discussed below.

### 2.5.2 Soft Multi-Issue Pipelines

The idea of using VLIW (Very Long Instruction Word) processors in which batches of independent instructions are submitted to the processor pipeline has been explored as

a way of increasing soft processor performance without the complexities of hardware scheduling. Saghir *et. al.* implemented a soft VLIW processor using a register file with 2 banks replicated 4 times to achieve the 4 read ports and 2 write ports necessary to sustain two instructions per cycle [57]. For an fir benchmark this configuration achieved up to 2.55x speedup with 3 data write ports and 2 address write ports over 1 data write port and 1 address write port. Bank conflicts and limits to instruction level parallelism limit the performance scaling possible on soft VLIW processors, moreover the increasing register file replication necessary would quickly become overwhelming. Jones *et. al.* implemented a 4-way VLIW processor by implementing the register file in logic instead of block RAMs [31]. This 4-way parallelism averaged only 29% speedup over single-issue, suggesting that the technique cannot easily scale performance.

A superscalar processor can issue multiple instructions concurrently, but unlike VLIW processors, a superscalar automatically identifies and schedules independent instructions in hardware. While this approach is popular in hard processors, there is presently no soft superscalar architectures in existence likely due to their complexity. Also, the large associative circuit structures and many-ported register file required to build a superscalar are not efficiently implementable in FPGAs. Carli designed an out-of-order single-issue soft MIPS processor that implements Tomasulo's algorithm and discusses the infeasibility of superscalar issue with respect to his architecture [12]. The soft MIPS was found to be up to twice as big as a Xilinx Microblaze and between 3x and 12x slower.

### 2.5.3 Soft Multi-Threaded Pipelines

A potentially promising method of scaling soft processor performance is to leverage multiple threads. Research into exploiting multiple threads in soft processors will only become more fruitful as advancements in parallel programming are made in the microprocessor industry. Nonetheless, auto-vectorization is a significantly simpler problem which exploits predominantly fine-grain data parallelism and is hence supported in many compilers including GCC.

The advanced architectural features needed to keep a pipeline fully utilized can be avoided by instead having multiple independent instruction streams (threads), which can also be used to hide system latencies. Fort *et. al.* showed that a multithreaded soft processor can save significant area while hiding memory latencies and performing as fast as a multiprocessor system when both use an uncached latent memory system [21]. Labrecque *et. al.* showed that multithreading can save logic by eliminating branch handling and data dependency hardware [37]. They also showed that with an off-chip DRAM memory system the amount of hardware threads, cache configuration, cache topology, and number of cores can be varied to achieve maximum throughput from the memory system [38]. Moussali [47] built a multi-threaded version of the Xilinx Microblaze and showed that 1.1x to 5x performance can be gained by hiding the latency caused by custom instructions and custom computation blocks.

The CUSTARD [15, 16] customizable threaded soft processor is an FPGA implementation of a parameterizable core supporting the following options: different number of hardware threads and types, custom instructions, branch delay slot, load delay slot, forwarding, and register file size. The primary purpose of the design was to be used with a tool for automatic custom instruction generation. However its uses as a parameterized soft processor is more applicable to our own work. While the available architectural axes are interesting the results show some overheads in the processor design: clock speed varied only between 30 and 50 MHz on the XC2V2000 FPGA (on which the Microblaze soft processor is clocked at 100 MHz), and overall performance is 6-61% worse than Microblaze. Also the single-threaded base processor consumed 1800 slices while the commercial Microblaze typically consumes less than 1000 slices on the same device. Nonetheless 4-way multi-threading can be added for only 28% more area but was shown to gain only 10% in performance.

#### 2.5.4 Soft Multiprocessors

Unnikrishnan *et. al.* created a tool for automating the parallelization of streaming code and making application-specific customizations to the targetted soft multiprocessor system [62]. The individual cores could be customized to their software eliminating unused hardware using our SPREE framework and achieving significant area savings. With 16 processors up to 5x increased performance can be achieved using this tool. Similarly, Plavec *et. al.* [53] developed a tool to generate a streaming architecture comprised of multiple processor cores from a streaming program. The Altera C2H behavioural synthesis tool is leveraged to convert processor nodes to custom hardware achieving further speed improvements. The generated and optimized streaming architecture can perform up to 8.9x faster than execution on a single soft processor, as well as 4.3x faster than using C2H on the entire benchmark kernel. Similar to our own work, these stream-based design flows can provide scalable soft processor performance if streaming languages are adopted by embedded system designers. An auto-vectorizing compiler or vectorized library could provide this scalability with minimal disruption to current design flows.

Ravindran *et. al.* built a soft multiprocessor system dedicated to IPv4 packet forwarding [55]. The 14-processor system was able to achieve a throughput of 1.8Gbps, which when normalized to area is 2.6x slower than the Intel IXP-2800 network processor. This case study show the potential of FPGA-based multiprocessors to compete with highly optimized and specialized commercial hard multiprocessors. Rigorous manual parallelization was required and the multiprocessor topology was customized, but customizing each individual core was not performed as the authors used standard Xilinx Microblaze cores. More aggressive customization would require extensive software and hardware labour, but can perhaps be automated in the future.

#### 2.5.5 Soft Vector Processors

Yu *et. al.* [75] first demonstrated the potential for vector processing as a simple-to-use and scalable accelerator for soft processors. In particular, through performance mod-

elling the authors show that (i) a vector processor can potentially accelerate data parallel benchmarks with performance scaling better than Altera’s C2H behavioural synthesis tool (even after manual code restructuring to aid C2H), and (ii) how FPGA architectural features can be exploited to provide efficient support for some vector operations. For example, the multiply-accumulate blocks internally sum multiple partial products from narrow multiplier circuits to implement wider multiplication operations. This same accumulator circuitry is used by Yu to efficiently perform vector reductions which sum all vector elements and produce a single scalar value. Also the block RAMs can be used as small lane-local memories for efficiently implementing table lookups and scatter/gather operations.

The work of Yu *et. al.* was done in parallel with our own development of VESPA and its infrastructure, but it left many avenues unexplored. Its memory system consisted of only the fast on-chip block RAMs—latent memory systems were never explored. Without this and without real execution of benchmarks, the scalability of soft vector processors remains unproven. Also few customization opportunities in soft vector processors were examined beyond the number of lanes and the maximum vector length: the width of the lanes, multiplier, and memory were parameterized and were individually set for each benchmark. Finally more sophisticated vector pipelines features such as vector chaining were never considered. Beyond the work of Yu, in this thesis, we offer a full and verified hardware implementation of a soft vector processor called VESPA, connected to off-chip memory, with GNU assembler vector support, and evaluation on vectorized industry-standard benchmarks. This thesis more thoroughly explores the scalability, customizability, and architecture of soft vector processors. In addition, we explore the design space of VESPA configurations and show how competitive it can be versus manual hardware design in Chapter 8.

## Chapter 3

# Experimental Framework

Our goal of improving soft processors to be more competitive with hardware requires a measurement infrastructure for accurately and thoroughly evaluating enhancements to soft processors. In this chapter we describe the infrastructure used for executing, verifying, and evaluating soft processors. Specifically, we describe the benchmarks, compiler, CAD software, hardware platforms, measurement methodology, measurement error, and verification process.

### 3.1 Overview

We employ a real and complete measurement infrastructure which implements soft processors in hardware executing benchmarks on real FPGA devices. An overview of the infrastructure is illustrated in Figure 3.1. Benchmark software programs are compiled with standard compilers and simulated at the instruction-level to verify their correctness. Architectural ideas are augmented into a complete Verilog design of a soft processor and simulated at the register transfer level (RTL) using an RTL simulator. Once the correctness of the architecture is verified, the design is synthesized using FPGA computer-aided design (CAD) software which emit hardware characteristics such as the area and clock frequency of the design. The soft processor is then configured onto a real FPGA and executes each benchmark from off-chip DRAM—at the end of each execution the to-

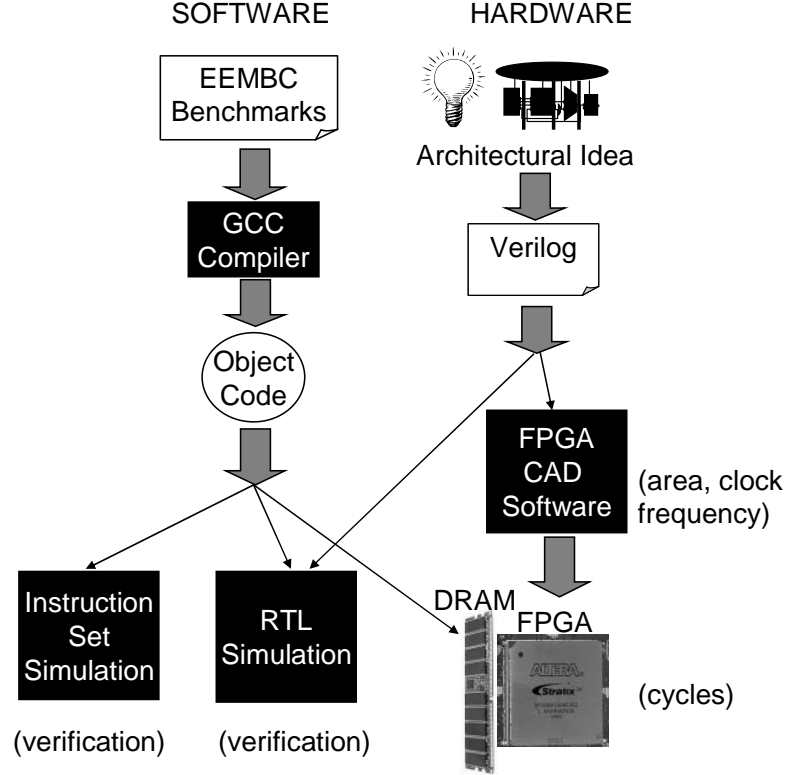


Figure 3.1: Overview of measurement infrastructure.

tal number of cycles are reported. The individual components of the infrastructure are discussed in detail in the remainder of this chapter.

### 3.2 Benchmarks

The benchmarks used in this study are predominantly from the industry-standard EEMBC (Embedded Microprocessor Benchmark Consortium) benchmark collection [18]. This EEMBC consortium is a non-profit corporation aiming to standardize embedded benchmarks and aid designers in selecting an appropriate embedded processor. The benchmarks are widely used in the embedded systems domain and since FPGAs are also used in the embedded domain, the EEMBC benchmarks are appropriate for evaluating soft processors. The benchmarks used in this study are selected from the Automotive 1.1, Office Automation 1.1, Telecom 1.1, Networking 2.0, and Digital Entertainment 1.0 suites. Our infrastructure is capable of compiling and executing all EEMBC benchmarks un-

Table 3.1: Vectorized benchmark applications.

Benchmark	Description	Source	EEMBC Suite (Dataset)	Input size (B)	Output size (B)	Num Loops
AUTCOR	auto correlation	EEMBC/VIRAM	Telecom (2)	1024	64	1
CONVEN	convolution encoder	EEMBC/VIRAM	Telecom (1)	522	1024	1
RGBCMYK	rgb filter	EEMBC/VIRAM	Digital Ent. (5)	1628973	2171964	1
RGBYIQ	rgb filter	EEMBC/VIRAM	Digital Ent. (6)	1156800	1156800	1
FBITAL	bit allocation	EEMBC/VIRAM	Telecom (2)	1536	512	2
VITERB	viterbi encoder	EEMBC/VIRAM	Telecom (2)	688	44	5
IP_CHECKSUM	checksum	EEMBC (kernel)	Net (handmade)	40960	40	1
IMGBLEND	combine two images	VIRAM	(handmade)	153600	76800	1
FILT3X3	image filter	VIRAM	(handmade)	76800	76800	1

compromised and with the complete test harness allowing us to report official EEMBC scores.

Our work on soft vector processors requires benchmarks with adequate data parallelism, so we assembled a subset of benchmarks for that purpose shown in Table 3.1. The top six are uncompromised EEMBC benchmarks vectorized in assembly and provided to us by Kozyrakis who used them during his work on the VIRAM processor [33] discussed in Section 2.2.6. Some debugging was subsequently performed on those benchmarks, which were also re-coded to eliminate dependencies to the original VIRAM processor configuration. The fifth benchmark is a kernel we extracted and hand-vectorized from the EEMBC IP\_PKTCHK benchmark. Since execution of this benchmark is independent of the data set values, we provide a hand-made data set of 10 arbitrarily filled 4KB packets. Similarly the last two benchmarks also execute independent of data set values, so we provide two arbitrarily filled 320x240 images (one byte per pixel) for FILT3X3 and one of those images for IMGBLEND. These two benchmarks were provided to us from the VIRAM group as well. The last three columns of Table 3.1 show the input data size, output data size, and total number of loops not including nested loops. All loops were vectorized except for one loop in both the FBITAL and VITERB benchmarks. Finally note that all benchmarks were written to be independent of the maximum vector length supported in the vector processor; no benchmark modifications were made nor required for any of our experiments.

### 3.3 Software Compilation Framework

Benchmarks are compiled using GNU GCC 4.2.0 ported to MIPS to match the MIPS-based SPREE scalar processors used throughout this work. Benchmarks are compiled with `-O3` optimization level. GCC has internal support for auto-vectorization potentially enabling soft vector processors to be employed without manual software changes. However, experiments with this feature showed that it failed to vectorize all key loops in the EEMBC benchmarks above. Using GCC 4.3.3 only the AUTCOR benchmark was successfully vectorized. We expect this technology to be better incorporated in GCC in the future. Commercial compilers such as the Intel C Compiler likely have better auto-vectorization support but is closed-source making it impossible to port to our VIRAM vector instruction set. Instead of relying on auto-vectorization, we ported the GNU assembler found in `binutils` version 2.1.6 to support our VIRAM vector instruction set, allowing us to hand-vectorize loops in assembly, compile it into a regular application binary, as well as disassemble the compiled result.

### 3.4 FPGA CAD Software

A key value of performing FPGA-based processor research directly on an FPGA is the ability to attain high quality measurements of the area consumed and the clock frequency achieved—these are provided by the FPGA CAD software. In this research we use Altera Quartus II version 8.1. There are many settings and optimizations that one can enable within the software, creating a wide range of synthesis results. In our work the settings used are those suggested in previous research [69] which identified them as a good area, clock frequency, and runtime tradeoff. First, we request that the CAD tool attempt to attain a 200 MHz clock frequency despite the fact that our soft processors are incapable of reaching such a high clock frequency. By doing this the CAD software thoroughly optimizes the clock frequency of the design. Second, we enable the optimizations for register retiming and register duplication as suggested. All other settings are left at their

default values.

### 3.4.1 Measuring Area

Area is comprised mostly of the FPGA programmable logic blocks described in Section 2.3. Throughout this work two generations of FPGAs are used: the Stratix I and Stratix III on which the programmable logic blocks are respectively referred to as *Logic Elements (LEs)* and *Adaptive Logic Modules (ALMs)*. Soft processors also make use of memory blocks and multiply-accumulate blocks in their designs creating a multi-dimensional area measurement, which we reduce to a single scalar measurement of the total silicon area used by all the occupied FPGA resources. The silicon areas of each FPGA resource relative to a single programmable logic block including its routing was provided to us from Altera [13] for the Stratix I and Stratix II. The relative silicon areas are proprietary and hence cannot be released in this document. We used these numbers for the Stratix I and extrapolated them for the Stratix III and measured the total silicon area consumed. We report the areas for the Stratix I and Stratix III respectively in units of *equivalent LEs* and *equivalent ALMs*.

### 3.4.2 Measuring Clock Frequency

The clock frequency of a synthesized design is reported by the timing analysis tool in the FPGA CAD software. In addition to the settings described above, the actual device targeted can affect these results because of differing architecture, circuit design, and IC fabrication process used in creating the FPGA. Rather than targeting the FPGA devices used in this work (which are slower mid-speed devices as described in the next section), we instead measure clock frequency by targeting a Stratix III EP3SL340H1152C2 which is a faster device than those on our hardware platforms. Doing this accurately reflects the speeds achievable on state-of-the-art FPGAs rather than limiting our results to the devices available to us.

### 3.5 Hardware Platforms

All soft processors explored in this work are fully synthesized using the CAD flow described above and implemented in hardware on an FPGA system. A hardware implementation is necessary to quickly benchmark a soft processor—an analysis of the execution speeds of hardware over software simulation is presented in Section 3.8. Benchmarks are executed in hardware and report the precise number of clock cycles required to complete execution. The majority of this work was done on the University of Toronto Transmogriifier-4 board, but prior to writing, we ported some of our work to the new Altera DE3 board. We describe each of these hardware platforms below and specify in our results which was used in the corresponding experiments.

#### 3.5.1 Transmogriifier-4

The Transmogriifier-4 [19] is a multi-FPGA platform with four Altera Stratix 1S80F1508C6 devices on it (a high-end large-capacity FPGA device fabricated in 130nm technology). This system was developed at the University of Toronto until completed in 2005 and was intended for graphics and other compute-intensive streaming applications. It is equipped with many peripherals such as video and Firewire connections, but the most important non-FPGA component for our purposes is the two 1GB DIMMs of DDR-266 SDRAM available for each of the four FPGAs. Only one Stratix I FPGA is used to host a soft processor design and one of the connected DIMMs is used to store the instruction and data for an application. The memory system is clocked at 133 MHz (266 MHz dual data rate).

The TM4 was selected for our studies of soft processor design for a few reasons. First, it provides a communication layer between user-designs on the FPGA(s) to a host Linux computer simplifying the design of an I/O subsystem. This communication package is referred to as the *TM4 Ports Package*. Second, it has a pre-verified memory controller design available. And finally, it has an abundance of DDR SDRAM on it whereas the

FPGA development kits at that time had only SRAM or only 16MB of DRAM. We believe it is important to use DRAM technology since the desktop market will continue to commoditize it making DRAM the cost-effective choice for embedded designs.

### 3.5.2 Terasic DE3

The Terasic DE3 boards were released in 2008 offering more up-to-date FPGA and DRAM technologies. We use the Terasic DE3-340 board equipped with a single Stratix III EP3SL340H1152C3 which is one of the largest state-of-the-art FPGAs available at the time this work was performed. The Stratix III is fabricated in a  $65nm$  CMOS technology process making it two generations more advanced than the Stratix I FPGAs on the TM4. We also use a 1GB DDR2-533 MHz memory device for the storage of instructions and data in a program. The Altera DDR2 memory controller connects the soft processor to the DDR2 DIMM and is clocked at the full-rate of 266 MHz.

### 3.5.3 Measuring Wall Clock Time

The implementation onto a real FPGA hardware platform enables accurate measurement of not just the execution cycles (which traditionally was only modelled in the computer architecture community) but also the wall clock time for executing a benchmark. Wall clock time considers both cycle performance and clock frequency of a processor. Measuring wall clock time is ideally performed by clocking the design at its highest clock rate, measuring the number of clock cycles to execute a benchmark, and then multiplying the number of cycles by the clock period. To avoid complications that arise from clocking each design at a custom rate, we clock all designs at one clock frequency. On the TM4 this is 50 MHz and on the DE3 it is 100 MHz. Thus our calculation of wall clock time is given by

$$WCT = N_{cycles@50or100MHz} / f_{cpu} \quad (3.1)$$

where  $f_{cpu}$  is the maximum clock frequency of the soft processor and  $N_{cycles@50or100MHz}$

is the number of cycles to complete the benchmark when clocked at 50 or 100 MHz depending on the platform. Typically the soft processor can be clocked higher than these frequencies, meaning we are underclocking the soft processors.

### 3.6 Measurement Error

Errors in our measurement methodology exist due to simplifications made, randomness in the CAD software, and physical effects in our realistic infrastructure. These errors affect the area, cycles, clock frequency, and wall clock time measurements and are detailed below.

1. **Area:** Area measurements are subject to two sources of errors: (i) the synthesis algorithms which can produce significantly different hardware implementations from minor perturbations to the Verilog source; and (ii) the approximation of the silicon areas of each resource on the Stratix III which we derived from the Stratix II. The first is difficult to mitigate, the second cannot be discussed to protect the intellectual property rights of the vendor.
2. **Cycles:** The number of cycles reported at the end of benchmark execution is precisely measured, but certain events can randomly occur during execution altering the measurement with each run. A DRAM refresh command is one such example, as is settling times between signals crossing clock domains. In general this affected only the least significant digit of cycle measurements while benchmarks executed between thousands and millions of cycles. The error is hence ignored.
3. **Clock Frequency:** Clock frequency measurements can vary significantly from the non-determinism in modern CAD algorithms which produce different clock frequencies depending on an integer *seed* selected by the user. To filter out the noise caused by this non-determinism, we select 8 different seeds and average the clock frequency across the 8 runs as suggested in [69]. This averaging minimizes the amount of measurement error in our methodology.

4. **Wall Clock Time:** As mentioned previously, measuring the maximum clock frequency of a design and achieving a design that can operate correctly at that frequency introduces additional complications. These complications are avoided by underclocking all designs at the same clock frequency and using Equation 3.1 which leads to time dilation effects between the processor and memory. Underclocking a processor design means fewer processor cycles are needed to match the memory latency. Scaling those cycles by a faster clock rate falsely accelerates the memory latency as well. In Chapter 4 we show that cache misses are not a major contributor to scalar soft processors, and in Chapter 6 we show that prefetching can minimize their impact on performance so we ignore these effects.

### 3.7 Verification

All soft processors were fully tested in hardware using the built-in verification encoded into each EEMBC benchmark. At the end of each benchmark a checksum is computed across the output data and compared to a built-in gold-standard value to determine if execution completed successfully. If the verification fails, it can be extraordinarily difficult to uncover and fix bugs given that manual modifications were made to the benchmarks, the assembler, the simulator, and the hardware design. As a result, developing a powerful test and debug infrastructure with multiple abstraction levels is imperative for in-hardware exploration of architectures.

#### 3.7.1 Instruction Set Simulation

One useful abstraction is simulation at the instruction-level which is performed independent of any architecture. Instruction set simulation can verify the correctness of the benchmark and assembler hence ruling out bugs in these components. However without a pre-verified VIRAM simulator available, considerable time was spent augmenting an existing simulator with VIRAM extensions and simultaneously debugging it with the

benchmarks and assembler.

Our simulator is based on the MINT [64] MIPS simulator which is pre-verified and can successfully execute the scalar MIPS code in our benchmarks. MINT models only the MIPS state and parses instructions in the binary and appropriately updates the state. We augmented this simulator with support for the VIRAM vector instruction set modelling all the vector state described in Section 2.2.6. In addition we parse and execute the vector instructions by correspondingly modifying the vector state. Once verified, the augmented MINT simulator was used to verify the benchmarks and compiler, analyze the instruction streams of the benchmarks, and even model caches and other processor components to predict their effectiveness. The most important use of the the simulator however is to generate traces of all modifications to the vector state which is used to compare against by the RTL simulation described below.

### 3.7.2 Register Transfer Level (RTL) Simulation

RTL simulation is performed using Modelsim SE version 6.3c which can simulate the Verilog design in software (avoiding hardware timing problems such as crossing a clock domain). The complete system is simulated including the processor, bus, and even DDR controller. The behaviour of the TM4 DDR DIMM is modelled in Verilog using a hand-made memory model, as is the TM4 communication package which is stimulated with bus transactions that emulate the TM4-to-host transactions. The DE3 DDR2 memory is modelled with the Altera generated memory model. With this level of simulation we can capture logic errors throughout the complete hardware system. Similar to MINT, the RTL simulation emits a complete trace of all modifications made to the vector state. By comparing this trace to that from MINT, we can identify: (i) the instruction which triggered the error; (ii) the incorrect value computed; and (iii) the exact time in the waveform the error occurred. This trace-guided debug infrastructure is used extensively before implementing a design in hardware.

Table 3.2: Benchmark execution speeds.

Platform	Instructions/s	Normalized Speedup
DE3	68970334	2383961
MINT	76458	2643
Modelsim	29	1

### 3.7.3 In-Hardware Debugging

Despite the simulation at the instruction and RTL level, inevitably some errors will manifest only in the hardware implementation. In such a case the benchmark will either report that it failed or execute indefinitely with no response. For either case the Altera SignalTap II Logic Analyzer is used to examine the internal state of the system. SignalTap inserts logic into the design allowing some signals to be sampled under some event and transmitted to the FPGA CAD software over a JTAG link. This tool provides very limited scope and debug features, highlighting the need to catch errors before the system is implemented in hardware.

## 3.8 Advantages of Hardware Execution

RTL simulation in Modelsim could be used in place of actual hardware execution while still achieving high-fidelity results. But execution in real hardware has the advantage of rapid benchmark execution which is necessary for benchmarking large design spaces using long-running applications. To quantify the advantages of hardware execution we measured the actual execution rates across: (i) our DE3 hardware platform hosting a soft processor; (ii) our MINT-based instruction set simulator which executes the benchmark without cycle-accurate hardware detail; and (iii) RTL simulation in Modelsim of the same soft processor. This was measured by executing the QSORT benchmark from the free MiBench [61] suite.

Table 3.2 lists the instruction execution rates and normalized speedup across the three platforms. RTL simulation is by far the slowest since the exact cycle-to-cycle behaviour of the processor is being emulated in software. The MINT simulator can execute 2643x

faster than modelsim by emulating only instruction-level behaviour without any cycle-level details. The hardware implementation on the DE3 can execute 2.4 million times faster than Modelsim, and approximately 1000x faster than MINT. The benchmarking speed available in hardware enables us to quickly execute large benchmarks across many soft processor configurations, while capturing full and realistic hardware behaviour.

### 3.9 Summary

In this chapter we presented our infrastructure for evaluating soft processors in real hardware. Using industry-standard benchmark applications compiled through standard software toolchains and executed from DRAM on real FPGA devices we achieve benchmarking accuracies never seen in traditional computer architecture research. In addition, with accurate area and clock frequency measurements from the FPGA CAD software, we achieve a more complete view of pertinent architectural metrics enabling us to draw accurate conclusions about soft processor architecture.

## Chapter 4

# Performance Bottlenecks of Scalar Soft Processors

A key goal of this research is to scale the performance of soft processors. This is best achieved by targeting the bottlenecks of current soft processors, hence motivating analysis of the bottlenecks in current soft processor systems under their typical workloads. For example, if soft processors were memory bound a soft processor can customize its memory system and scale performance with area costs less than adding vector extensions. The subsequent sections implement a soft processor system with off-chip memory, analyze that system, explore different cache configurations, and finally compare it to an IBM PowerPC hard processor. The observations gained from this analysis will be used to guide system-level scalability enhancements for soft processors.

### 4.1 Integrating Scalar Soft Processors with Off-Chip Memory

Our previous work with the SPREE soft processor generator [70, 71] used only *on-chip* memory, where memory latency is not a concern since FPGA block-RAMs typically operate at higher speeds than the soft processors that use them. However, our consultations with both Xilinx and Altera revealed [8, 65]: (i) that commercial soft processors were most often used in systems with off-chip memory which requires several processor clock

cycles to access—referred to as *latent memory accesses*; and (ii) that internally both companies benchmark their processors with embedded systems benchmarks, believing these represent typical soft processor workloads. The first suggests a disconnect between the prior research and commercial uses of soft processors hence necessitating new studies into soft processors with off-chip memory. The second confirms our benchmark selection, yet motivates an off-chip memory system for supporting benchmarks with larger data sets such as those from EEMBC as discussed in Chapter 3. Systems with only on-chip memory have limited data and instruction memory available preventing them from executing many of the EEMBC benchmarks (data set sizes for the vectorized benchmarks are given in Chapter 3, Table 3.1). We therefore implemented a SPREE soft processor on the TM4 using the DDR DRAM for memory.

The specific scalar processor design selected for our study was automatically generated by the SPREE processor generator [70, 71]. We chose a 3-stage pipelined processor with full forwarding and a 1-bit branch history table for branch prediction as we found it to be the most area-efficient (good performance with low area). The processor suffers a single pipeline stall on any branch misprediction or instance of a shift, multiply, load, or store instruction. SPREE initially supported only on-chip memory, so we modified SPREE to export an external memory bus allowing the connection of a memory subsystem and hence allowing varying additional stalls for loads and stores depending on the response of the memory subsystem. The DDR memory on the TM4 has 64 pins resulting in 128 bits accessible per clock cycle since data is transmitted on both positive and negative edges of the 133 MHz clock. To connect the processor and memory, we use instruction and data caches to hide the memory latency. The caches have a 16-byte line size to match the 128-bit interface of the DDR memory for simplicity. To fully utilize the Stratix I block RAMs required to achieve this line size, we implement 4KB deep caches. The data cache implements a write-back, write-allocate write policy.

Using the TM4 hardware platform, the processor and caches are clocked together at 50 MHz while the DDR controller is clocked at 133 MHz as discussed in Chapter 3.

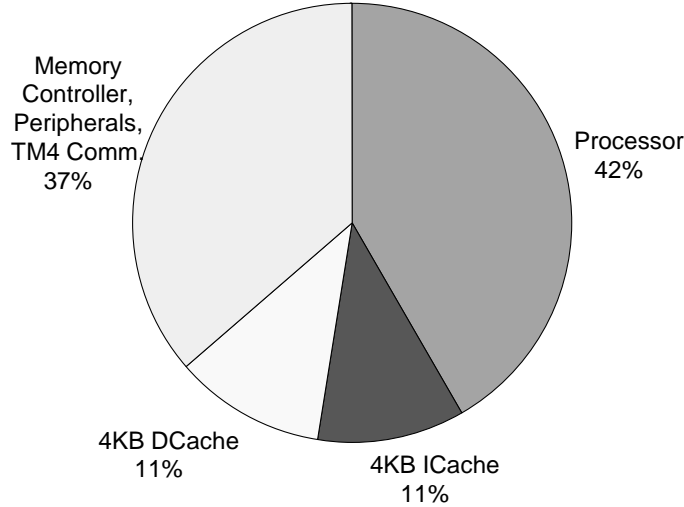


Figure 4.1: Area breakdown of scalar SPREE processor with off-chip memory system.

There are three main reasons for the reduced clock speed of the processor and caches: i) the original 3-stage pipelined processor with on-chip memory could only be clocked at 72 MHz on the slower speed grade Stratix I FPGAs on the TM4; ii) adding the caches and bus handshaking further reduced the clock frequency to 64 MHz; and iii) to relax the timing constraints when crossing clock domains, we chose a 20 ns clock period which is a rational multiple of the 133 MHz (7.5 ns) DDR clock. Doing this means the worst case offset between these two clock edges is 2.5ns. This large delay makes it easier for the CAD tools to meet timing constraints.

#### 4.1.1 Scalar Soft Processor Area Breakdown

Figure 4.1 shows the relative area of components in our soft processor system with off-chip DDR memory. The areas were measured in terms of silicon area as described in Chapter 3. The figure shows that the system is comprised of the processor core (42%), 4KB direct-mapped L1 data cache (11%), 4KB direct-mapped L1 instruction cache (11%), and the rest of the system including memory controller, peripherals, and communication logic between the TM4 and Linux host (37%). Note that cache accounts for less than a quarter of system area, despite the simplicity of the processor core. While this is quite different from conventional processors whose silicon area is typically dominated by cache,

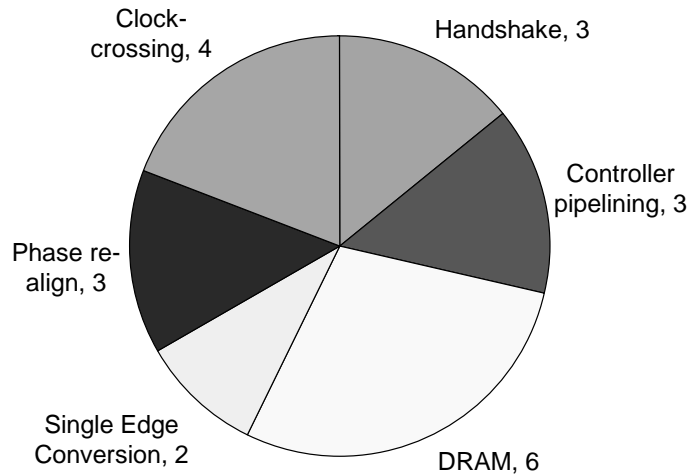


Figure 4.2: Breakdown of the 21 cycle memory latency in TM4-based soft processor system measured in clock cycles of the memory core clock (133 MHz).

it is expected in FPGA technology since caches are composed mostly of memory which can be built efficiently using block RAMs. Similarly, in contrast with hard systems, cache area is also dominated by area devoted to the memory controller and other peripherals.

#### 4.1.2 Scalar Soft Processor Memory Latency

A load miss penalty of only 9 cycles exists on our system with a processor clock of 50MHz and a memory system clock of 133MHz. In terms of the memory system clock, the latency is 21 cycles and can be broken-down as seen in Figure 4.2. The processor uses a 3-cycle handshaking scheme to communicate a memory request to the DDR controller. Pipelining within the DDR controller and the row and column access latencies are responsible for a 9-cycle delay before the data is available at the pins of the FPGA.<sup>1</sup> Conversion from the 64-bit dual-data-rate signal to a 128-bit wide single-edge signal requires 2 cycles, followed by 3 cycles for phase realignment since data returns offset from the original clock edge. Crossing back into the processor's clock domain with some handshaking then consumes an additional 4 cycles. This memory controller implementation can have its latency further improved by: (i) tracking open DRAM pages and avoiding redundant row access latencies; (ii) allowing multiple outstanding memory operations to be requested;

<sup>1</sup>Note the controller uses a closed-page policy meaning every request opens a DRAM row and then closes it.

and (iii) fusing the single edge conversion, phase re-alignment, and clock crossing which together amount to a single clock crossing. Thus, we are confident the memory system is not overly-optimized and hence is representative of the memory latencies typical in an FPGA.

Table 4.1: Memory latencies on soft and hard processor systems.

	SPREE on TM4	SPREE on DE3	Pentium 4 desktop
Processor Clock	50MHz	100MHz	2.8GHz
DRAM	DDR	DDR2	DDR
Memory Clock	133MHz	266MHz	160MHz
CAS Latency	2.5	4	2.5
Miss Penalty	9	11	325

Our first key observation is therefore that off-chip memory latency for FPGA-based soft processors is not as significant as it is for ASICs and other hard processors, because the clock frequency of typical soft processors is much slower as seen in Table 4.1. The memory latency after missing in both the L1 and L2 caches on a 2.8GHz Pentium 4 (Northwood) processor with 160MHz DDR SDRAM was measured as 325 cycles using the RightMark Memory Analyzer software [10]. This latency is 36 times higher than the 9-cycle latency observed in our 50MHz soft processor on the TM4. Since the soft processor is being underclocked as discussed earlier, the observed memory latency can be higher with a faster processor clock frequency. But even with an optimistic 133MHz processor clock, the 21 cycle latency is still very small compared to the 325 cycles on the Pentium 4. Using the DE3 platform and DDR2 DRAM, the latency is increased to 11 cycles when the SPREE processor is clocked at 100 MHz. Clocking it optimistically at 266MHz results in a 30 cycle latency which is still one-tenth of that on the Pentium 4 desktop system. These small memory latencies suggest that research into improved memory systems for soft processors can be deferred until perhaps sometime in the future. In this thesis we address the more immediate need for increased computational capability by implementing vector extensions.

The increased latency observed on the DE3 platform over the TM4 is due to the

Altera DDR2 High Performance Memory Controller used, which is much more sophisticated than the DDR controller we designed ourselves for the TM4. The Altera DDR2 controller supports multiple outstanding memory requests, though our soft processor does not exploit this as it can service only one memory operation at a time. It also tracks open DRAM pages, so that a cache misses to an already open page would exhibit a shorter latency. Finally, the memory controller is aggressively pipelined since it must satisfy timing constraints in many different designs on many different devices. After two generations of CMOS technology improvements, this increased latency can at best suggest a gradual worsening soft processor-memory performance gap. We expect that going forward, soft processors will continue to observe memory latencies much smaller than conventional microprocessors. Despite the small memory latencies, the memory system may be a significant bottleneck in a scalar soft processor if the latency could not be effectively hidden. This is explored in the subsequent section.

## 4.2 Scaling Soft Processor Caches

If the memory latency was a significant bottleneck, then hiding that latency would greatly increase the performance of the system. In this section we explore the impact of cache configuration on performance to measure the significance of memory latency in our scalar soft processor system. We extrapolate our results and model an ideal memory system (effectively on-chip memory) to determine an upper bound on the speedup that could be achieved by eliminating the memory latency.

In this experiment we use the parameterized data cache depth in our scalar soft processor to vary the capacity of the cache. This data was collected from an in-hardware execution of the EEMBC benchmarks on the TM4. The *measured* line in Figure 4.3 shows the geometric-mean speedup across our EEMBC benchmarks for varying direct-mapped data-cache sizes, relative to a 4KB data cache. Compared to the 4KB data cache, an enormous 256KB data cache provides only a 9% additional speedup at the cost of a

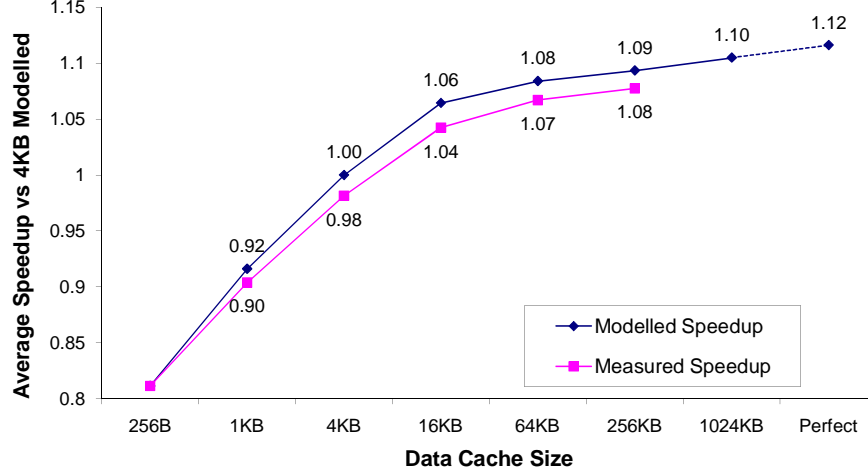


Figure 4.3: Geometric mean speedup across our EEMBC benchmarks for varying direct-mapped data-cache sizes, relative to a 4KB data cache. Speedup is both *measured* in real hardware and *modeled* according to Equation 4.1, both with a 64KB instruction-cache. For the modeled speedup, the *perfect* point shows the impact of a perfect data cache.

64-fold increase in area devoted to cache.

To extrapolate these results further, we used our hardware system and an instruction set simulator to derive a model of the system. To model the impact of a given cache, we use the equation:

$$Speedup = CPI_{perfect} + (f_{ld}M_{ld}P_{ld}) + (f_{st}M_{st}P_{st}) \quad (4.1)$$

where  $CPI_{perfect}$  is the cycles-per-instruction measured with a perfect memory system,  $f_{ld}$  is the frequency of loads,  $M_{ld}$  is the load miss rate,  $P_{ld}$  is the load miss penalty in processor cycles. The third term in the equation is analogous to the second and uses equivalent parameters specifically for stores instead of loads. Using the CPI values measured previously for our processors with only on-chip memory [70] as an estimate, the frequency of memory references and miss rates measured using our instruction simulator as seen in Appendix A, and miss penalties reported by the Altera SignalTap II Logic Analyzer software, we plot the *modelled speedup* line shown in Figure 4.3. The figure shows that the modelled speedup tracks the measured speedup very closely, with the modelled speedup being slightly larger since it models neither instruction misses nor bus contention. According to this model a perfect data cache improves performance only

12% over the 4KB data cache. Caches with increased associativity may be ineffective at achieving this performance because they would increase the cache access latency. The diminishing returns seen in the larger cache sizes and the idealized cache point out that the memory system is not a significant bottleneck. While vector extensions can also aid in relieving memory bottlenecks, soft processors are uniquely able to adapt to their memory access patterns to effectively hide memory latency. In a memory bound system it is likely that this would produce performance scaling with significantly less area cost than a vector processor. Since soft processors are not presently memory bound we forego this potentially large research topic and are hence motivated to explore a means of translating additional area into improved performance other than increasing memory system performance.

### 4.3 Soft vs Hard Processor Comparison

Recall that our goal is to use software-programmed soft processors to replace much of the manual hardware design in an FPGA system. To enable greater capability in soft processors we also seek performance scaling significantly beyond that achieved by improving the memory system. To provide a context for these goals, we compare soft processor performance to hard processor performance. This allows us to approximate the large performance losses associated with implementing a processor on an FPGA substrate. Note it is not our goal to make FPGAs the desired substrate for all microprocessors, rather, soft processors are already adequately motivated despite their lack of performance as discussed below.

An FPGA design which includes a software component can execute that software on (i) an off-chip hard processor, (ii) an on-chip hard processor such as the PPC 405 included on various Xilinx FPGAs, and (iii) on a soft processor. The first option requires additional board space and power, the second option raises the costs of FPGAs, while the soft processor option likely performs the worst. By leveraging the reprogrammability

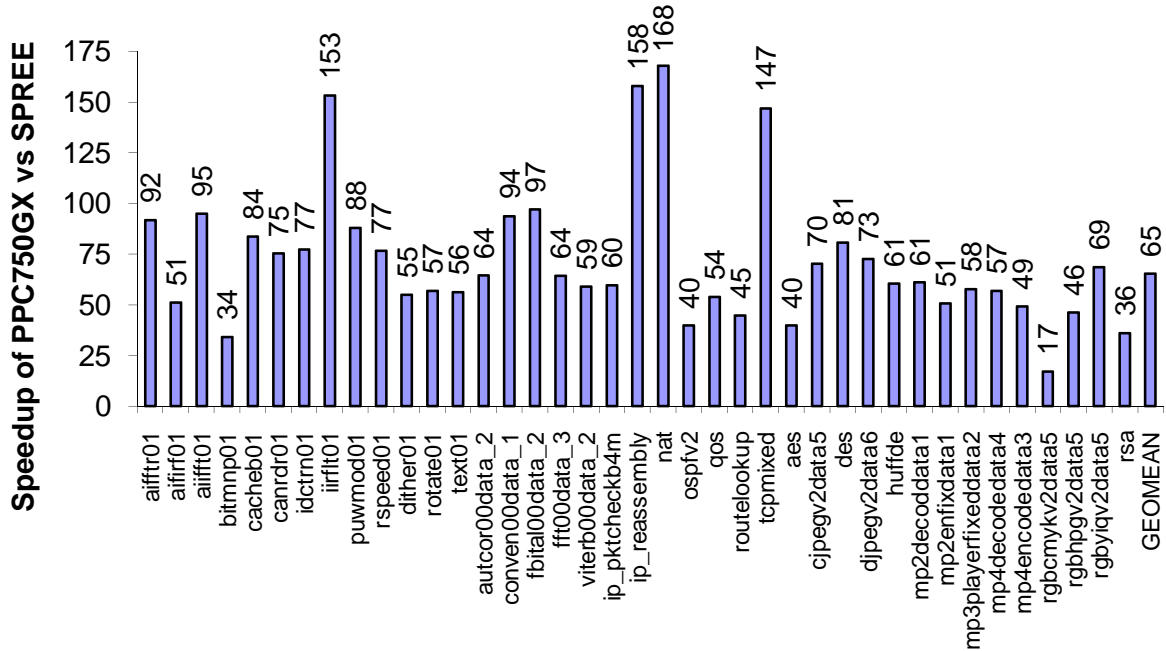


Figure 4.4: Speedup of IBM 750GX 1GHz laptop processor versus the 3-stage 50 MHz SPREE-based processor system.

in soft processors to customize them to their application, we hope to improve their performance and make them an effective vehicle for avoiding hardware design by making software sufficient. Quantifying the performance gap between soft and hard processors will suggest the magnitude of performance scaling necessary to make soft processors significantly more useful in this regard. Using our SPREE processor with 3-stage pipeline, full forwarding, 1-bit branch history, and separate 4KB L1 direct-mapped caches, we measure the performance of the EEMBC benchmarks on the TM4. Since EEMBC scores are listed on the EEMBC website [18], we can easily compare this SPREE processor to a real hard processor implemented in the same 130nm CMOS technology used in our Stratix 1S80 platform. However, the number of processors listed on the EEMBC website are relatively few so we chose the IBM PowerPC 750GX based on its reputation, high-performance, and 130nm design. Other options were not very well-known and had low performance.

We used the complete EEMBC benchmark suite choosing the largest datasets for each application, and eliminating any benchmarks dominated by floating point or integer

division operations as our processor did not have hardware support for these operations. Certain benchmarks such as `nat` and `iirflt01` still contain a significant amount of division and hence additionally suffer in our system which performs division in software. Figure 4.4 shows the performance of our SPREE processor against the IBM PowerPC 750GX which was used in laptop computers and greatly outperforms typical embedded processors. The PPC750GX is a 1GHz out-of-order multi-issue processor with 32KB 4-way set associative L1 caches, a shared 1MB L2 cache, and a 200 MHz memory bus clock. On average, the PPC750GX performs 65x faster than our 50 MHz in-order single-issue processor with separate 4KB direct-mapped caches and a 133-MHz memory clock with 9-cycle memory access latency. The `RGBCMYK` benchmark is executed only 17x faster than our soft processor. This datum seems to be an anomaly, but without access to the PPC750GX or its compiler further investigation is impeded. A likely cause of this are the conditional statements within the small loop which cannot be accurately predicted since they are data dependent. Our SPREE processor with its short pipeline is only slightly affected by mispredicted branches, a more highly aggressive design such as the PPC750GX may be more heavily impacted.

The large 65x performance gap is in part accounted for by the 20x faster processor clock speed of the PPC750GX. Differing processor architecture, memory hierarchy, and memory technology presumably contribute to the remainder of the gap. As we showed in the last section, idealizing the complete memory system does not significantly increase the performance of the soft processor. This suggests that soft processors need to be equipped with far more powerful compute capabilities than currently available, and that the order of performance gains necessary to truly make soft processors useful beyond their current niche is in the 10-50x range. Our goal is to make significant progress in this direction through the use of soft vector processors.

## 4.4 Summary

In this chapter we investigated a system comprised of a commercially competitive scalar soft processor connected to off-chip DDR RAM in real hardware. The observed memory latency was only 9 cycles, significantly smaller than in traditional hard processors which are clocked in the GHz range. We noted that the size of a 4KB data cache is just one quarter the size of the soft processor. We also saw that expanding this cache to 256KB provided only a 9% increase in performance as measured in hardware, and when we model an ideal memory system, only 12% better performance is possible. Thus, the small 4KB direct-mapped cache has largely solved the memory problem for current soft processors running embedded benchmarks. Further increases to the computational capabilities of soft processors are necessary to widen their adoption. Against a hard laptop processor our commercially competitive soft processor was 65x slower with a 20x slower clock rate. By reducing this gap we hope soft processors will provide a more affordable, simple, and effective means of implementing computation in FPGAs. Rather than performing incremental improvements to soft processors, the magnitude of the gap motivates research into highly scalable soft processor architectures.

## Chapter 5

# The VESPA Soft Vector Processor

In this chapter we motivate, design, and build a soft vector processor called Vector Extended Soft Processor Architecture or VESPA.

### 5.1 Motivating Soft Vector Processors

Recall that our goal is to scale the performance of soft processors so that they might be used as an alternative to laborious hardware design. Since FPGAs are often used in embedded systems, their workloads include telecommunication and multimedia applications which are known to have ample data level parallelism [33]. Thus, to achieve our goal of scaling the performance of soft processors, we are motivated to exploit this DLP so that these workloads might be implemented more easily in software instead of hardware.

While DLP can be exploited in many ways, we chose a soft vector processor for a number of reasons. First, supporting and using soft vector processors requires only extending the instruction set. Commercial soft processors already have infrastructures for adding custom instructions, so vector extensions can be comfortably used by existing FPGA designers. Second, vector processors provide a built-in abstraction between software and hardware through the maximum vector length MVL parameter. This allows the designer to vary the number of vector lanes and hence control the area/performance trade-off without rewriting or re-compiling software. Third, auto-vectorization has been

thoroughly researched and already exists in compilers such as `GCC` [14] because detecting the fine-grain data parallelism used by vector processors is far simpler than the general parallelization problem. With high-quality auto-vectorization, soft vector processors could be seamlessly used in a typical `C`-based design flow and the FPGA designer would need only to choose the number of lanes depending on the space available on their device. On going research in auto-vectorization algorithms [50] could help enable this seamless design flow. Finally, the biggest reason is that a vector architecture is well-suited to FPGA implementation. A vector processor with all lanes operating in lockstep requires very little inter-lane coordination making the design scalable in hardware. Moreover, the architecture does not require any large associative lookups, many ported register files, or other structures that are inefficient to implement in FPGAs. Other architectures such as superscalar processors could require such inefficient FPGA structures. For all these reasons we believe soft vector processors can effectively exploit DLP on an FPGA and hence promote simpler software implementations of components instead of manual hardware design.

## 5.2 VESPA Design Goals

In deriving the design goals for VESPA, it is useful to target the computational tasks that a soft vector processor is likely to be used for. The decision to use a soft vector processor implementation depends not only on the amount of DLP in a computation, but also on how critical the given computation is to the overall performance of the system. A digital system is comprised of many components each implementing different computational tasks which vary in both their DLP and their performance requirements (or criticality). Computations with little or no DLP, as well as highly critical computations which justify highly-optimized hardware design are unsuitable candidates for execution on a soft vector processor. Thus, as shown in Figure 5.1, the class of computations targeted in this thesis is low to medium critical computations with sufficient DLP. The benchmarks used in

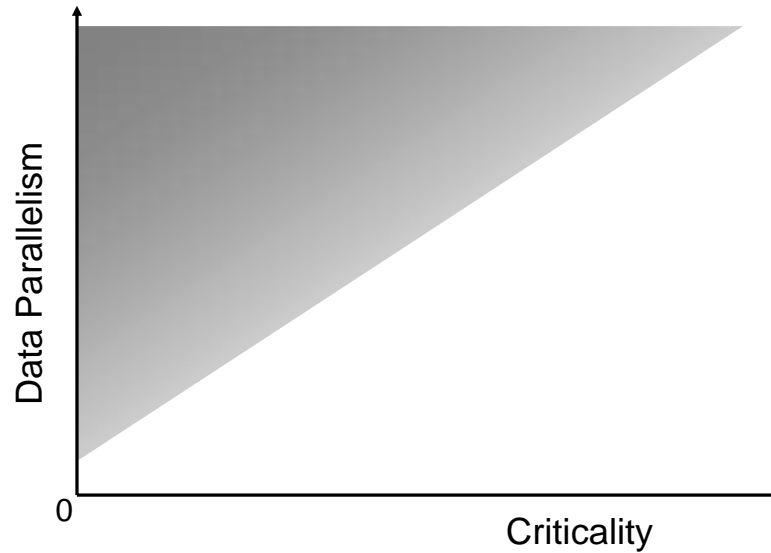


Figure 5.1: A view of the space of computations divided along the axes of DLP and performance criticality. Computations with low DLP and criticality are near the origin and are likely candidates for implementation on a scalar soft processor, while computations with sufficient DLP and low to medium criticality are shown in grey and are targeted in this thesis for implementation on a soft vector processor.

this thesis typically have very high DLP. Increased amounts of DLP motivate soft vector processor implementations for more critical computations. As a result the design goals for VESPA are as follows:

1. **Scalability** – The more VESPA can scale performance, the more likely it is to be used for computation with higher criticalities. Since our goal is to reduce the amount of hardware design, converting these more critical computations into software is key for this thesis.
2. **Flexibility** – Aside from the number of lanes, there are several other parameters that can dramatically affect the area and performance of a soft vector processor. To exploit the unique ability of FPGAs to quickly implement custom hardware, VESPA was designed with many architectural parameters which designers can use to meet their area/performance needs.
3. **Portability** – Although less crucial than the first two goals, it is also important that a soft vector processor can be easily ported to different FPGA architectures.

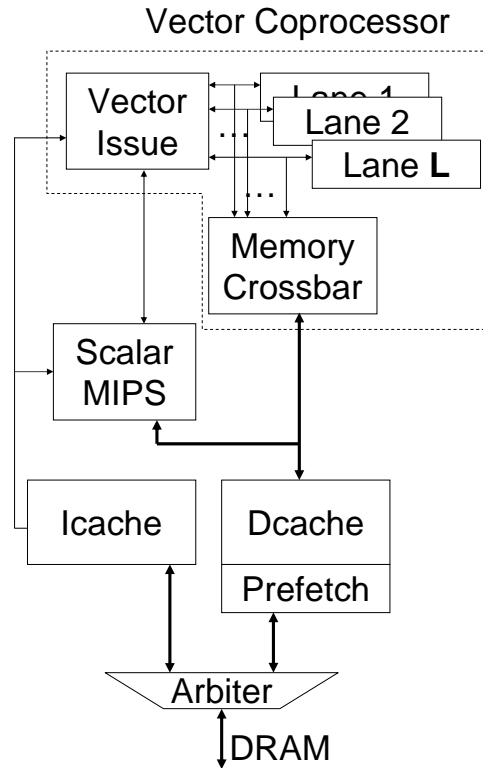


Figure 5.2: VESPA processor system block diagram.

With this property, FPGA vendors and users are more likely to adopt soft vector processors since maintaining the design across their many FPGA families is simplified.

To achieve these goals and verify the feasibility of soft vector processors on FPGAs we implemented VESPA on the FPGA hardware platforms described in Chapter 3.

### 5.3 VESPA

The VESPA soft vector processor was designed to meet the aforementioned goals. VESPA is composed of a scalar processor and an attached vector coprocessor. A diagram including both components as well as their connection to memory is shown in Figure 5.2. The figure shows the MIPS-based scalar and VIRAM-based vector coprocessor both fed by one instruction stream read from the instruction cache. Both cores can execute out-of-order with respect to each other except for communication and memory instructions

which are serialized to maintain sequential memory consistency. Vector instructions enter the vector coprocessor, are decoded into element operations which are issued onto the vector lanes and executed in lockstep. The vector coprocessor and scalar soft processor share the same data cache and its data prefetcher though the prefetching strategy can be separately configured for scalar and vector memory accesses. The four sections below describe the scalar processor, the vector instruction set implemented by the vector coprocessor, the vector coprocessor memory architecture and the VESPA pipeline in more detail.

### 5.3.1 MIPS-Based Scalar Processor

The instruction set architecture (ISA) used for our scalar processor core is a subset of MIPS-I [46] which excludes floating-point, virtual memory, and exception-related instructions; floating point operations are supported through the use of software libraries. This subset of MIPS is the set of instructions supported by the SPREE system [70, 71] which is used to automatically generate our scalar soft processor FPGA implementation in synthesizable Verilog HDL. The generated scalar processor is a 3-stage MIPS-I pipeline with full forwarding and a 4Kx1-bit branch history table for branch prediction.

The SPREE framework was modified in two ways to better meet the needs of the vector processor. First, an integer divider unit was added to the SPREE component library along with instruction support for MIPS divide instructions. This was necessary to accommodate the FBITAL benchmark which requires scalar division. Second, to support the vector coprocessor, the MIPS coprocessor interface instructions were implemented in SPREE. These instructions allow the SPREE processor to send data to the coprocessor and vice versa. With these changes in place we can automatically generate new scalar processor cores and attach them directly to the memory system and vector coprocessor without modification, allowing future studies to consider both scalar and vector architectures in tandem.

Table 5.1: VIRAM instructions supported

Type	Instruction
Vector	vadd vadd.u vsub vsub.u vmulhi vmulhi.u vcmp.eq vcmp.ne vcmp.lt vcmp.u.lt vcmp.le vcmp.u.le vmin vmin.u vmax vmax.u vmullo vabs vand vor vxor vnor vsll vsrl vsra vsat.b vsat.h vsat.w vsat.su.b vsat.su.h vsat.su.w vsat.su.l vsat.u.b vsat.u.h vsat.u.w vsadd vsadd.u vssub vssub.u vsrr vsrr.u vsls vsls.u vxumul vxumul.u vxlmul vxlmul.u
Vector Manipulation	vins.vv vins.sv vext.vv vext.sv vext.u.sv vmerge vexthalf vhalf
Flag	vfand vfor vfxor vfnor vfcfr vfset
Memory	vld.b vld.h vld.w vld.l vld.u.b vld.u.h vld.u.w vlds.b vlds.h vlds.w vlds.l vlds.u.b vlds.u.h vlds.u.w vldx.b vldx.h vldx.w vldx.l vldx.u.b vldx.u.h vldx.u.w vst.b vst.h vst.w vst.l vsts.b vsts.h vsts.w vsts.l vstx.b vstx.h vstx.w vstx.l vstxo.b vstxo.h vstxo.w vstxo.l
Control	vsatvl vmcts vmstc cfc2 ctc2 mtc2

### 5.3.2 VIRAM-Based Vector Instruction Set

While many vector processor implementations exist, we used an existing vector ISA to leverage prior design effort, but implemented our architecture from scratch to take advantage of FPGA-specific features. The instruction set architecture of the VESPA vector coprocessor is based on the VIRAM [60] instruction set summarized in Chapter 2, Section 2.2.6. The specifics of VESPA’s vector instruction set is described below.

The vector coprocessor implements all of the vector state of the VIRAM instruction set which is shown in Chapter 2, Figure 2.2 (on page 14). While VIRAM implements 64-bit vector elements and control/scalar registers, in VESPA this is reduced to 32-bits since none of our vectorized benchmarks listed in Chapter 3, Table 3.1 (on page 29) require 64-bit processing. All of the state is efficiently implemented in FPGA block RAMs with the vector and flag register files both having two copies of their state to provide the 2 read ports and 1 write port required by the vector pipeline. Since block RAMs have only two access ports, we replicate the register files and broadcast writes to both copies of the register file while each copy provides its own read access port.

The vector coprocessor supports most of the integer, fixed-point, flag, and vector

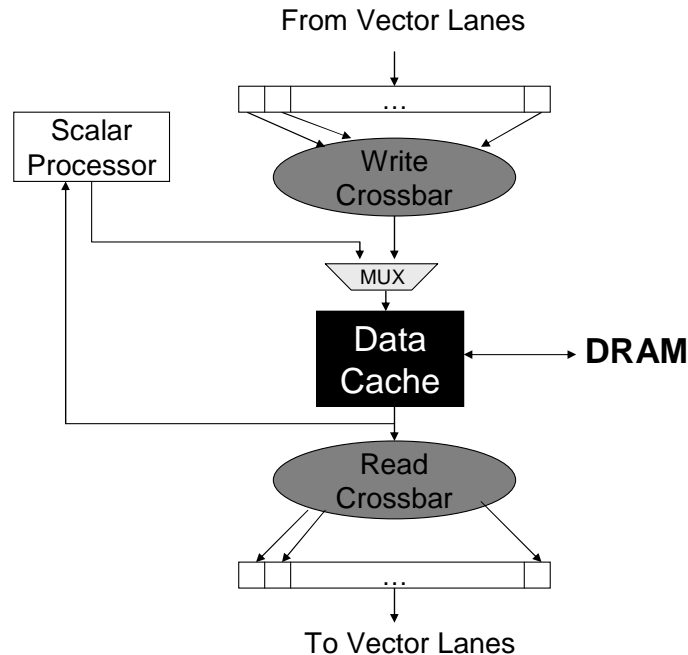


Figure 5.3: The VESPA memory architecture shares the data cache between the scalar processor and vector coprocessor. The memory crossbar maps individual requests from the vector lanes to the appropriate byte(s) in the cache line.

manipulation instructions in the VIRAM instruction set, as listed in Table 5.1. Some instruction exclusions were necessary to better accommodate an FPGA implementation: for example, the VIRAM multiply-accumulate instructions (which require 3 reads and 1 write) were eliminated since they would require further register file replication, banking, or a faster register file clock speed to overcome the 2-port limitations on FPGA block RAMs. Floating-point instructions are not implemented since they are generally not used in embedded applications as seen in our benchmarks; also we do not support virtual memory since it is not implemented in SPREE. Unlike the scalar processor, the vector coprocessor does not support integer division and modulo instructions since they do not appear in our benchmarks in vectorized form. Finally there is no support for exceptions—no vector instruction causes an exception and all vector state must either be saved or remain unmodified during exception processing.

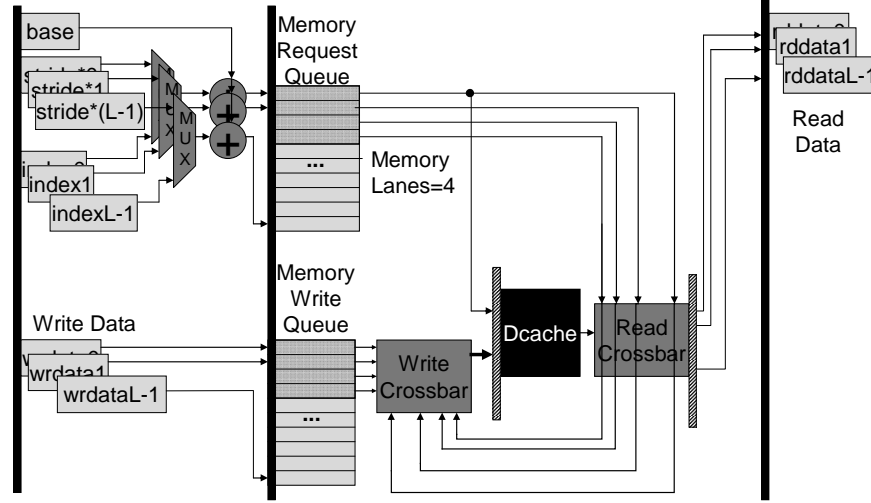


Figure 5.4: The VESPA memory unit buffers all memory requests from each lane and satisfies up to  $M$  requests a time from a single cache access. In this example  $M=4$ . The black bars shows pipeline stages, the grey bars show cycle delays which require pipeline stalls.

### 5.3.3 Vector Memory Architecture

Figure 5.3 shows the VESPA memory architecture. Each vector lane can request its own memory address but only one cache line can be accessed at a time which is determined by the requesting lane with the lowest lane identification number. For example, lane 1 will request its address from the cache then each byte in the accessed cache line can be simultaneously routed to any lane through the *memory crossbar*. Thus, the spatial locality of lane requests is key for fast memory performance since it reduces the number of cache accesses required to satisfy all lanes. The original VIRAM processor [34] had a memory crossbar for connecting the lanes to different banks of the on-chip memory. We use the same concept for connecting the lanes to different words in a cache line. There is one such crossbar for reads and another for writes; we treat both as one and refer to the pair as the memory crossbar (with the bidirectionality assumed). This crossbar is the least scalable structure in the vector processor design but should be configured to sustain the performance of the memory system it is connected to.

Figure 5.4 shows the vector memory unit in more detail. The black bars indicate pipeline stages while the grey bars show registers which require pipeline stalls. In the first stage the addresses being accessed by each lane is computed and loaded into the

Memory Request Queue. The memory unit will then attempt to satisfy up to  $M$  of these lane requests at a time from a single cache access. When all  $M$  requests have been satisfied the Memory Request Queue shifts all its contents up by  $M$ . If the instruction is a vector store, the Memory Write Queue duplicates this behaviour. When the Memory Request Queue is empty the vector memory unit de-asserts its stall signal and is ready to accept a new memory operation.

Many options exist for connecting the vector coprocessor to memory, including though a cache shared with the scalar processor, a separate cache, or no cache. The original VI-RAM processor used the last approach and was connected directly to its on-chip memory without a cache. However for off-chip memories caches are more likely required to hide the memory latencies. While this may not be true for heavily streaming benchmarks, in some cases the cache may be so important that the vector coprocessor requires its own separate data cache to avoid competing for cache space with the scalar core. This range of different memory system configurations could be interesting to explore in the future, but for this work a shared data cache is used primarily to avoid memory consistency issues which complicate the design. The decision is further supported for the following reasons: (i) its low area cost as seen in Section 4.1.1 provides little motivation to avoid using a cache; (ii) it is certainly required for the scalar core which the vector coprocessor can “piggyback” on, especially since (iii) there is very little competition for cache space between the scalar and vector cores in our applications. This decision may need to be revisited for applications with significant interaction between the scalar and vector cores, but most of our benchmarks have only a small amount of supportive scalar operations.

The data cache blocks on any access, stalling execution until the transaction has been completed. The memory controller for the TM4 also blocks on any memory access, while the Altera DDR2 memory controller for the DE3 allows multiple outstanding requests. VESPA was not improved to take advantage of this feature since the memory bus used in commercial soft processors does not support it. In the future more scalable vector architectures could take advantage of non-blocking memory systems.

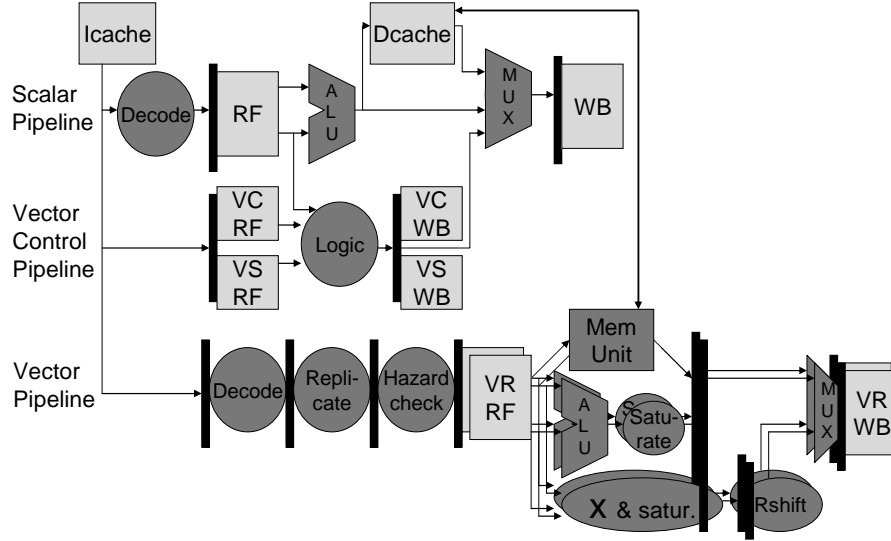


Figure 5.5: The VESPA architecture with 2 lanes. The black vertical bars indicate pipeline stages, the darker blocks indicate logic, and the light boxes indicate storage elements for the caches as well as the scalar, vector control (vc), vector scalar (vs), and vector (vr) register files.

### 5.3.4 VESPA Pipelines

Figure 5.5 shows the VESPA pipelines with each stage separated by black vertical bars. The topmost pipeline is the 3-stage scalar MIPS processor discussed earlier. The middle pipeline is a simple 3-stage pipeline for accessing vector control registers and communicating between the scalar processor and vector coprocessor. The instructions listed in the last row of Table 5.1 are executed in this pipeline while the rest of the vector instructions are executed in the longer 7-stage pipeline at the bottom of Figure 5.5. Vector instructions are first decoded and proceed to the *replicate* pipeline stage which divides the elements of work requested by the vector instruction into smaller groups that are mapped onto the available lanes; in the figure only two lanes are shown. The *hazard check* stage observes hazards for the vector and flag register files and stalls if necessary (note the flag register file and processing units are not shown in the figure). Since there are two lanes, the pipeline reads out two adjacent elements for each operand, referred to as an element group, and sends them to the appropriate functional unit. Execution occurs in the next two stages (or three stages for multiply instructions) after which results are written back to the register file. The added stage for multiplication is due to

Table 5.2: Configurable parameters for VESPA.

	Parameter	Symbol	Value Range
Compute	Vector Lanes	L	1,2,4,8,16,...
	Memory Crossbar Lanes	M	1,2,4,8,... L
	Multiplier Lanes	X	1,2,4,8,... L
	Register File Banks	B	1,2,4,...
	ALU per Bank	APB	true/false
ISA	Maximum Vector Length	MVL	2,4,8,16,...
	Vector Lane Bit-Width	W	1,2,3,4,..., 32
	Each Vector Instruction	-	on/off
Memory	ICache Depth (KB)	ID	4,8,...
	ICache Line Size (B)	IW	16,32,64,...
	DCache Depth (KB)	DD	4,8,...
	DCache Line Size (B)	DW	16,32,64,...
	DCache Miss Prefetch	DPK	1,2,3,...
	Vector Miss Prefetch	DPV	1,2,3,...

the fixed-point support which performs a right shift after multiplication. The multiplier and barrel shifter necessary to do so require an extra stage of processing compared to the ALU.

## 5.4 Meeting the Design Goals

Recall that the design goals for VESPA were for it to be scalable, flexible, and portable. The scalability of VESPA is explored in the next chapter, while its flexibility and portability are discussed in this section beginning with the former.

### 5.4.1 VESPA Flexibility

VESPA is a highly parameterized design enabling a large design space of possible vector processor configurations as seen in Chapter 7. These parameters can modify the VESPA compute architecture (pipeline and functional units), instruction set architecture, and memory system. All parameters are built-in to the Verilog design so a user need only modify the parameter value and have the correct configuration synthesized with no additional source modifications. Each of these parameters are explored in detail in subsequent chapters, but we concisely describe them below.

Table 5.2 lists all the configurable parameters and their acceptable value ranges—

many integer parameters are limited to powers of two to reduce hardware complexity. The number of vector lanes ( $L$ ) determines the number of elements that can be processed in parallel; this parameter is the most powerful means of scaling the processing power of VESPA. The width of each vector lane ( $W$ ) can be adjusted to match the maximum element size required by the application: by default all lanes are 32-bits wide, but for some applications 16-bit or even 1-bit wide elements are sufficient. The maximum vector length ( $MVL$ ) determines the capacity of the vector register file; hence larger  $MVL$  values allow software to specify greater parallelism in fewer vector instructions, but increases the register file capacity required in the vector processor.

The number of memory crossbar lanes ( $M$ ) determines the number of lane memory requests that can be satisfied concurrently, where  $1 < M < L$ . For example, if  $M$  is half of  $L$ , then in Figure 5.3, this means the crossbar connects to half the lanes in one cycle, and the other half in the next cycle.  $M$  is independent of  $L$  for two reasons: (i) a crossbar imposes heavy limitations on the scalability of the design, especially in FPGAs where the multiplexing used to build the crossbar is comparatively more expensive than for conventional IC design; and (ii) the cache line size limits the number of lane memory requests that can be satisfied concurrently. Thus we may not need a *full memory crossbar* which routes to all  $L$  lanes, rather the parameter  $M$  allows the designer to choose a subset of lanes to route to in a single cycle. This trade-off is explored in Chapter 7, Section 7.1.3.

The user can similarly conserve multiply-accumulate blocks by choosing a subset of lanes to support multiplication using the  $X$  parameter. The  $B$  and  $APB$  parameters control the amount of vector chaining VESPA can perform as seen in Chapter 7, Section 7.2. Also each vector instruction can be individually disabled thereby eliminating the control logic and datapath support for it as seen in Chapter 7, Section 7.4.

The memory system includes an instruction cache, a data cache, and a data prefetcher. The instruction cache is direct-mapped with depth  $ID$  and cache line size  $IW$ . Similarly, the data cache is direct-mapped with depth  $DD$  and cache line size  $DW$ . The prefetcher can be configured with a variety of prefetching schemes which respond to any data access

using DP or exclusively to vector memory operations using DPV. All these memory system parameters are explored in Chapter 6.

As seen in Chapter 7, the parameters in Table 5.2 provide a large design space for selecting a custom configuration which best matches the needs of an application. Since soft processors are readily customizable, we require only software for automatically selecting a configuration for an application. The development of this software is beyond the scope of this thesis and is hence left as future work.

### 5.4.2 VESPA Portability

The portability of soft vector processors is a major factor in whether FPGA vendors will adopt them in the future. Since FPGA vendors have many different FPGA devices and families, a non-portable hardware IP core would require more design effort to support across all these devices. The discussion below describes our attempts to minimize the porting effort.

VESPA is fully implemented in synthesizable Verilog but was purposefully designed to have no dependencies to a particular FPGA device or family. In fact we ported VESPA from the Stratix 1S80 on the TM4 to the Stratix III 3S340 on the DE3 and required zero source modifications. Although we do not port VESPA across different vendors or families, we instead explain that the FPGA structures needed to efficiently build a soft vector processor exist in most modern FPGA devices.

To maintain device portability in VESPA, the architected design makes very few device-specific assumptions. First, it assumes the presence of a full-width multiply operation which is supported in virtually all modern day FPGA devices and does not assume any built-in multiply-accumulate or fracturability support since the presence of these features can vary from device to device. Second, with respect to block RAMs, VESPA assumes no specific sizes or aspect ratios, nor any particular behaviour for read-during-write operations on either same or different ports. VESPA only uses one read port and one write port for any RAM hence limiting the need for bi-directional dual-port RAMs.

These few assumptions allow the VESPA architecture to port to a broad range of FPGA architectures without re-design. However, although VESPA was not aggressively designed for high clock frequency, any timing decisions made *are* specific to the Stratix III it was designed for, hence some device-specific retiming may be needed to achieve high clock rates on other devices.

## 5.5 FPGA Influences on VESPA Architecture

Our goal of improving soft processors to compete with hardware design is largely pursued by matching the architecture to the application. However, soft processors can also be improved by matching their architectures to the FPGA substrate. Conventional notions of processor architecture are based on CMOS design, but the tradeoffs on an FPGA substrate can lead to different architectural conclusions. Several previous works considered the influence of the FPGA substrate on the architecture of soft processors [26, 45, 49, 69]. These works often identify low-level circuit engineering differences but have not proposed high-level architectural differences between soft and hard processors. Doing so is complicated by two main factors: (i) designer effort and skill varies between academics, FPGA vendors, and microprocessor companies; and (ii) the level of performance required varies significantly between soft processors which are used largely as controllers and microprocessors which are used for general purpose computation. As a result, it is difficult to draw high-level conclusions about the architectures of soft processors since the performance attainable on such an architecture is highly dependent on skill, effort, and desired performance of the designer.

The VESPA architecture was influenced in a number of ways by the FPGA substrate. These influences are discussed in more detail throughout this thesis in sections devoted to the affected architectural component. We collect the key points and summarize them here. First, the multiply-accumulate blocks are obvious choices for efficiently implementing processor multipliers. This performance is still significantly less than an

FPGA adder circuit leading to accommodations in the pipeline similar to hard microprocessors. However, the multipliers are also efficient [45] for implementing shifters since multiplexers are relatively expensive on FPGAs. This shared multiplier/shifter functional unit means vector chaining on soft vector processors exhibits different behaviour than traditional vector processors since vector multiplies and vector shifts cannot be executed simultaneously. Second, the block RAMs provide relatively inexpensive storage helping to motivate the existence of caches even when they are not strongly motivated in our vectorized applications. The low area cost of storage also helps motivate vector processors since the large vector register files required can be efficiently implemented. Finally, the two ports on FPGA block RAMs also impose architectural differences from traditional processors. For 3-operand instruction sets such as MIPS, the register file must sustain 2 reads and 1 write per cycle. Since FPGA block RAMs have only two ports, a common solution is to leverage the low area cost of block RAMs to duplicate them as discussed in section 5.6. Additional ports are required to support multiple vector instruction execution. Chapter 7.2 describes how banking is performed to overcome the port limitations. This approach is reminiscent of vector processors before VLSI design, and marks a key architectural difference between VESPA and modern vector processors such as the T0 [7] and VIRAM [34]. In general, the lack of ports and expensive multiplexing logic make FPGAs less amenable to any architecture with multiple instructions in flight such as traditional superscalar out-of-order architectures, though it may be possible for clever circuit engineering by a skilled designer to make such architectures prevalent in soft processors.

## 5.6 Selecting a Maximum Vector Length (MVL)

Before further evaluating VESPA we must determine an appropriate maximum vector length (MVL). This parameter abstracts the number of hardware vector lanes from the software vector length and hence affects both the hardware implementation of a vector

processor and the software implementation of vectorized code. It represents a contract between the processor and programmer to support at the very least storage space for  $MVL$ -number of elements, thereby allowing the programmer to use vector lengths up to this length while leaving the processor free to implement between 1 and  $MVL$  vector lanes. Note that all of our vectorized benchmarks are designed to use vectors with the full  $MVL$  length and require no modification for changes to  $MVL$  or any other parameter.

Increasing the  $MVL$  allows a single vector instruction to encapsulate more element operations, but also increases the vector register file size and hence the total number of FPGA block RAMs required. This growth is potentially exacerbated by the fact that the entire vector register file is replicated to achieve the three ports necessary (2-read and 1-write), since current FPGAs have only dual-ported block RAMs. The performance impact of varying the  $MVL$  results in an interesting tradeoff: higher  $MVL$  values result in fewer loop iterations, in turn saving on loop overheads—but this savings comes with more time-consuming vector reduction operations. For example, as  $MVL$  grows, the  $\log_2(MVL)$  loop iterations required to perform a tree reduction that adds all the elements in a vector grows with it. We examine the resulting impact on both area and performance below on the TM4 platform; the results are analogous for the DE3.

The area impact of increasing  $MVL$  increases some control logic due to the increased sizes of register tags and element indices, but primarily affects the vector register file and hence its FPGA block RAM usage. Because of the discrete sizes and aspect ratios of those block RAMs, these results are specific to the FPGA device chosen. Given block RAMs with maximum width  $W_{BRAM}$  bits and total capacity (or depth) of  $D_{BRAM}$  bits, and using the parameters from Table 5.2, the number of block RAMs will be the greater of Equations 5.1 and 5.2.

$$N_{BRAMs} = \lceil L \cdot W \cdot B / W_{BRAM} \rceil \quad (5.1)$$

$$N_{BRAMs} = \lceil 32MVL \cdot W / D_{BRAM} \rceil \quad (5.2)$$

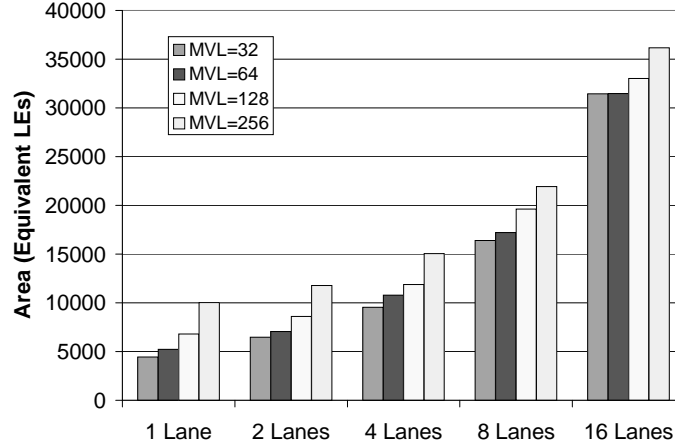


Figure 5.6: Area of the vector coprocessor across different MVL and lane configurations.

For example, the Stratix I M4K block RAM has  $D_{BRAM}=4096$  bits and can output a maximum of  $W_{BRAM}=32$ -bits in a single cycle, hence a 16-lane vector processor with 1 bank requires 16 of these M4Ks to output the 32-bit elements for each lane using Equation 5.1. This results in 64Kbits being consumed which exactly matches the demand of the  $MVL=64$  case according to Equation 5.2. But when  $MVL=32$  the block RAMs are only half-utilized resulting only in wasted area instead of area savings. The Stratix III has block RAMs which are twice as big, so this phenomenon would be observed between  $MVL$  values of 64 and 128 for the 16-lane VESPA.

Figure 5.6 shows the area of the vector processor for different values of  $MVL$  and for a varying number of lanes. The graph shows that increasing the  $MVL$  causes significant growth when the number of lanes are few, but as the lanes grow and the functional units dominate the vector coprocessor area, the growth in the register file becomes less significant as seen in the 16 lane vector processor. Of particular interest is the identical area between the 16 lane processors with  $MVL$  equal to 32 and 64. This is an artifact of the discrete sizes and aspect ratios of FPGA block RAMs as previously described. At 16 lanes the vector processor demands such a wide register file that Equation 5.1 dominates. As a result, the storage space for vector elements is distributed among these block RAMs causing, in the  $MVL=32$  case, only half of each block RAM's capacity to be used. We avoid this under-utilization by setting  $MVL$  to 64 and doubling it to 128 for 32 lanes. For

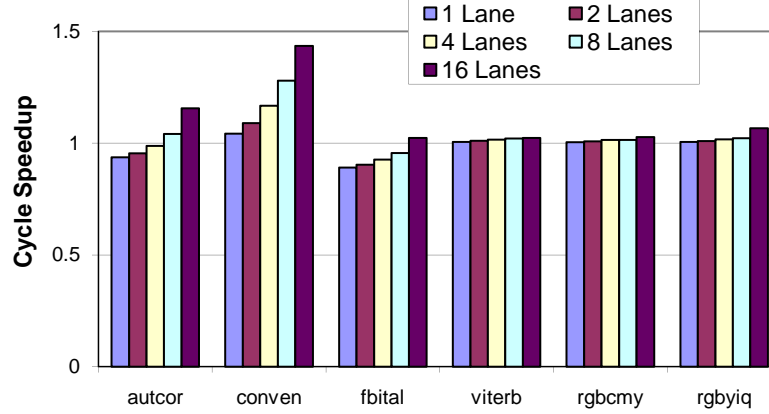


Figure 5.7: Cycle speedup measured when MVL is increased from 32 to 256.

Stratix III which has block RAMs twice as deep, we also double the MVL. Note that in our area measurements we count the entire silicon space of the block RAM used regardless of the number of memory bits actually used. By doing so we accurately reflect the incentive to fully utilize consumed FPGA resources.

Figure 5.7 shows the performance of a set of vector processors with varying numbers of lanes and MVL=256, each normalized to an identically-configured vector processor with MVL=32. The benchmarks AUTCOR and FBITAL both have vector reduction operations and hence show a decrease in performance caused by the extra cycles required to perform these reductions. The performance degradation is more pronounced for low numbers of lanes as the number of lanes increase the reduction operations themselves execute more quickly, until finally the amortization of looping overheads dominates and results in an overall benchmark speedup for 16 lanes. The remaining benchmarks do not contain significant reduction operations and hence experience faster execution times for the longer vectors when MVL=256. For CONVEN, which performs vector operations based on some scalar processing, increasing the MVL has a dramatic affect on performance as both the loop overhead and this scalar processing is amortized. The speedup reaches up to 43% for 16 lanes. The remaining benchmarks have larger loop bodies which already amortize the loop overhead and hence have only very minor speedups.

## 5.7 Summary

This chapter described the VESPA soft vector processor which was built to evaluate the concept of vector processors for FPGAs using off-chip memory systems on real FPGAs and executing industry-standard embedded benchmarks. VESPA is a complete hardware design of a scalar MIPS processor and a VIRAM vector coprocessor written in Verilog. Only a portion of the VIRAM vector instruction set is supported by VESPA which is described in this chapter. VESPA has many parameterized architectural parameters briefly summarized here but more thoroughly explored in later chapters. The MVL is one such parameter explored in this chapter.

## Chapter 6

# Scalability of the VESPA Soft Vector Processor

The key goal of this work is to achieve performance significantly beyond current soft processors to make it easier to leverage the computational power of FPGAs without complicated hardware design. The scalability of a vector processor is potentially a powerful method of doing so. In this chapter we evaluate whether this scalability holds true on FPGAs and improve it by exploring the area and performance of several architectural modifications.

### 6.1 Initial Scalability (L)

To highlight and quantify the importance of the architectural modifications subsequently proposed in this research, we first measure the scalability of a base initial design which lacks these features. Specifically, the initial VESPA design is identical to that described in Chapter 5 but supported only parameterization of the number of lanes and the MVL value (which is set to 64 for this scalability study). Its memory system was hard-coded with two 4KB direct-mapped instruction and data caches each with 16B lines sizes. This section evaluates the scalability of this design and presents those findings as measured across the EEMBC benchmarks executed on the TM4 hardware platform. Note that the

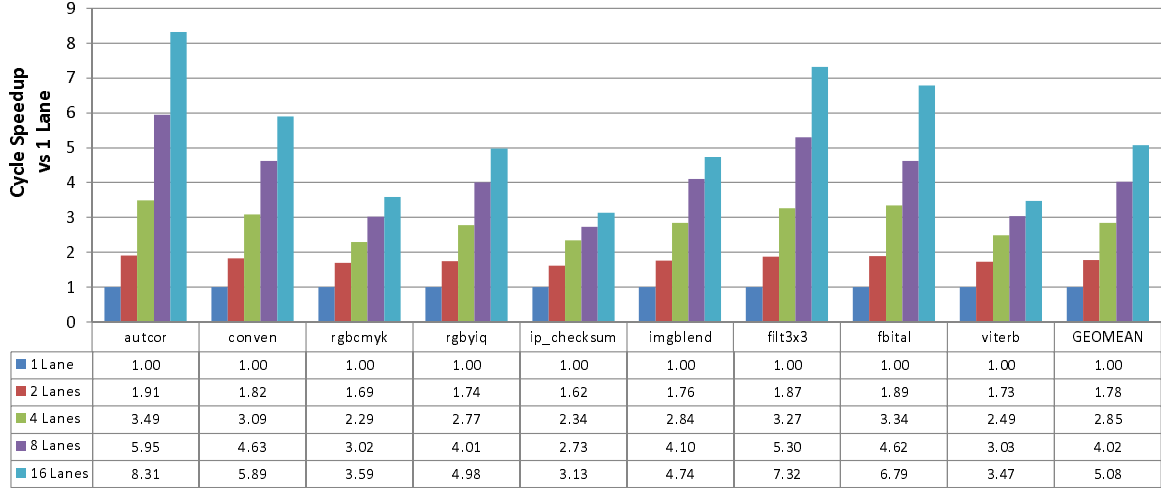


Figure 6.1: Cycle performance of increasing the number of lanes on the initial VESPA design with 4KB data cache size and 16B cache line size.

TM4 is used only in this chapter because the improved VESPA which was ported to the DE3 cannot be easily reverted to this initial design.

Figure 6.1 shows the cycle speedup (the speedup achieved when measuring only clock cycles) attained by increasing the number of vector lanes. Speedup is measured relative to the single-lane VESPA configuration executing the identical benchmark binary—we do not compare against the non-vectorized benchmark here. Chapter 8 explores the performance between VESPA and a scalar soft processor executing non-vectorized code. The figure shows speedups ranging inclusively across all benchmarks from 1.6x to 8.3x. On average the benchmarks experience a 1.8x speedup for 2 lanes, with a steady increase to 5.1x for 16 lanes. We are unable to scale past 16 lanes because of the number of multiply-accumulate blocks on the Stratix 1S80 on the TM4 (we later port the improved VESPA design to the DE3 to overcome this limitation). The observed scaling may be adequate, but for most of the benchmarks the performance gains appear linear despite the exponential growth in lanes.

Since scalability is such an important aspect of a soft vector processor, we are motivated to pursue architectural improvements which enable greater performance scaling than seen in Figure 6.1. The following section analyzes the scaling bottlenecks in the system.

### 6.1.1 Analyzing the Initial Design

Assuming a fully data parallel workload with a constant stream of vector instructions (which closely represents many of our benchmarks), poor scaling can be caused by either inefficiencies in the vector pipeline or the memory system. Since VESPA executes vector ALU operations without any wasted cycles it is therefore the vector memory instructions inhibiting the performance scaling. The vector memory unit stalls one cycle upon receiving any memory request and then stalls for each necessary cache access. In addition cache misses result in cycle stalls for the duration of the memory access latency. In this section we evaluate whether the memory system is indeed throttling the scalability in VESPA.

The impact of the memory system is measured using cycle-accurate RTL simulation of the complete VESPA system including the DDR memory controller for four of the benchmarks<sup>1</sup> using the Modelsim simulation infrastructure described in Chapter 3. Hardware counters were inserted into the design to count the number of cycles the vector memory unit is stalled, as well as the number of cycles it is stalled due specifically to a cache miss.

Our measurements demonstrate that this initial VESPA design with 16 lanes, 16B data cache line size and 4KB depth spends approximately 67% of all cycles stalling in the vector memory unit, and 45% of all cycles servicing data misses. This cache line size was selected for the initial configuration because it matches the 128-bit width of the DRAM interface—cache lines smaller than 16B would waste memory bandwidth. The 4KB depth is then selected to fully utilize the capacity of the block RAMs used to create the 16B line size. Depths less than 4KB (for the Stratix I) would waste FPGA RAM storage bits because of the discrete aspect ratios of the block RAMs. The large number of cycles spent in the vector memory unit, and specifically the misses, suggests that the memory system is significantly throttling VESPA’s performance.

---

<sup>1</sup>The other benchmarks are not included because their data sets are too large for simulation

## 6.2 Improving the Memory System

Standard solutions for improving memory system performance include optimizing the cache configuration and the implementation of an accurate data prefetching strategy. We pursue these same solutions within VESPA but with an appreciation for the application-dependence of these solutions since in a soft processor context, an FPGA designer can select a cache and prefetcher to match their specific application. The data cache is hence parameterized along its depth (or capacity) and its line size, while a data prefetcher is implemented with parameterized prefetching strategies.

### 6.2.1 Cache Design Trade-Offs (DD and DW)

The most obvious approach to increasing memory system performance is to alter the cache configuration to better hide the memory latency. In this section we parameterize and explore the speed/area trade-offs for different data cache configurations for direct-mapped caches. Set-associative caches require multiplexing between the entries in a set, which is expensive especially in an FPGA and hence deters us from including this option in our initial exploration. Also, banking the cache was not explored since all of our benchmarks use mostly contiguous memory accesses. We vary data cache depth from 4KB to 64KB and the cache line size from 16B to 128B. Note, our system experiences some timing problems caused by the large size of the memory crossbar on the TM4 for a cache line size of 128B which limits the measurements we can make for that configuration and cache lines greater than 128B.

Some conclusions from this study can be hypothesized with further examination of the benchmarks. Many of our vectorized benchmarks are streaming in nature with little data re-use. For such benchmarks we anticipate that cache depth will not impact performance significantly while widening the cache line and hence increasing the likelihood of finding needed data in a single cache access may considerably improve performance. In addition, the longer cache lines provide some inherent prefetching by caching larger blocks of

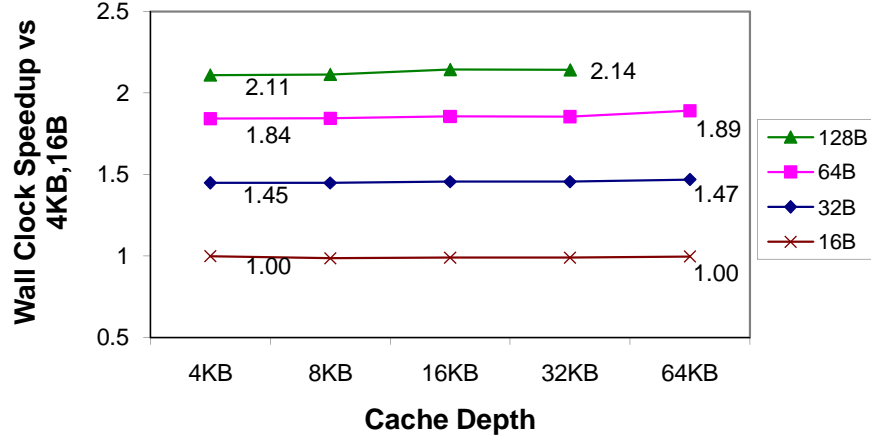


Figure 6.2: Average wall clock speedup (excluding VITERB benchmark) attained for a 16-lane VESPA with different cache depths and cache line sizes, relative to the 4KB cache with 16B line size. Each line in the graph depicts a different cache line size.

contiguous memory on a miss.

Figure 6.2 shows the average wall clock speedup across all our benchmarks except VITERB for each data cache configuration normalized against the 4KB cache with a 16B cache line size. We first note that as predicted, the streaming nature of these benchmarks makes cache depth affect performance only slightly. For the 16B cache line configuration the performance is flat across a 16-fold increase in cache depth, while for the 128B cache line this 16-fold growth in depth increases performance from 2.11x to 2.14x. In terms of improving our baseline 4KB deep 16B line size default configuration for these benchmarks, the cache line size plays a far more influential role on performance. Each doubling of line size provides a significant leap in performance reaching up to 128B with an average of more than double the performance of the 16B line size.

Figure 6.3 shows the wall clock speedup for just the VITERB benchmark across the same cache configurations. The VITERB benchmark is significantly different than the other benchmarks: it passes through multiple phases which have varying amounts of data parallelism and in some cases none at all. Because of this, cache conflicts appear to be an issue. The figure shows that once the cache depth reaches 16KB the performance plateaus for all cache line configurations and results similar to the rest of the benchmarks are observed where only increases to cache line provide significant performance boosts. For

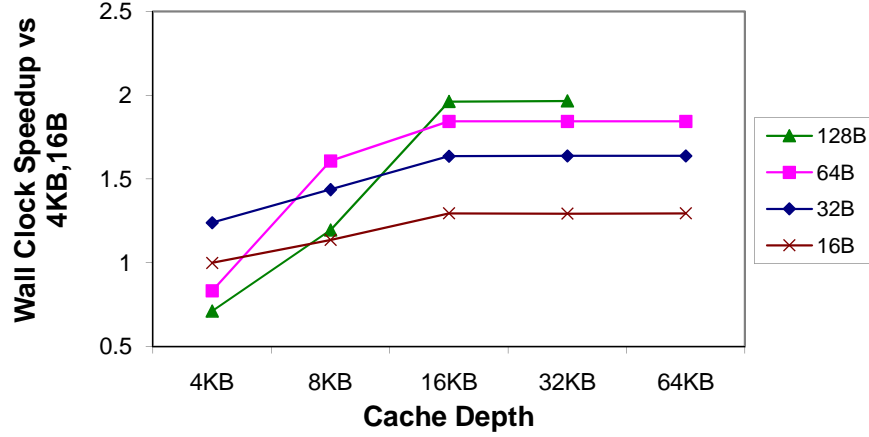


Figure 6.3: Wall clock speedup of VITERB benchmark attained for a 16-lane VESPA with different cache depths and cache line sizes, relative to the 4KB cache with 16B line size. Each line in the graph depicts a different cache line size.

Table 6.1: Clock frequency of different cache line sizes for a 16-lane VESPA.

Cache Line Size (B)	Clock Frequency (MHz)
16B	128 MHz
32B	127 MHz
64B	123 MHz
128B	122 MHz

4KB cache depths, increasing the cache line size past 32B actually decreases performance. For an 8KB cache the same phenomenon occurs at 64B instead. In both cases the cause is increased conflicts since with constant depth, a wider cache line size creates fewer cache sets. Unlike the other benchmarks, VITERB has significant data re-use and capturing that working set in a 16KB cache is imperative before applying further memory system improvements.

In contrast with the scalar soft processors shown in Chapter 4, the increase in computational power via multiple lanes in the vector processor makes the memory system more influential in determining overall performance. Chapter 4 demonstrated that the impact of the memory system is limited to 12% additional performance for the scalar soft processor, whereas in both Figure 6.2 and Figure 6.3 performance is more than doubled.

Table 6.1 shows that the clock frequency is slightly reduced as the cache line size increases. This clock frequency degradation is due to the multiplexing needed to get data

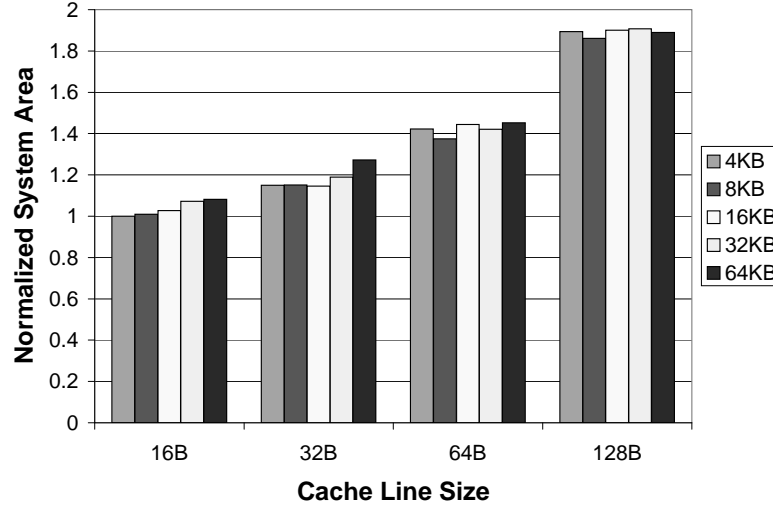


Figure 6.4: System area of different cache configurations on a 16-lane VESPA normalized against the 4KB cache with 16B line size. Each coloured bar in the graph depicts a different cache depth.

words out of the large cache lines and into the vector lanes via the memory crossbar. In other words, by doubling the cache line size, the memory crossbar is also doubled in size and is responsible for the frequency degradation. Further logic design effort through pipelining and retiming can mitigate these effects, resulting in slightly more pronounced benefits for the longer cache lines.

Figure 6.4 shows the silicon area of the VESPA system normalized against that of the 4KB cache with 16B line size. The area cost can be quite significant, in the worst case almost doubling the system area. However, the area trends are quite different than what one would expect with traditional hard processors. We discuss the effect on area of cache depth and cache line size below.

Increases in cache depth have a minimal effect on area and in many cases are hidden by the noise in the synthesis algorithms: for example, the 4KB cache with 64B line size is larger than its 8KB counterpart. This is a synthesis anomaly since the number of block RAMs and multiply-accumulate blocks is the same for both designs, yet the 4KB configuration consumes 900 additional LEs. In fact all caches with a 64B line size have the same number of block RAMs except for the 64KB depth configuration, in which case the added block RAMs for cache depth does not contribute significantly more area than

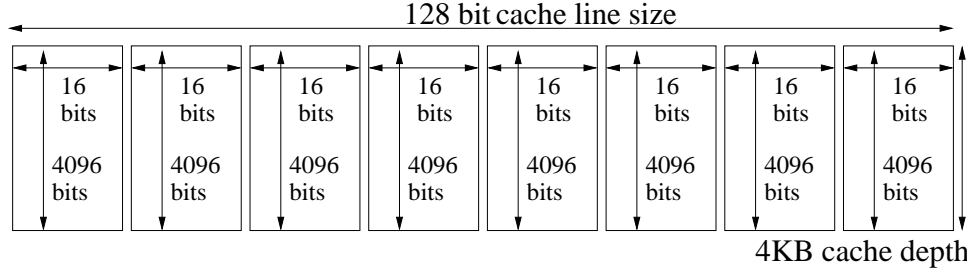


Figure 6.5: Multiple block RAMs are needed to create the width necessary for 16B cache lines, and the cache depth should be 4KB to fully-utilize the capacity of those block RAMs.

the rest of the 64B configurations. Such results are expected for an FPGA since cache depth only affects the block-RAM storage required, which is more efficiently implemented relative to programmable logic.

Increasing the cache line size can also increase the number of block RAMs consumed. Certainly the largest contributor to the increased area with cache line size is the multiplexers in the vector memory crossbar which routes each byte to each vector lane; however it is also due to the increase in FPGA block RAMs being used, a phenomenon unique to FPGAs. In their current configuration, the block RAMs are limited to a maximum of 16-bit wide data ports: to create a cache with 16B (128-bit) line sizes we require at least 8 such FPGA block RAMs in parallel, as shown in Figure 6.5, hence consuming all 8 of those block RAMs and their associated silicon area. Any increases in cache line sizes will result in corresponding increases in the number of used block RAMs and with it an automatic increase of physical storage bits used (whether they are logically used by the design or not). Therefore we generally choose the depth to fill the capacity of the fewest number of block RAMs required to satisfy the line size.

In terms of supporting VESPA configurations with many lanes, such as the 16-lane configuration used throughout this section, we believe the 40% additional area is worth the performance increase of a data cache with 64 byte line size and 16KB depth to fill the used block RAMs. The two factors that contribute to these performance improvements are: (i) wider cache lines require fewer cache accesses to satisfy memory requests from all the lanes; and (ii) wider cache lines bring larger blocks of neighbouring data into

the cache on a miss providing effective prefetching for our streaming benchmarks which access data sequentially. Of course, the latter benefit can be achieved through hardware prefetching which comes without significant area cost.

### 6.2.2 Impact of Data Prefetching (DPK and DPV)

Due to the predictable memory access patterns in our benchmarks, we can automatically prefetch data needed by the application before the data is requested. We hence augment VESPA by supporting hardware data prefetching where a cache miss translates into a request for the missing cache line as well as additional cache lines that are predicted to soon be accessed. This section describes the data prefetcher in VESPA as well as evaluates its effect across our benchmarks.

#### 6.2.2.1 Prefetching Background

Data prefetching is a topic thoroughly studied in the computer architecture community [63]. The simplest scheme, known as *sequential prefetching*, fetches the missed cache line as well as the next  $K$  cache lines in memory. All our prefetching schemes are based on sequential prefetching since this maps well to our many streaming benchmarks.

Fu and Patel had investigated prefetching particularly in the context of a vector processor [22]. They limited prefetching to vector memory instructions with strides less than or equal to cache line size and found that prefetching is generally useful for up to 32 cache blocks. But in an FPGA context we can appreciate the application-dependent nature of prefetching since the FPGA-system can be reconfigured with a custom prefetcher configuration. We further experiment with a *vector length* prefetch where the vector length is used to calculate the number of cache lines to prefetch.

#### 6.2.2.2 Designing a Prefetcher

The data prefetcher is configured using the parameters DPK and DPV from Table 5.2. DPK is the number of consecutive cache lines prefetched on any cache miss—note that

prefetching is triggered for both scalar and vector instructions since both share the same data cache and its prefetcher. To minimize cache pollution we introduce a copy of that parameter, DPV, to prefetch specifically for vector instructions having strides within two cache lines (as done by Fu and Patel [22]) which can be prefetched more aggressively since they are known to access the cache sequentially. We refer to these misses as *sequential vector misses*.

A key advantage of the data prefetcher is that it leverages the high bandwidth from burst mode transfers; after an initial miss penalty, all cache lines including the prefetched lines are streamed into the cache at the full DDR rate. This bandwidth is vital for VESPA which processes batches of memory requests for each vector memory instruction. Complications arise from handling such large memory transfers when the evicted cache lines are dirty. To ensure that these dirty lines are properly written-back to memory we must either drop the prefetched line, or else buffer the dirty cache lines and write them back to memory later; this write back buffer approach is used in VESPA, and prefetching is halted when the 2KB buffer is full. For simplicity, we also halted prefetching at the end of the DRAM row that the miss initially accessed.

The prefetcher is currently limited to working only with cache lines greater than or equal to 64B. With smaller cache lines the prefetcher has fewer cycles between the loading of successive cache lines to probe the cache entries and decide whether to allow the prefetch or not. For example if a cache entry is dirty and a prefetch request seeks to replace it with a stale copy of its data from memory, that prefetch must be blocked. As a result we use only 64B cache lines and 16KB depth to fully-utilize the block RAM capacity. As mentioned previously, cache line sizes of 128B and larger are unstable in our design so we are confined to evaluating prefetching on only the 64B line size.

### 6.2.2.3 Cache Line Size and Prefetching

As discussed in Section 6.2.1, in general we expect wider cache lines to perform some inherent prefetching and hence reduce the impact of our hardware prefetcher. Conversely,

hardware prefetching can have more impact on narrower cache lines. Hence, one can reduce area by shrinking the cache line size (and with it the large memory crossbar) while using hardware prefetching to explicitly perform the inherent data prefetching of longer cache lines. However, the long cache lines are typically required to capture more of the spatial locality that is used to satisfy multiple lane requests. Without it more cache accesses (and hence cycles) are required to satisfy the lane requests.

#### 6.2.2.4 Evaluating Prefetching

This section explores the impact of the different data prefetching configurations. The aggressiveness of the prefetcher is increased by doubling the number of cache lines it loads and is varied using both the DPK and DPV parameters from 0 (no prefetching) to 63 (enough prefetching to fill one quarter of the data cache). As discussed earlier, our sequential prefetcher can be activated by either (i) *any* cache miss or (ii) only sequentially-accessing vector memory instructions; however, our benchmarks generally use very few scalar loads and stores, and generally have vector strides of less than a cache line, thus nearly all memory operations are initiated by sequential vector instructions. We therefore anticipate that both of these activation strategies will perform similarly.

Figure 6.6 shows the performance of prefetching on either any cache miss or sequential vector misses, both normalized against the performance without prefetching. Using the same base vector architecture of 16 lanes and full memory crossbar, we configure the data cache with 16KB depth and 64B line size and explore the impact of the different data prefetching configurations. The figure shows that, as expected, whether prefetching is performed on all cache misses or just on known sequential vector instructions, the performance is very similar—they essentially overlap in the graph. The speedup achieved is quite significant, almost reaching 30% average faster performance. As we increase the number of cache lines prefetched, and hence the aggressiveness of the prefetcher, we see diminishing returns on the performance gains until the cache pollution dominates, reducing the speedup at 63 cache line prefetches. Note that we found that the implementation

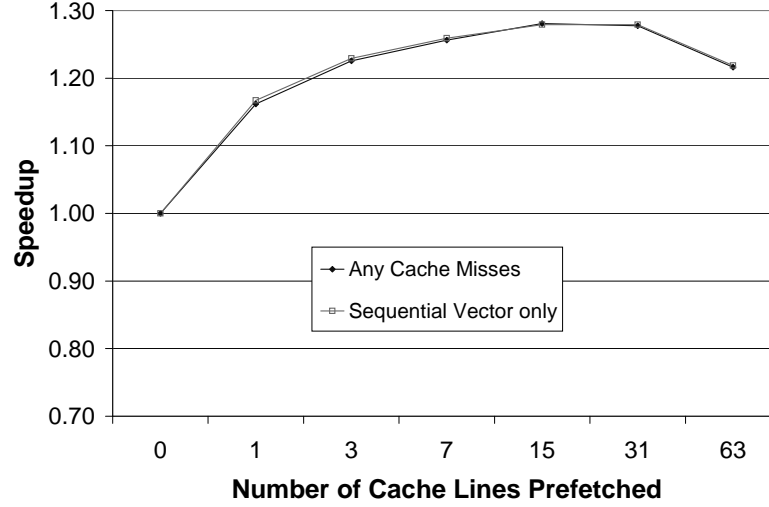


Figure 6.6: Average speedup, relative to no prefetching, of prefetching  $n$  cache lines using two strategies: (i) on *any data cache miss*; (ii) on any miss from a sequentially-accessing vector memory instruction (called *sequential vector miss*). While the number of prefetched cache lines can be any integer, we selected prefetches such that the total number of cache lines fetched including the missed cache line is a power of two.

of the prefetcher did not impact clock frequency.

Figure 6.7 shows the performance of each benchmark as the aggressiveness is increased for prefetches triggered by any cache miss. The graph shows that four of the benchmarks, AUTCOR, CONVEN, VITERB, and FBITAL do not benefit significantly from prefetching, while the other benchmarks achieve speedups as high as 2.2x. For large prefetches the performance tapers off and then begins a downward trend as cache pollution begins to dominate. In the case of CONVEN and FBITAL the performance becomes worse than with no prefetching. As long as the number of cache lines being prefetched is moderate, we can speed up benchmarks that benefit from prefetching without slowing down benchmarks that do not. On average we observe a peak 30% performance improvement when prefetching 31 cache lines. Of course the benefit of using a soft vector processor is that one can tune the amount of prefetching for each application. For example, 15 is often the best number of cache lines to prefetch on average, but for IMGBLEND prefetching 15 cache lines performs worse than many other configurations.

With respect to area, the cost of prefetching is relatively small requiring mostly control logic for tracking and issuing multiple successive memory requests. But additional area

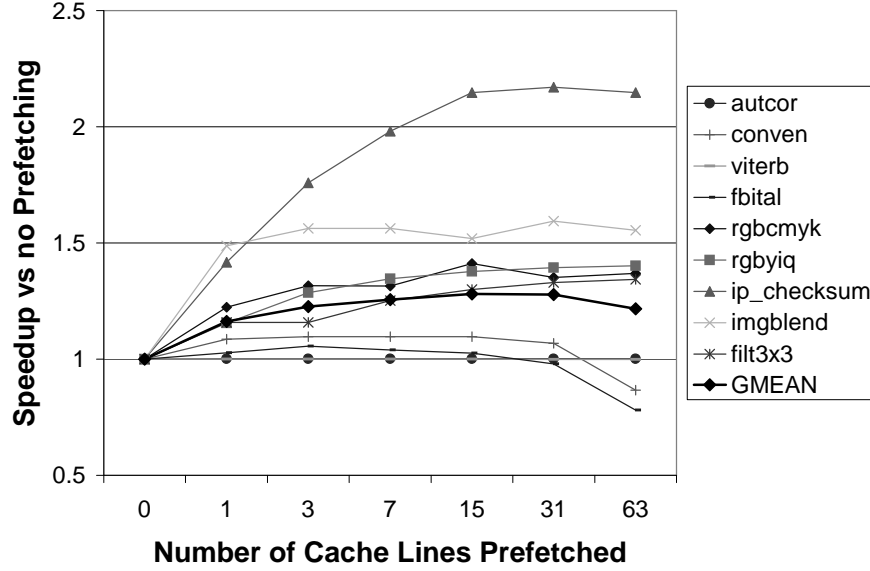


Figure 6.7: Speedup when prefetching a constant number of consecutive cache lines on any data cache miss, relative to no-prefetching.

is required by the writeback buffer which stores the evicted dirty cache lines. In general the buffer needs to have the greater of  $DPK+1$  or  $DPV+1$  entries for the case where all evicted lines are dirty. With prefetching disabled this cost is reduced to a single register, but otherwise is generally implemented in FPGA block RAMs where the effect of discrete aspect ratios as discussed in Figure 6.5 results in a constant 1.6% area cost if prefetching is between 1 and 15 cache lines. For more than 15 cache lines this area cost doubles, but there is little additional performance gain seen in our benchmarks to justify the added area cost.

#### 6.2.2.5 Vector Length Prefetching

Choosing a good value for the amount of prefetching,  $DPK$ , depends on the mix of vector lengths used in the program. Recall each vector memory instruction instance explicitly specifies its vector length providing a valuable hint for the number of cache lines to prefetch. In this section our goal is to make use of this hint to achieve a high quality prefetch configuration without requiring a brute force exploration. We therefore recast  $DPK$  as  $DPV$  which is a multiplier of the current vector length. Note that the actual vector

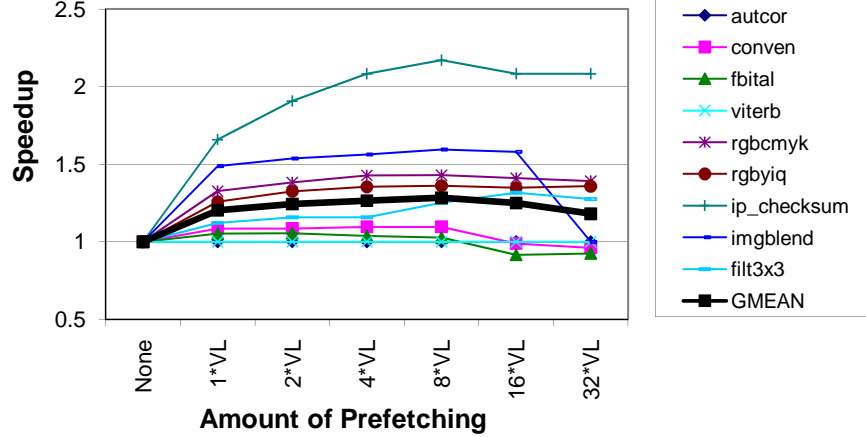


Figure 6.8: Wall clock speedup achieved for different configurations of the vector length prefetcher.

length used is the *remaining vector length*, which is the portion of the vector length not yet processed after the miss which triggers the prefetch. For example, if the first eight elements of a vector load were cache hits and a miss occurred on the ninth element of a 64 element vector, the prefetcher would use 55 as the vector length.

Figure 6.8 shows the performance of a range of vector length prefetchers. Prefetching 8 times the vector length ( $8VL$ ) cache lines performs best achieving a maximum speedup of 2.2x for IP\_CHECKSUM and 28% on average. Of specific interest is the  $1VL$  configuration which prefetches the remaining elements in a vector miss and hence has zero cache pollution. This configuration has no speculation, it guarantees no more than one miss per vector memory instruction and is ideal for heavily mixed scalar/vector applications, but only achieves 20% speedup on average across our benchmarks. Greater performance can be achieved by incorporating the right amount of speculation in the prefetching. The figure shows that adding speculation gains performance, but too much can undo the performance gains as seen in IMGBLEND where large prefetches of the input stream conflicts in the cache with the output stream causing thrashing between the two streams.

The area cost of the vector length prefetcher is essentially the same as that of the constant number of cache lines prefetcher, but there is a slight additional area cost of 0.3% for computing the number of cache lines to prefetch. This computation includes a multiply operation making the area cost non-negligible.

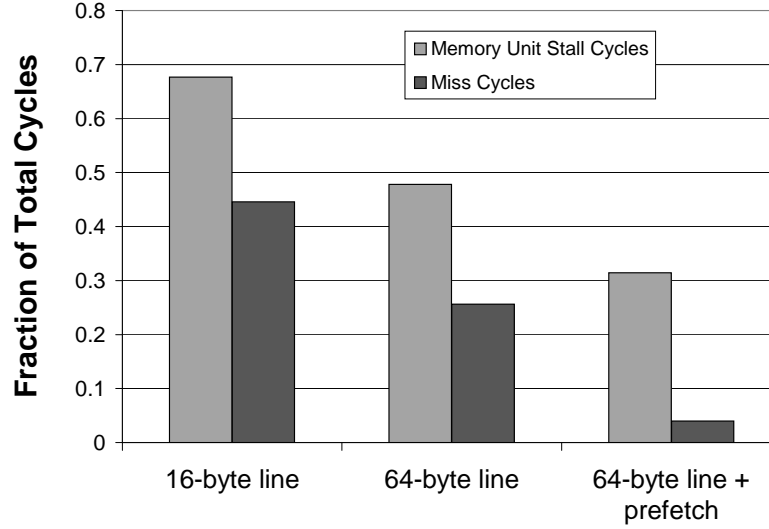


Figure 6.9: Average fraction of simulated cycles spent waiting in the vector memory unit or servicing a miss for a 16-lane full memory crossbar VESPA processor when cache lines are widened to 64B and prefetching is enabled for the next 15 cache lines.

The vector length prefetcher provides an important mechanism for capturing non-speculative prefetches with the 1VL configuration. A good soft vector processor should always perform this non-speculative prefetching but should also add some speculative prefetching. With regard to a speculative prefetching strategy, the vector length prefetcher does not quite reach the 30% performance gain from prefetching 15 cache lines using DPK but comes very close at 28%. While several other speculative strategies can be considered, the following section shows that prefetching 15 cache lines largely solves the problem of cache misses.

### 6.2.3 Reduced Memory Bottleneck

With the parameterized data cache and prefetcher, the memory bottleneck is drastically reduced. Recall that for the initial design the percentage of cycles spent in the vector memory unit was 67% and the percentage of all cycles spent servicing misses in the vector memory unit was 45%. This is shown in the first two bars of Figure 6.9. By increasing the cache line size, and correspondingly the depth to fill the block RAMs, these values are decreased to 47% and 25% respectively. With prefetching enabled for

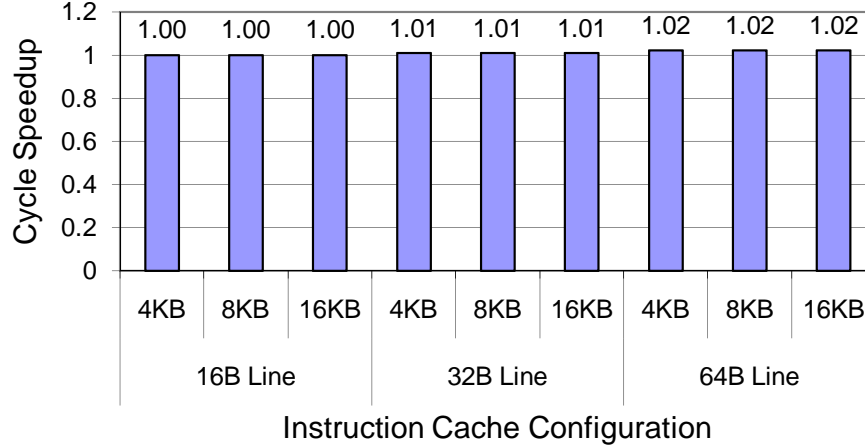


Figure 6.10: Average cycle performance across various icache configurations for a 16-lane VESPA with 64B dcache line, 16KB dcache capacity, and data prefetching of 7 successive cache lines.

the next 15 64B cache lines the fraction of time spent waiting on misses is reduced to just 4%. Thus prefetching appears to have largely solved the problem of miss cycles in our benchmarks. The memory unit otherwise stalls to accommodate multiple cache accesses. Further improvements could be made in the future to improve cache-to-lane throughput by better integrating the cache into the pipeline and providing multiple cache ports.

#### 6.2.4 Impact of Instruction Cache (IW and ID)

The analysis of the initial design assumed a constant stream of vector instructions, however this stream can be potentially interrupted by instruction cache misses. Since each vector instruction communicates many cycles of computational work to be performed by the vector processor, we generally do not anticipate that instruction cache misses would be significant. In addition the loop-centric nature of our benchmarks would result in few instruction cache misses. Since the data cache was parameterized, doing the same to the instruction cache was trivial so in this section, we briefly explore the space of instruction cache configurations. Using the TM4 platform we verify that the instruction cache does not severely impact the execution of VESPA even for a 16-lane configuration which processes vector instructions very quickly.

Figure 6.10 shows the effect of varying the instruction cache line size and depth for

Listing 6.1: Vectorized IP\_CHECKSUM loop

```

LOOP:
  vld.u.h  vr0 , vbase0 , vinc1 # Vector
  vadd.u   vr1 , vr1 , vr0      # Vector
  ctc2     r2 , v1              # Vector Ctl
  vsatvl   # Vector Ctl
  sub      r2 , r2 , r14        # Scalar
  bgtz     r2 , LOOP            # Scalar

```

a 16-lane VESPA with a 16KB data cache with 64B lines and hardware prefetching of the 7 neighbouring cache lines. The results show at most 2% performance gain averaged across our benchmarks. This is somewhat expected since many of the benchmarks are streaming in nature and spend most of the execution time iterating in one or a few loops. The system area cost of the largest 16KB-64B configuration is 10% greater than the 4KB-16B configuration. Although this cost is much smaller than seen in the data cache (due to the memory crossbar which is not required for instructions), the performance improvement is too small to justify this area cost. All configurations in this thesis use the 4KB instruction cache with 16B line size.

### 6.3 Decoupling Vector and Control Pipelines

The assumption of a constant stream of *vector* instructions is also violated in practice by the presence of scalar code and vector control instructions. The scalar pipeline was decoupled from the vector coprocessor in the initial design meaning cycles spent processing scalar code can be done while the vector coprocessor is busy processing vector instructions. But the vector coprocessor must still stall for vector control instructions to complete. As more lanes are added to VESPA, less time is spent processing vector instructions causing these vector control operations to possibly become significant. In this section we examine the effect of also decoupling the vector control pipeline allowing out-of-order execution between all three pipelines shown in Chapter 5, Figure 5.5. This optimization was motivated by visual inspection of the benchmark discussed below.

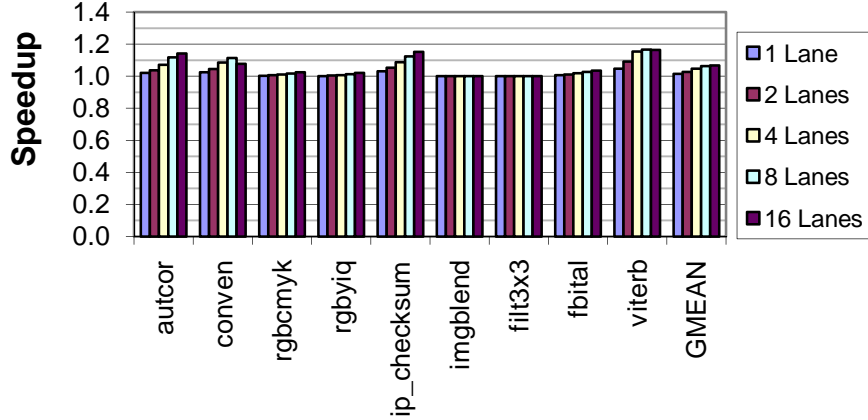


Figure 6.11: Performance improvement of decoupling the vector control pipeline from the vector pipeline, effectively supporting zero-overhead loops.

Listing 6.1 shows the vectorized kernel of the IP\_CHECKSUM benchmark which consists of a vector load and vector add instruction, followed by two vector control instructions for modifying the current vector length, then two scalar control instructions for handling the branching. The loop overhead, consisting of the two scalar instructions and two vector control instructions, is usually small in cycles compared to the vector load and add instructions—but when VESPA is configured with a large number of lanes these first two instructions are executed more quickly, making the control instructions more significant.

The improved VESPA has decoupled the two vector coprocessor pipelines shown in Chapter 5, Figure 5.5 allowing vector, vector control, and scalar instructions to execute simultaneously and out-of-order with respect to each other. As long as the number of cycles needed to compute the vector operations is greater than the cycles needed for the vector control and scalar operations, a loop will have no overhead cycles. Before this modification vector control operations and vector operations were serialized, but scalar operations could be hidden by executing concurrently with any vector instruction.

Figure 6.11 shows the impact on performance from this decoupling for various VESPA processors with 16KB data cache with 64B line size is shown. For 16 lanes, this technique improves performance by 7% on average and by 17% in the best case, while the area cost is negligible. Specifically, the benchmarks AUTCOR, IP\_CHECKSUM, and VITERB achieve

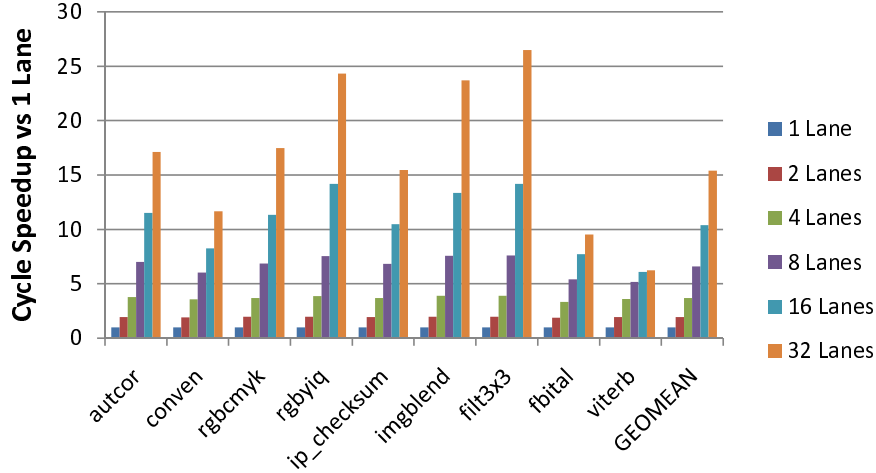


Figure 6.12: Performance scalability as the number of lanes are increased from 1 to 32 for a fixed VESPA architecture with *full memory support* (full memory crossbar, 16KB data cache, 64B cache line, and prefetching enabled).

between 15-17% speedup in the 16-lane configuration. This improved VESPA was used in all VESPA configurations presented in this thesis.

## 6.4 Improved VESPA Scalability

With all the above improvements we are motivated to re-evaluate the scalability of VESPA previously seen in Section 6.1. Furthermore, we use the new DE3 platform with its larger Stratix III FPGA to explore even larger 32-lane VESPA configurations that were not possible on the TM4. With good scalability implemented on real FPGAs, we hope to make a compelling case that soft vector processors are indeed attractive implementation vehicles over manual hardware design for data parallel workloads. This section thoroughly evaluates the improved scalability of VESPA.

### 6.4.1 Cycle Performance

Figure 6.12 shows the cycle performance improvement for each of our benchmarks as we increase the number of lanes on an otherwise aggressive VESPA architecture with *full memory support* (full memory crossbar, 16KB data cache with 64-byte cache lines and hardware prefetching—while a variety of prefetching schemes are possible we prefetch

Table 6.2: Performance measurements for VESPA with 1-32 lanes. Clock frequency is averaged across 8 runs of the CAD tools targeting the Stratix III 3S340C2, speedups are geometric means normalized to the 1-lane configuration.

	1 Lane	2 Lanes	4 Lanes	8 Lanes	16 Lanes	32 Lanes
Clock Frequency (MHz)	131	129	128	123	117	96
Average Cycle Speedup	1.00	1.95	3.7	6.5	10.4	15.4
Average Wall Clock Speedup	1.00	1.96	3.6	6.3	9.3	11.3

the next  $8 \times (\text{current vector length})$  elements since this is reliable across our benchmarks as seen in Section 6.2.2.4). The figure illustrates that impressive scaling is possible as seen in the 27x speedup for FILT3X3 executed on 32 lanes. The compute bound nature of soft processors is also exemplified in the 2-lane configuration which performs 1.95x faster on average than 1 lane. Had the processor been memory bound the performance gains from adding twice as many processing lanes would be significantly less than 2x. Overall we see that indeed a soft vector processor can scale cycle performance on average from 1.95x for 2 lanes, to 10x for 16 lanes, to 15x for 32 lanes. The improved VESPA achieves significantly better scaling than the initial VESPA design seen in Section 6.1 which achieved only 5.1x speedup for 16 lanes.

Ideally, the speedup would increase linearly with the number of vector lanes, but this is prevented by a number of factors: (i) only the vectorizable portion of the code can benefit from extra lanes, hence benchmarks such as CONVEN that have a blend of scalar and vector instructions are limited by the fraction of actual vector instructions in the instruction stream; (ii) some applications do not contain the long vectors necessary to scale performance, for example VITERB executes predominantly with a vector length of only 16; (iii) the movement of data becomes a limiting factor specifically for RGBCMYK, and RGBYIQ which access streams in a strided fashion requiring excessive cache accesses, and FBITAL which uses an indexed load to access an arbitrary memory location from each lane. Indexed vector memory operations are executed serially in VESPA, severely limiting the scalability of workloads that use them.

### 6.4.2 Clock Frequency

While the cycle performance was shown to be very scalable, in an FPGA context we can verify that the processor clock speed degradation caused by instantiating more lanes does not nullify or overwhelm the cycle improvements. In general as a hardware design grows in size it becomes more challenging to architect and design the circuit to achieve a high clock frequency. Our measurements of clock frequency on the VESPA architecture demonstrate that a vector processor implemented on an FPGA can retain scalable performance without whole design teams to optimize the architecture and circuit design. Certainly VESPA could further benefit from such optimizations.

Table 6.2 shows the clock frequency for each configuration produced by the FPGA CAD tools as described in Chapter 3. The clock frequency starts at 131 MHz for the 1 lane, decays to 123 MHz for 8 lanes, 117 MHz for 16 lanes, and finally 96 MHz for 32 lanes. The effect on wall clock time is moderate at 16 lanes reducing the 10x cycle speedup to 9x in actual wall clock time speedup. At 32 lanes the clock frequency drops significantly reducing the 15x cycle speedup to 11x in wall clock time. Despite these clock frequency reductions, the average wall clock time across our benchmarks continues to increase with more lanes. At 64 lanes the clock frequency is reduced to 80 MHz and the performance is worse than the 32-lane configuration. Because of timing problems with the 64-lane configuration, it cannot be accurately benchmarked and is hence not shown in Table 6.2.

In both the 16 and 32 lane configurations, the critical path is in the memory crossbar which routes all 64 bytes in a cache line to each of the lanes. The  $M$  parameter can be used to reduce the size of the crossbar and raise the clock frequency, but the resultant loss in average cycle performance often overwhelms this gain and produces a slower overall processor as shown in Chapter 7, Section 7.1.3. The clock frequency reduction can instead be addressed by pipelining the memory crossbar as well as additional engineering effort in retiming these large designs. Ultimately scaling to larger lanes requires careful design of a high-performing memory system, and may require a hierarchy of memory storage

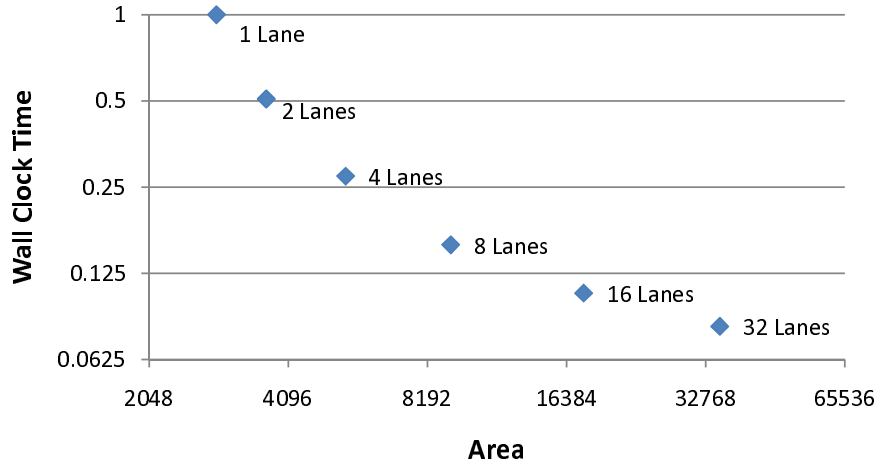


Figure 6.13: Performance/area design space of 1-32 lane VESPA cores with full memory support. Area measures just the vector coprocessor area.

units as seen in graphics processors. The following section shows that these many-lane configurations consume such a large portion of resources that they are questionably useful in many embedded systems application with tight constraints. Thus, we leave additional research into higher memory throughput and clock frequency for these large designs as future work likely better motivated in the high-performance computing domain.

### 6.4.3 Area

Figure 6.13 shows the area of each VESPA vector coprocessor (excluding the memory controller, system bus, caches, and scalar processor) on the x-axis and the wall clock time execution plotted on the y-axis. The initial cost of a vector coprocessor is considerable costing 2900 ALMs of silicon area due to the decode/issue logic, 1 vector lane, and the vector state with 64 elements in each vector ( $MVL=64$ ). As the vector lanes are increased a linear growth in area is eventually observed as the constant cost of the state and decode/issue logic are dominated. This additional area cost becomes quite substantial, for example growing from 8 to 16 lanes requires about 9000 ALMs worth of silicon. At 32 lanes one third of the resources on the Stratix III-340 are consumed, since this is the largest currently available FPGA device, a 32-lane configuration seems beyond the grasp of most embedded systems designs. Nonetheless performance scaling is still possible with

32-lanes and likely beyond with additional processor design effort.

## 6.5 Summary

This chapter first demonstrated the modest scalability in a naive VESPA design. Modified caches, hardware prefetching, and decoupled pipelines were then added to achieve significantly more scaling. Wider cache lines were the most significant improvement since they provide some inherent prefetching and also allows a single cache access to satisfy multiple lanes assuming spatial locality between the memory requests in the lanes. However the cost of increasing cache lines is large due to the growing memory crossbar. Prefetching can provide drastically reduced miss rates for a very low area cost, but its effectiveness is application-dependent. Finally the decoupled vector control pipeline allowed vector control instructions to be executed in parallel with vectorized work. Overall, the improved VESPA achieved significant scaling of up to 27x for 32 lanes and on average 15x. The next chapter will demonstrate that more thorough exploration of soft vector processor architecture can yield an even larger and more fine-grain VESPA design space.

## Chapter 7

# Expanding and Exploring the VESPA Design Space

One of the most compelling features of soft processors is their inherent reconfigurability. An FPGA designer can ideally choose the exact soft processor architecture for their application rather than be limited to a few off-the-shelf variants. If the application changes, a designer can easily reconfigure a new soft processor onto the FPGA device. In addition, the designer need not modify the software toolchain, which is often necessary with the purchase of a new hard processor in an embedded system.

The previous chapter explored a variety of architectural parameters of the VESPA soft vector processor including the number of lanes, the cache configurations, and the prefetching strategy. All of these parameters can be tuned to match an application with respect to its amount of data parallelism and memory access patterns. In this chapter we explore the computational capability of VESPA, specifically the functional units in its vector lanes. These functional units can significantly impact the performance of VESPA and also account for a significant amount of overall area especially when multiple lanes are present. Thus we explore architectural parameters that allow an FPGA designer to tune the functional units to their application in three aspects: (i) reducing the number of functional units in low demand hence creating *heterogeneous lanes* [74]; (ii) param-

eterizing the number of vector instructions that can be simultaneously executed using vector chaining [74]; and (iii) eliminating hardware not required by the application [72]. All evaluation in this chapter is performed on the DE3 hardware platform.

## 7.1 Heterogeneous Lanes

In this section we examine the option of reducing the number of copies of a given functional unit which is in low demand. For example, a benchmark with vector multiplication operations will require the multiplier functional unit, but if the multiplies are infrequent the application does not necessarily require a multiplier in every vector lane. In the extreme case a 32-lane vector coprocessor can have just one lane with a multiplier and have vector multiplication operations stall as the vector multiply is performed at a rate of one operation per cycle. We use this idea to parameterize the hardware support for vectorized multiplication and memory instructions as described below.

### 7.1.1 Supporting Heterogeneous Lanes

The VESPA vector datapath contains three functional units: (i) the ALU for addition, subtraction, and logic operations; (ii) the multiplier for multiplication and shifting operations; and (iii) the memory unit for load and store operations. Increasing the vector lanes with the  $L$  parameter duplicates all of these functional units, so all vector lanes are identical, or homogeneous. We provide greater flexibility by allowing the multiplier units to appear in only some of the lanes specified with  $X$ . Similarly the number of lanes attached to the memory crossbar can be selected using  $M$ . This allows for a heterogeneous mix of lanes where not all lanes will have each of the three functional unit types. A user can specify the number of lanes with ALUs using  $L$ , the number of lanes with multipliers with  $X$ , and the number of lanes with access to the cache with  $M$ .

Some area overhead is required to buffer operands and time-multiplex operations into the lanes which have the desired functional units, so the area savings from removing

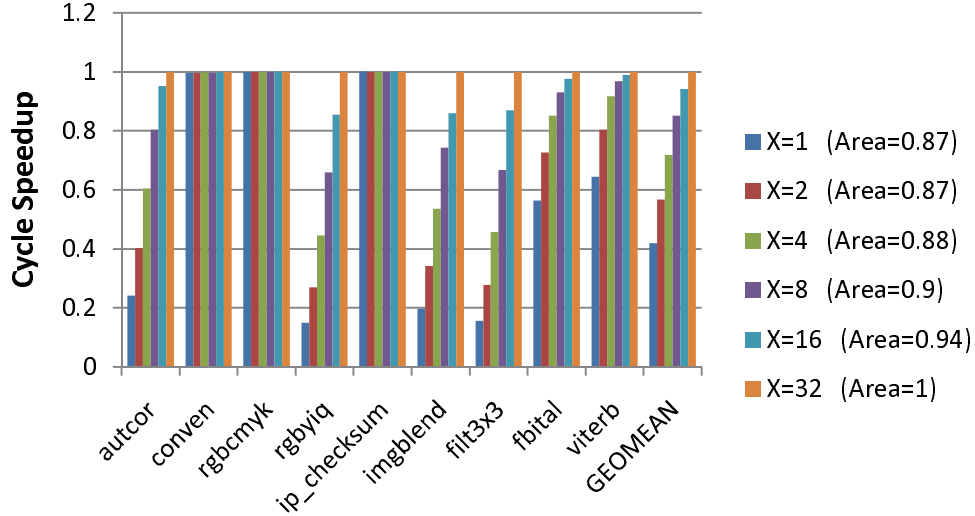


Figure 7.1: Performance impact of varying  $X$  for a VESPA with  $L=32$ ,  $M=16$ ,  $DW=64$ ,  $DD=16K$ , and  $DPV=8*VL$ , area and performance is normalized to the  $X=32$  configuration.

multipliers and shrinking the crossbar must offset this. In place of the missing functional units are shift registers for shifting input operands to the necessary lane and shifting back the result. Because of the frequency of ALU operations across the benchmarks and because of their relative size compare to the overhead, we do not support the elision of ALUs. This is a reasonable limitation since the multipliers are generally scarce, and the memory crossbar generally large, so reducing those units will have greater impact on area savings while being more likely to only mildly affect performance.

### 7.1.2 Impact of Multiplier Lanes ( $X$ )

The  $X$  parameter determines the number of lanes with multiplier units. The effect of varying  $X$  is evaluated on a 32-lane VESPA processor with 16 memory crossbar lanes (halved to reduce its area dominance) and a prefetching 16KB data cache with 64B line size. Each halving of  $X$  doubles the number of cycles needed to complete a vector multiply. We measure the overall cycle performance and area and normalize it to the full  $X=32$  configuration. Note that clock frequency was unaffected in these designs.

Figure 7.1 shows that in some benchmarks such as `FILT3X3` the performance degradation is dramatic, while in other benchmarks such as `CONVEN` there is no impact at all.

Programs with no vector multiplies can have multipliers removed completely with the instruction-set subsetting technique explored in Section 7.4.3, but programs with just few multiplies such as VITERB can have its multipliers reduced saving 10% area and suffering a small 3.1% performance penalty. The resulting saved area can then be used for other architectural features or components of the system.

The area savings from reducing the multipliers is small starting at 6% for halving the number of multipliers to 16, the savings asymptotically grow and saturate at 13%. Since the multipliers are efficiently implemented in the FPGA as a dedicated block, the contribution to the overall silicon area is small, and the additional overhead for multiplexing operations into the few lanes with multipliers ultimately outweigh the area savings. However, multipliers are often found in short supply, so a designer might be willing to accept the performance penalty if another more critical computation could benefit from using the multipliers.

### 7.1.3 Impact of Memory Crossbar (M)

A vector load/store instruction can perform as many memory requests in parallel as there are vector lanes, however the data cache can service only one cache line access per clock cycle. Extracting the data in a cache line to/from each vector lane requires a full and bidirectional crossbar between every byte in a cache line and every vector lane. Such a circuit structure imposes heavy limitations on the scalability of the design, especially within FPGAs where multiplexing logic is comparatively more expensive than in traditional IC design flows. Because of this, the idea of using heterogeneous lanes to limit the number of lanes connected to the crossbar as described in Chapter 5, Section 5.3.3 can be extremely powerful.

The parameter,  $M$ , controls the number of lanes the memory crossbar connects to and hence directly controls the crossbar size and the amount of parallelism for memory operations. For example, a 16-lane vector processor with  $M$  equal to 4 can complete 16 add operations in parallel, but can only satisfy up to 4 vector loads/store operations provided

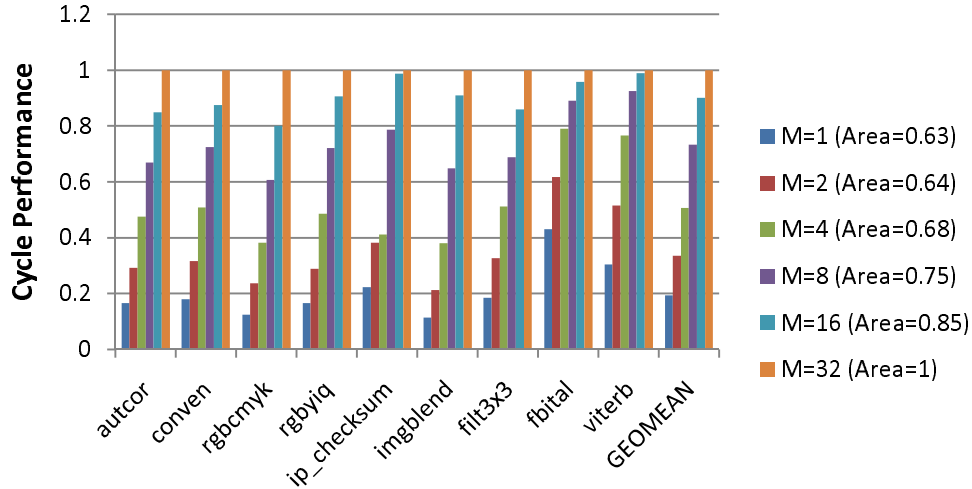


Figure 7.2: Cycle performance of various memory crossbar configurations on a 32-lane vector processor with 16KB data cache, 64B line size, and 8\*VL prefetching. Performance is normalized against the full M=32 configuration. Area is shown in parentheses and is also normalized to the M=32 configuration.

all 4 were accessing the same cache line. Decreasing M reduces area and decreases cycle performance of vector memory instructions. Also, clock frequency can be increased by reducing M when the memory crossbar is the critical path in the design.

Figure 7.2 shows the effect on cycle performance and vector coprocessor area as the memory crossbar size is varied on a 32-lane vector processor with 16KB data cache, 64B line size, and 8\*VL prefetching. Both cycle performance and area are normalized to the full memory crossbar (M=32). For the smallest crossbar, where M=1 and memory operations are serialized, average performance is reduced to one-fifth of the full memory crossbar, but 37% of area is saved. For M=4 performance is halved and 32% of area is saved. All configurations with  $M \leq 4$  lose significantly more in performance than is gained in area savings. For M=8 the tradeoff almost breaks even saving 25% of area and reducing performance by an average of 26.6%. With a half-size memory crossbar at M=16 area savings is 15% while average performance degradation is 9.8%. For some benchmarks such as VITERB and IP\_CHECKSUM there is no performance degradation between the M=32 and M=16 configurations, meaning the 15% area reduction can be achieved for free. In other cases such as FBITAL the performance degradation is small (only 4.3%). This provides an effective lever for customizing the size of the crossbar to the memory demands

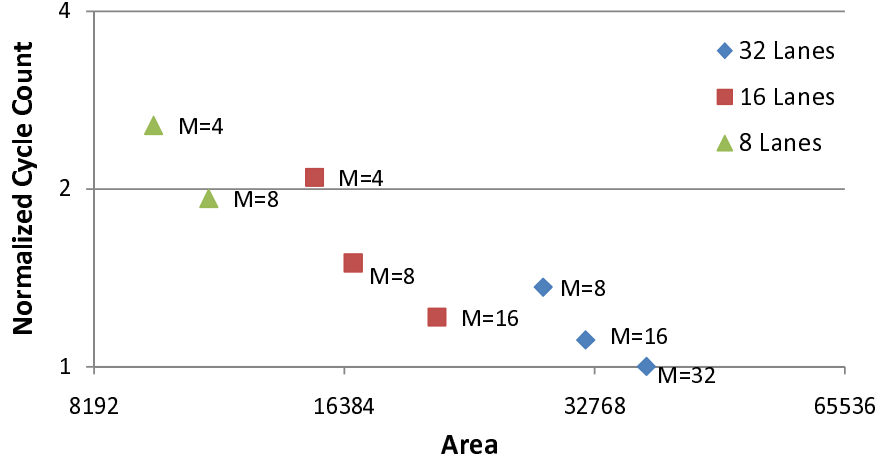


Figure 7.3: Average normalized cycle count versus area for various memory crossbar configurations on various numbers of lanes. All VESPA configuration have 16KB data cache, 64B line size, and 8\*VL prefetching. Cycles are normalized against the full  $M=32$  configuration on a 32-lane VESPA.

of the application, however it can also be used to mitigate clock frequency degradation caused by the large crossbars.

Figure 7.3 highlights the area/speed tradeoff possible using the memory crossbar reduction. The figure shows the average cycle count of an 8, 16, and 32 lane VESPA each with full, half, and quarter-sized memory crossbars all normalized to the 32-lane VESPA with full memory crossbar. The 16-lane VESPA with  $M=8$  is a half-sized memory crossbar providing a useful area/performance design point between the full memory crossbar 8-lane VESPA and the full 16-lane VESPA. Similarly the half-sized crossbar for 32 lanes provides a mid-point between the full memory crossbars of the 16 and 32-lane VESPA configurations. The quarter-sized crossbar with  $M=4$  and 16 lanes performs worse and is larger than the 8-lane full memory crossbar. In general, half-sized memory crossbars are useful design points, while the quarter-sized memory crossbars are dominated by the full crossbars with half as many lanes.

Figure 7.4 shows the effect on wall clock performance and clock frequency across all values of  $M$  (normalized to  $M=32$ ) on a 32-lane VESPA with 16KB data cache, 64B line size, and 8\*VL prefetching. For such a large vector processor, the many lanes and the full crossbar limits clock frequency to 98 MHz compared to the 131 MHz achievable on

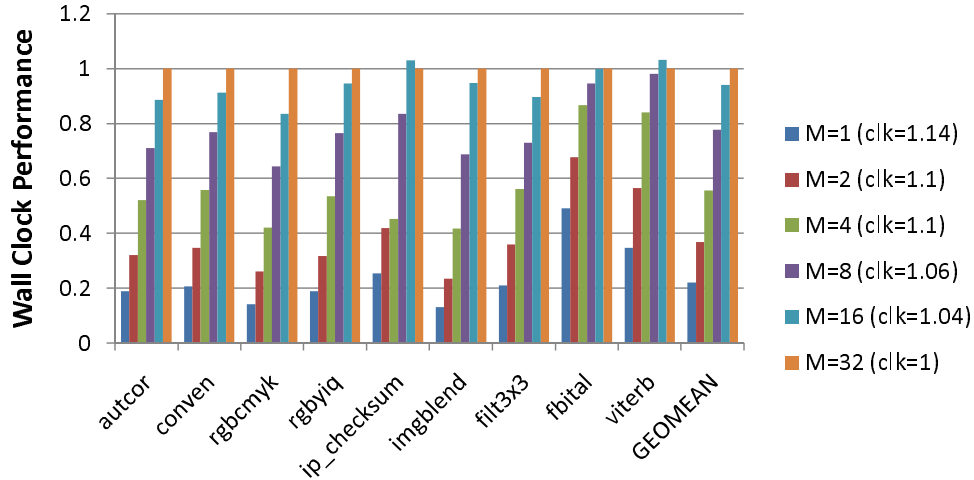


Figure 7.4: Wall clock performance of various memory crossbar configurations on a 32-lane vector processor with 16KB data cache, 64B line size, and 8\*VL prefetching. Performance is normalized against the full M=32 configuration. Clock frequency is shown in parentheses and is also normalized to the M=32 configuration.

a 1-lane VESPA. Reducing the memory crossbar to M=1 raises the clock frequency to 110 MHz but still leaves overall wall clock time at one-fifth the performance of the full memory crossbar. In the cases where no cycle degradation was observed such as M=16 for VITERB and IP\_CHECKSUM, the wall clock performance is actually better than the full memory crossbar because of the 4% gain in clock frequency. In FBITAL the clock frequency gain makes M=16 and M=32 equal in wall clock performance and hence allows a free 15% area savings. This clock frequency improvement phenomenon occurs because the memory crossbar is the critical path of the design. For configurations with fewer lanes, or for a more highly-pipelined and highly-optimized design we would expect clock frequency to remain relatively constant.

## 7.2 Vector Chaining in VESPA

Our goal of scaling soft processor performance is largely met by instantiating multiple vector lanes using a soft vector processor. However, additional performance can be gained by leveraging a key feature of traditional vector processors: the ability to concurrently execute multiple vector instructions via vector chaining, as discussed in Chapter 2, Sec-

tion 2.2.4. By simultaneously utilizing multiple functional units, VESPA can more closely approach the performance and efficiency of a custom hardware design. In this section, VESPA is augmented with parameterized support for chaining designed in a manner that is amenable to FPGA architectures.

### 7.2.1 Supporting Vector Chaining

VESPA has three functional unit types: an ALU, a multiplier/shifter, and a memory unit, but only one functional unit type can be active in a given clock cycle. Additional parallelism can be exploited by noting that vector instructions operating on different elements can be simultaneously dispatched onto the different functional unit types, hence permitting more than one to be active at one time. Modern vector processors exploit this using a large many-ported register file to feed operands to all functional units keeping many of them busy simultaneously. This approach was shown to be more area-efficient than using many banks and few ports as in historical vector supercomputers [7]. But since FPGAs cannot efficiently implement a large many-ported register file, our solution is to return to this historical approach and use multiple banks each with 2 read ports and 1 write port. The three-port banks were created out of two-port block RAMs by duplicating the register file as described in Chapter 5.

Figure 7.5 shows how we partition the vector elements among the different banks for a vector processor with 2 banks, 4 lanes, and  $MVL=16$ . Each 4-element group is stored as a single entry so all 4 lanes can each access their respective operand on a single access. Element groups are interleaved across both banks so that elements 0-3 and 8-11 are in bank 0, and elements 4-7 and 12-15 are in bank 1. As a result, sequentially accessing all elements in a vector requires alternating between the two banks allowing instructions operating on different element groups to each use a register bank to feed their respective functional unit. The number of chained instructions is limited by the number of register banks. In this example, with two banks at most two instructions can be dispatched.

Figure 7.6 shows an example of our implementation of vector chaining using two

Bank 1	15	7	...	15	7	15	7
	14	6		14	6	14	6
	13	5		13	5	13	5
	12	4		12	4	12	4
Bank 0	11	3	...	11	3	11	3
	10	2		10	2	10	2
	9	1		9	1	9	1
	8	0		8	0	8	0
vr31				vr1		vr0	

Figure 7.5: Element-partitioned vector register file banks shown for 2 banks, 4 lanes, and maximum vector length 16. Note that accessing all elements in a vector requires oscillating between both banks.

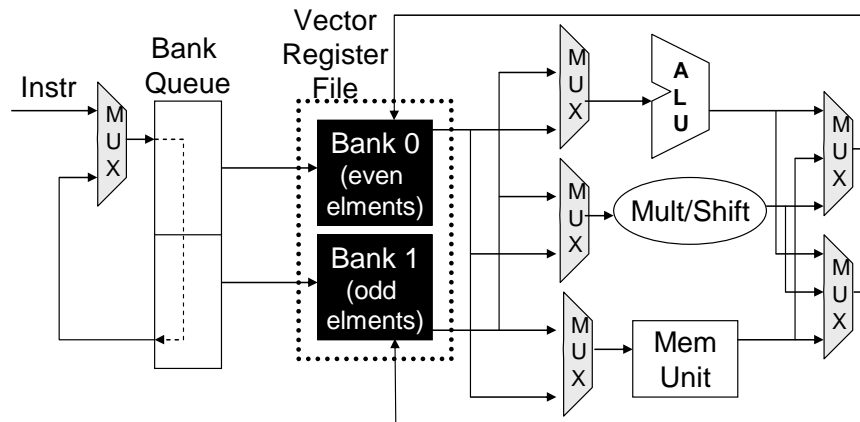


Figure 7.6: Vector chaining support for a 1-lane VESPA processor with 2 banks.

register banks to support a maximum of 2 vector instructions in flight for a 1-lane VESPA processor. Once resource, read-after-write, and bank conflicts are resolved, instructions will enter the Bank Queue and cycle between the even and odd element banks until all element operations are completed. During that time another instruction can enter the queue and rotate through the cyclical Bank Queue resulting in 2 element operations being issued per cycle. As each operation completes the result is written back to the appropriate register bank. Using a cyclical queue simplifies the control logic necessary for assigning a bank to an element operation, but causes one or more cycle delays for the few vector instructions which cannot start on an even element (most vector instructions

start with element 0).

The number of register banks,  $B$ , used to support vector chaining is parameterized and must be a power of two. A value of 1 reduces VESPA to a single-issue vector processor without vector chaining support eliminating the Bank Queue and associated multiplexing illustrated in Figure 7.6. VESPA can potentially issue as many as  $B$  instructions at one time, provided they each have available functional units. To increase the likelihood of this, VESPA allows replication of the ALU for each bank, the `APB` parameter enables or disables this feature. For example, with two banks and `APB` enabled, each vector lane will have one ALU for each bank and in total two ALUs. Since multipliers are generally scarce we do not support duplication for the multiply/shift unit, and we also do not support multiple memory requests in-flight because of the system’s locking cache.

### 7.2.2 Impact of Vector Chaining

We measured the effect of the vector chaining implementation described above across our benchmarks using an 8-lane vector processor with full memory support (16KB data cache, 64B cache line, and prefetching of  $8 \times VL$ ) implemented on the DE3 platform. We vary the number of banks from 2 to 4 and for each toggle the ALU per bank `APB` parameter and compare the resultant four designs to an analogous VESPA configuration without vector chaining.

Figure 7.7 shows the cycle speedup of chaining across our benchmarks as well as the area normalized to the 1 bank configuration. The area cost of banking is considerable, starting at 27% for the second register bank and the expensive multiplexing logic needed between the two banks. The average performance improvement of this 27% area investment is approximately 26%, and in the best case is 54%. Note that if instead of adding a second bank, the designer opted to double the number of lanes to 16, the average performance gain would be 49% for an area cost of 77%. Two banks provide half that performance improvement at one third the area, and is hence a more fine-grain trade-off than increasing lanes.

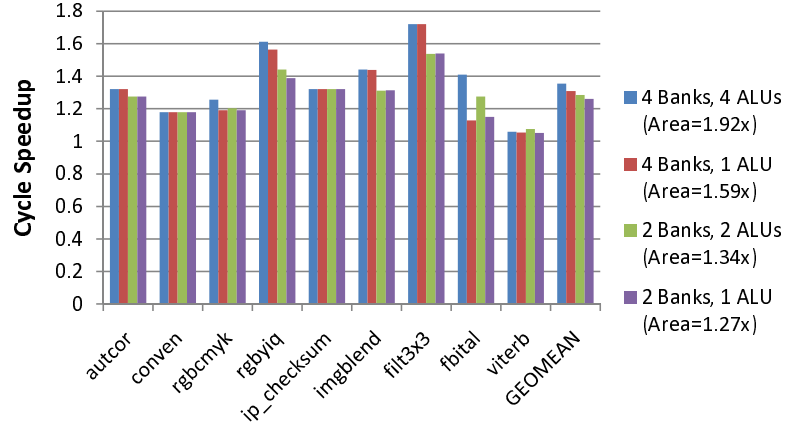


Figure 7.7: Cycle performance of different banking configurations across our benchmarks on an 8-lane VESPA with full memory support. Area is shown in parentheses for each configuration. Both cycle speedup and area area normalized to the same VESPA without vector chaining.

Replicating the ALUs for each of the 2 banks (2 banks, 2 ALUs) provides some minor additional performance, except for FBITAL where the performance improvement is significant. FBITAL executes many arithmetic operations per datum making demand for the ALU high and hence benefiting significantly from increased ALUs and justifying the additional 7% area. Similarly the 4 bank configuration with no ALU replication benefits only few benchmarks, specifically RGBYIQ, IMGBLEND, FILT3X3. These benchmarks have a near equal blend of arithmetic, multiply/shifting, and memory operations and thus benefit from the additional register file bandwidth of extra banks. However the area cost of these four banks is significant at 59%. Finally, with 4 banks and 4 ALUs per lane the area of VESPA is almost doubled exceeding the area of a VESPA configuration with double the lanes and no chaining, which performs better than the 4 banks and 4 ALUs; as a result we do not further study this inferior configuration. Though the peak performance of the 4 bank configuration is 4x that of the 1 bank configuration, our benchmarks and single-issue in-order pipeline with locking cache cannot exploit this peak performance. Note that instruction scheduling in software could further improve the performance of vector chaining, but in many of our benchmarks only very little rescheduling was either necessary or possible, so we did not manually schedule instructions to exploit chaining.

Figure 7.8 shows that the speedup achieved from banking is reduced as the lanes

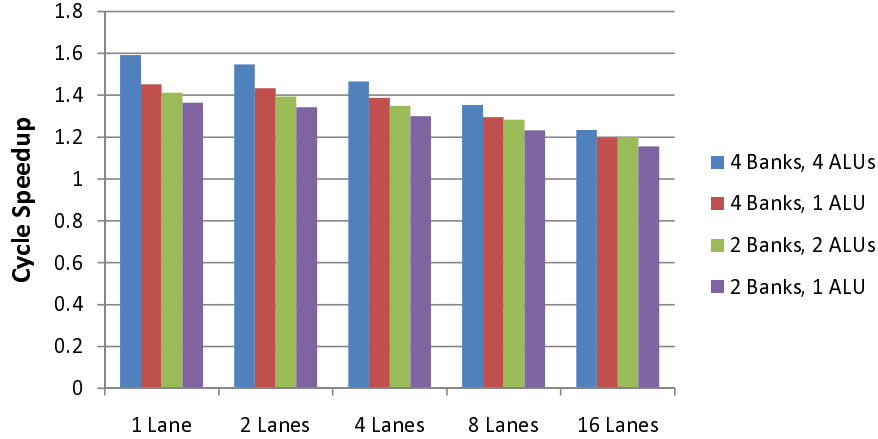


Figure 7.8: Cycle performance averaged across our benchmarks for different chaining configurations for a VESPA with varying number of lanes and all with full memory support. Cycle speedup is normalized to that measured on the same VESPA without vector chaining.

are increased. Chaining allows multiple vector instructions to be executed if both the appropriate functional unit and register bank are available. However, because only one instruction is fetched per cycle, chaining is only effective when the vector instructions are long enough to stall the vector pipeline, in other words, when the length of a vector is greater than the number of lanes. As the number of lanes increases, vector instructions are completed more quickly providing less opportunity for overlapping execution. In the vector processors with one lane, speedups from banking can average as high as 60% across our benchmarks, while in the fastest 16-lane configuration banking achieves only 23% speedup. The 1 lane vector processor represents an optimistic speedup achievable on extremely long vector operations.

The area cost of chaining is due largely to the multiplexing between the banks, but also to the increase in block RAM usage. The vector register file is comprised of many FPGA block RAMs given by the greater of the two Equations 5.1 and 5.2 as discussed in Chapter 5. For vector processors with few lanes there is no increase in the number of block RAMs. However, for vector processors with many lanes, making Equation 5.1 greater, adding more banks proportionally increases the number of block RAMs used. For example increasing from 1 to 4 banks with no ALU replication on a 16 lane VESPA with  $MVL=128$  adds 38% area just in block RAMs and 56% in total. For a system with

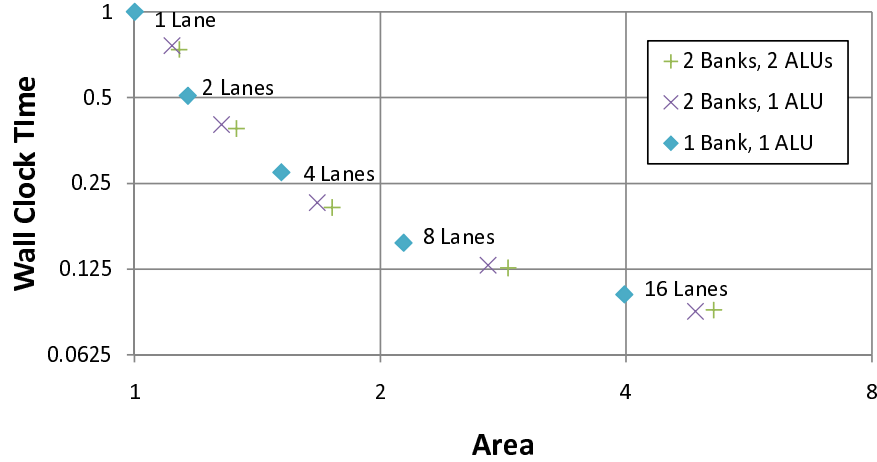


Figure 7.9: Performance/area space of 1-16 lane vector processors with no chaining (1 bank with 1 ALU), and 2-way chaining (2 banks with 1 ALU and 2 banks with 2 ALUs). Area and performance are normalized to the 1 lane, 1 bank, 1 ALU configuration.

many unused block RAMs this increase can be justified even though only a fraction of the capacity of each block RAM may be used. In fact, the unused capacity of the block RAMs can be fully utilized by the vector processor with a corresponding increase in MVL as seen in Equation 5.2.

Figure 7.9 shows the wall clock time versus area space of the no chaining configurations from 1 to 16 lanes (depicted with solid diamonds). We overlay two vector chaining configurations on the same figure and observe that the points with 2 banks and no ALU replication appear about one third of the way to the next solid diamond, illustrating that chaining can trade area/performance at finer increments than doubling the number of lanes. Adding ALU replication slightly increases the performance and area of the soft vector processor. Note that the 4-bank configurations are omitted since the area cost is significant and the additional performance is often modest compared to 2 banks. Since we have complete measurement capabilities of the area and performance we are able to identify that vector chaining in an FPGA context is indeed a trade-off and not a global improvement (it did not move VESPA toward the origin of the figure).

### 7.2.3 Vector Lanes and Powers of Two

Another option for fine-grain area/performance trade-offs is to use lane configurations that are not powers of two, resulting in cumbersome control logic which involves multiplication and division operations. For example the `vext.sv` instruction extracts a single element given by its index value in the vector. If a 9-lane vector configuration is used, determining the element group to load from the register file would require dividing the index by 9. By using a power of two this operation reduces to shifting by a constant, which is free in hardware. Since this extra logic can impact clock frequency, and the additional area overhead can be significant, this approach would generate inferior configurations that, in terms of Figure 7.9, would form a curve further from the origin than the processors with lanes that are powers of two. Chaining, on the other hand, is shown to directly compete with these configurations, and in Section 7.3 is shown to even improve performance per unit area.

## 7.3 Exploring the VESPA Design Space

Using VESPA we have shown soft vector processors can scale performance while providing several architectural parameters for fine-tuning and customization. This customization is especially compelling in an FPGA context where designers can easily implement an application-specific configuration. In this section we explore this design space more fully by measuring the area and performance of hundreds of VESPA processors generated by varying almost all VESPA parameters and implementing each configuration on the DE3 platform.

### 7.3.1 Selecting and Pruning the Design Space

Our aim is to derive a design space that captures many interesting tradeoffs without an overwhelming number of design points. Each design point must be synthesized nine times (once for implementing on the DE3, and 8 times across different seeds to average

Table 7.1: Explored parameters in VESPA.

	Parameter	Symbol	Value Range	Explored
Compute	Vector Lanes	L	1,2,4,8,16,...	1,2,4,8,16,32
	Memory Crossbar Lanes	M	1,2,4,8,... L	L, L/2
	Multiplier Lanes	X	1,2,4,8,... L	L, L/2
	Register File Banks	B	1,2,4,...	1,2,4
	ALU per Bank	APB	true/false	true/false
ISA	Maximum Vector Length	MVL	2,4,8,16,...	L*4,128,512
	Vector Lane Bit-Width	W	1,2,3,4,..., 32	-
	Each Vector Instruction	-	on/off	-
Memory	ICache Depth (KB)	ID	4,8,...	-
	ICache Line Size (B)	IW	16,32,64,...	-
	DCache Depth (KB)	DD	4,8,...	8, 32
	DCache Line Size (B)	DW	16,32,64,...	16, 64
	DCache Miss Prefetch	DPK	1,2,3,...	-
	Vector Miss Prefetch	DPV	1,2,3,...	off, 7, 8*VL

out the non-determinism in FPGA CAD tools as described in Chapter 3). Each synthesis can take between 30 minutes to 2.5 hours with an average of approximately one hour. Exploring 1000 design points hence requires more than 1 year of compute time. To reduce this compute time we are motivated to prune the design space.

We vary all combinations of the explored parameter values listed in the last column of Table 7.1 and implement each architectural configuration. The selection of these parameter values were guided by our research in the previous chapters. The instruction cache was not influential as seen in Chapter 6, Section 6.2.4 so it is not explored here. The data cache has a depth of either 8KB or 32KB to fill the block RAMs for either 16B or 64B cache lines. Prefetching is enabled only for the 64B configuration as a result of a limitation discussed in Chapter 6, Section 6.2.2. The same section shows the different prefetch triggers DPK and DPV to perform similarly across our benchmarks so we explore only the latter.

Lanes are varied by doubling the number of lanes from 1 to 32 inclusively. The memory crossbar is either full or half-sized since anything less than this was found in Section 7.1.3 to be generally inferior to full-sized crossbars with half as many lanes. The number of multiplier lanes was also varied between all lanes and half the lanes, despite the observation that some benchmarks required no multiplier lanes. Chaining

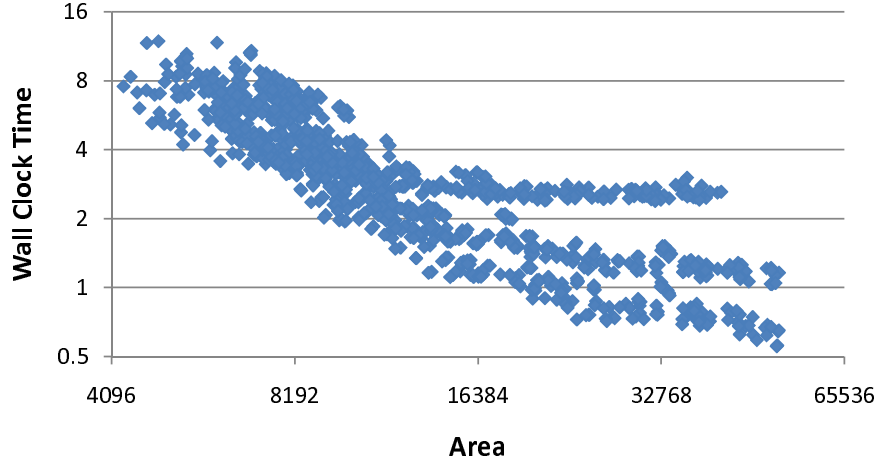


Figure 7.10: Average normalized wall clock time and area (in equivalent ALMs) of several soft vector processor variations.

is varied from no chaining, to two-way chaining, to four-way chaining. For the latter two configurations the ALU replication `APB` parameter is toggled both on and off. Note that 4-way chaining on 32-lanes is not performed because of the exceedingly large area required for this configuration. With the selected parameters and value ranges shown in the last column of Table 7.1, a brute force exploration of the complete 2400-point design space would result in 2-3 years of compute time. Further design space pruning was performed to cull certain parameter *combinations* which generally result in inferior design points.

As an example of inferior configurations, consider Figure 7.10 which shows the average wall clock performance and area of a set of VESPA configurations. The design space is similar to the one described above but excludes the `DPV=7` and `MVL=4*L` values. As area is increased, three branches emerge: the topmost (slowest) being the designs throttled by a small 16B cache line size, and the middle branch throttled by cache misses without prefetching. With both larger cache lines and prefetching enabled the fastest and largest designs in the bottom branch can trade area for performance competitively with the smaller designs. The top two branches are hence comprised entirely of inferior configurations which can be pruned to save compilation time.

To limit our exploration time we use Figure 7.10 as well as our intuition to exclude

configurations with:

1. ( $L < 8$ ) and ( $MVL = 512$ ) – Configurations with few lanes can seldomly justify the area for such large amount of vector state.
2. ( $L \geq 8$ ) and ( $DW = 16B$ ) – Configurations with many lanes require wider cache lines as seen in Figure 7.10.
3. ( $L \geq 8$ ) and ( $DPV = 0$ ) – Configurations with many lanes require prefetching as seen in Figure 7.10.
4. ( $DD = 8KB$ ) and ( $DW = 64B$ ) – Configurations which do not fully utilize their block RAMs.
5. ( $DD = 32KB$ ) and ( $DW = 16B$ ) – Configurations with extra block RAMs used only to expand the cache depth which was shown to be ineffective in accelerating benchmark performance as seen in Section 6.2.1.

As a result of this pruning, the 2400 point design space resulting from all combinations of parameter values in the last column of Table 7.1 is reduced to just 768 points. With less than one-third the number of design points the exploration time is reduced proportionately.

### 7.3.2 Exploring the Pruned Design Space

Our goal is to measure the area and performance of this 768-point design space and confirm VESPA's ability to: (i) span a very broad design space; and (ii) fill in this design space allowing FPGA designers to choose an exact-fit configuration.

Figure 7.11 shows the vector coprocessor area and cycle count space of the 768 VESPA configurations. The design space spans a total of 28x in area and 24x in performance providing a huge range of design points for an FPGA embedded system designer to choose from. Moreover, the data shows that VESPA provides fine-grain coverage of this design space indeed allowing for precise selection of a configuration which closely matches the

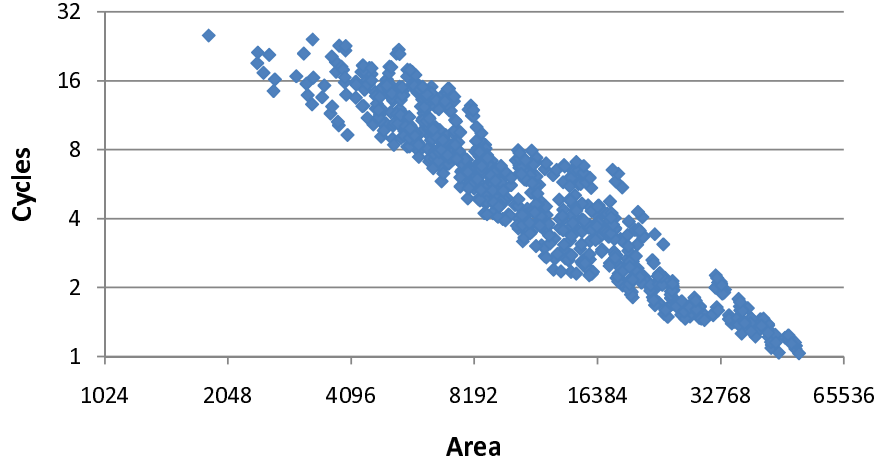


Figure 7.11: Average cycle count and vector coprocessor area of 768 soft vector processor variations across the pruned design space. Area is measured in equivalent ALMs, while the cycle count of each benchmark is normalized against the fastest achieved cycle count across all configurations and then averaged using geometric mean.

area/speed requirements of the application. By inspection, the pareto optimal points in the figure closely approximate a straight line providing steady performance returns on area investments. Also the configurations are all relatively close to the pareto optimal points meaning our exploration was indeed focused on useful configurations. In addition notice no wasteful branches such as those in Figure 7.10 exist because of the pruning.

Figure 7.12 shows the area and wall clock time space of the same 768 VESPA design points. This data includes the effect of clock frequency which decays only slightly throughout the designs up to 8 lanes but is eventually reduced by up to 25% in our largest designs (the points in the bottom right of the figure). Since these largest designs are also the fastest, the maximum speed achieved is reduced considerably by the clock frequency reduction. The design space spans 18x in wall clock time instead of the 24x spanned in cycle count. This is in line with the 25% performance reduction expected because of the clock frequency decay. Additional retiming or pipelining can mitigate this decay, motivating a separate VESPA pipeline for supporting many lanes or even a pipeline generator such as SPREE [69]. Nonetheless the design space is still very large and even the designs with reduced clock frequencies in the lower right corner of the figure provide useful pareto optimal design points.

Table 7.2: Pareto optimal VESPA configurations.

DD	DW	DPV	APB	B	MVL	L	M	X	Clock (MHz)	Vector Coproc. Area (Equiv. ALMs)	Normalized Wall Clock Time
8KB	16B	0	0	1	4	1	1	1	134	1838	18.91
8KB	16B	0	0	1	8	2	1	1	132	2415	14.46
8KB	16B	0	0	1	8	2	1	2	132	2503	13.15
8KB	16B	0	0	1	8	2	2	2	131	2646	11.07
8KB	16B	0	0	2	8	2	2	1	127	3209	10.90
8KB	16B	0	0	2	8	2	2	2	125	3290	10.15
8KB	16B	0	0	1	16	4	2	2	129	3650	8.92
8KB	16B	0	0	1	16	4	2	4	127	3804	8.35
8KB	16B	0	0	1	16	4	4	2	128	3825	8.02
8KB	16B	0	0	1	16	4	4	4	128	4015	7.26
8KB	16B	0	0	2	16	4	4	2	126	4848	7.25
8KB	16B	0	0	1	128	4	4	4	125	5168	7.12
8KB	16B	0	0	2	16	4	4	4	122	5207	6.90
8KB	16B	0	0	2	128	4	4	2	123	5620	6.74
32KB	64B	0	0	1	16	4	2	4	129	5983	6.64
32KB	64B	8*VL	0	1	16	4	2	4	129	5990	6.49
8KB	16B	0	0	1	32	8	4	4	123	5993	6.42
8KB	16B	0	0	2	128	4	4	4	121	5996	6.17
8KB	16B	0	0	1	32	8	8	4	124	6361	5.72
32KB	64B	7	0	1	16	4	4	2	128	6506	5.19
32KB	64B	7	0	1	16	4	4	4	128	6817	4.54
32KB	64B	7	0	2	16	4	4	2	124	7580	4.44
32KB	64B	7	0	2	16	4	4	4	121	7899	4.05
32KB	64B	7	0	2	128	4	4	2	123	8387	3.99
32KB	64B	8*VL	0	2	128	4	4	2	124	8463	3.90
32KB	64B	7	0	2	128	4	4	4	121	8671	3.50
32KB	64B	8*VL	0	2	128	4	4	4	121	8809	3.46
32KB	64B	8*VL	1	2	128	4	4	4	121	9363	3.37
32KB	64B	8*VL	0	1	32	8	8	4	123	10400	3.02
32KB	64B	7	0	1	32	8	8	4	123	10498	2.94
32KB	64B	7	0	1	32	8	8	8	125	10759	2.54
32KB	64B	8*VL	0	1	128	8	8	8	124	11603	2.45
32KB	64B	7	0	2	128	8	8	4	117	12177	2.35
32KB	64B	8*VL	0	2	128	8	8	4	119	12288	2.27
32KB	64B	7	0	2	128	8	8	8	118	12787	2.02
32KB	64B	8*VL	0	2	128	8	8	8	118	13341	2.00
32KB	64B	7	1	2	128	8	8	8	119	14123	1.98
32KB	64B	8*VL	1	2	128	8	8	8	119	14545	1.94
32KB	64B	8*VL	0	2	128	16	8	8	112	18414	1.91
32KB	64B	8*VL	0	1	64	16	16	8	116	18748	1.80
32KB	64B	8*VL	0	1	128	16	16	8	114	18872	1.80
32KB	64B	8*VL	0	2	128	16	8	16	111	19510	1.78
32KB	64B	8*VL	0	1	64	16	16	16	114	19777	1.64
32KB	64B	8*VL	0	1	128	16	16	16	115	19990	1.58
32KB	64B	8*VL	0	2	128	16	16	8	109	22653	1.55
32KB	64B	7	0	2	128	16	16	16	111	23837	1.38
32KB	64B	7	1	2	128	16	16	16	111	26256	1.37
32KB	64B	8*VL	1	2	128	16	16	16	111	26848	1.32
32KB	64B	7	0	1	128	32	32	32	96	36864	1.31
32KB	64B	8*VL	0	2	512	32	16	32	99	38871	1.30
32KB	64B	7	0	1	512	32	32	32	99	39841	1.28
32KB	64B	8*VL	0	1	512	32	32	32	99	39843	1.24
32KB	64B	8*VL	0	2	128	32	32	32	94	43449	1.24
32KB	64B	7	0	2	128	32	32	32	91	43675	1.24
32KB	64B	8*VL	0	2	512	32	32	32	92	45469	1.13
32KB	64B	8*VL	1	2	512	32	32	32	96	50950	1.08

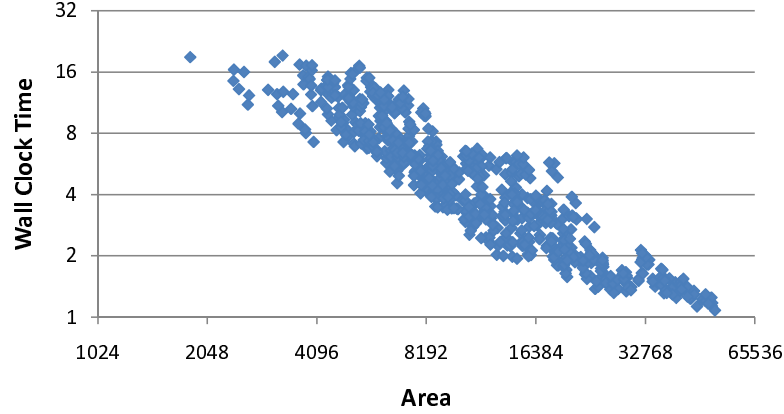


Figure 7.12: Average wall clock time and vector coprocessor area of 768 soft vector processor variations across the pruned design space. Area is measured in equivalent ALMs, while the wall clock time of each benchmark is normalized against the fastest achieved time across all configurations and then averaged using geometric mean.

Table 7.2 lists the pareto optimal VESPA configurations from the area/wall clock time design space. These 56 configurations dominate the rest of the 712 designs meaning only 7.3% of the design space was useful. While this analysis is based on an average across our benchmarks, on a per-application basis we expect a larger set of points to be useful. The table is sorted starting from the smallest area design at the top, to the largest at the bottom.

The smallest area design has 1 lane, 8KB data cache with 16B line size, MVL of 4, and no chaining, prefetching or heterogeneous lanes. There are few neighbouring points surrounding this configuration since most parameter values are not applicable or cause large area investments. More small designs can be found in this region by including more small MVL values in the exploration. As seen in Section 5.6 the MVL value can either modestly or substantially affect the area for designs with few lanes. Had our search space included a more fine-grain exploration of MVL values we would expect more neighbouring points around this smallest area design—our current exploration has only one low value of MVL ( $4 \times L$ ) with the next smallest value being 128 which is very large for a one-lane vector processor.

The pareto optimal configurations listed in the table highlight the contribution of the VESPA parameters in creating useful designs. The full range of MVL values and

vector lanes are used, many of them with half-sized crossbars, or half as many lanes with multipliers. All memory system configurations were used including all the prefetching strategies. Chaining varied between off and 2-way chaining through two banks—no pareto optimal points were created using 4-way chaining. Finally the ALU replication parameter, **APB**, was enabled for some of the designs with chaining. Overall we see that the architectural parameters in VESPA each provide an effective means of trading area for performance and each contribute towards selecting an efficient soft vector processor configuration.

The clock frequency of each configuration is shown in the third-last column of the table and quantifies the clock degradation previously discussed. The smallest configuration achieves 134 MHz while the largest is reduced to 96 MHz. In general the clock frequency is relatively stable across configurations with the same number of lanes. Despite the clock degradation, increasing the number of lanes still provides ample performance acceleration.

### 7.3.3 Per-Application Analysis

A key motivation for FPGA-based soft processors is their ability to be customized to a given application. This application-specific customization can aid FPGA designers in meeting their system constraints. Since these constraints vary from system to system, in the next two sections we examine the effect of two common cost functions: performance and performance-per-area.

#### 7.3.3.1 Fastest Per-Application Configurations

Across the complete 768-point design space the fastest overall processor is typically the fastest for each benchmark. Most of VESPA’s parameters trade additional area for increased performance, hence without an area constraint all benchmarks benefit from adding more lanes, bigger caches, and more chaining. The prefetching strategy and **MVL** value however can positively or negatively affect the performance for a given application. Aside from these two parameter the other parameters can only increase performance

Table 7.3: Configurations with best wall clock performance for each benchmark.

Application	VESPA Configuration									Performance vs GP
	DD	DW	DPV	APB	B	MVL	L	M	X	
autcor	32KB	64B	8*VL	1	2	512	32	32	32	1.000
conven	32KB	64B	7	1	2	512	32	32	16	1.036
rgbcmyk	32KB	64B	8*VL	1	2	512	32	32	16	1.022
rgbyiq	32KB	64B	8*VL	1	2	512	32	32	32	1.000
ip_checksum	32KB	64B	8*VL	1	2	128	32	32	16	1.260
imgblend	32KB	64B	8*VL	1	2	512	32	32	32	1.000
filt3x3	32KB	64B	8*VL	1	2	512	32	32	32	1.000
fbital	32KB	64B	8*VL	1	2	128	16	16	16	1.024
viterb	32KB	64B	8*VL	0	1	128	16	16	16	1.168
GEOMEAN										1.053
General Purpose (GP)	32KB	64B	8*VL	1	2	512	32	32	32	1

assuming clock frequency is not significantly reduced.

Table 7.3 shows the fastest configuration for each application. The last row shows the configuration that is the fastest on average across all the benchmarks, referred to as the *general purpose* configuration. All configurations have the same memory system including prefetching strategy except for CONVEN. With more fine grain exploration of prefetching strategies we would expect to see more variation here. But certainly all benchmarks benefit from the deeper and wider cache configuration.

The number of lanes is 32 across all configurations except for FBITAL and VITERB which are the benchmarks which scale the least. These two benchmarks are better served with the increased clock frequency of the 16 lane configurations over the 32-way parallelism of 32-lanes. Similarly CONVEN, RGBCMYK and IP\_CHECKSUM benefit from the slightly increased clock from eliminating half the multipliers. All other benchmarks have homogeneous lanes since there is no area incentive to reducing the number of functional units in this analysis. Two-way chaining and the APB parameter are enabled for all configurations except for VITERB which has insufficient DLP to exploit chaining and instead benefits from the slightly increased clock frequency attainable without chaining.

The last column shows how much faster the per-application configuration is compared to the general purpose configuration, and for most benchmarks there is little additional performance gained. In fact the general purpose configuration is identical to the fastest configurations for AUTCOR, RGBYIQ, IMGBLEND and FILT3X3. However the

Table 7.4: Configurations with best performance-per-area for each benchmark.

Application	VESPA Configuration									Performance per Area vs GP
	DD	DW	DPV	APB	B	MVL	L	M	X	
autcor	8KB	16B	0	0	2	128	8	8	8	1.068
conven	32KB	64B	8*VL	0	2	128	8	8	4	1.054
rgbcmk	32KB	64B	8*VL	0	1	64	16	16	8	1.071
rgbyiq	32KB	64B	7	0	2	128	16	16	16	1.058
ip_checksum	32KB	64B	7	0	2	32	8	8	4	1.087
imgblend	32KB	64B	7	0	2	128	16	16	16	1.025
flt3x3	32KB	64B	8*VL	0	4	512	16	16	16	1.070
fbital	8KB	16B	0	0	1	32	8	4	8	1.246
viterb	8KB	16B	0	1	2	4	1	1	1	1.356
GEOMEAN										1.110
General Purpose (GP)	32KB	64B	7	0	2	128	8	8	8	1

IP\_CHECKSUM benchmark is significantly faster with a smaller MVL value than the general purpose configuration. A 26% speed improvement is seen as a result of the shorter time required to sum all the elements in a vector. The VITERB configuration gains 17% performance due largely to clock frequency.

On average the fastest per-application configuration is 5.3% faster than the general purpose configuration, but most of this is due to the large performance difference seen with IP\_CHECKSUM and VITERB. To better understand the efficiency gained by selecting a processor on a per-application basis, one must consider the area costs in addition to performance. Focussing only on performance acceleration leads to exorbitant area investments for small performance improvements. In actual fact, other computations could potentially use available FPGA area to more dramatically accelerate their execution and better serve the complete system. We therefore seek configuration with the best performance-per-area.

### 7.3.3.2 Best Performance-Per-Area Configurations

Performance-per-area is a commonly used metric for measuring efficiency which considers both performance and area. To calculate performance-per-area we take the inverse of the product between area and wall clock time, both measured as described in Chapter 3. The measured area includes the complete processor system excluding the memory controller and host communication hardware; the wall clock time is measured on the DE3 platform.

Table 7.4 shows the VESPA configuration with the best performance-per-area for each benchmark selected out of the 768 explored designs. The last row shows the general purpose configuration that achieves the best performance-per-area averaged arithmetically across all benchmarks. The per-application configurations can achieve up to 35.6% (average of 11%) better performance-per-area over the general purpose configuration. The selected configurations for each benchmark vary significantly from the general purpose 8-lane configuration with  $MVL=128$ , 2 banks, 32KB data cache, 64B line size, and 7 cache line prefetching. Three of the benchmarks work best instead for the  $8*VL$  prefetching strategy, while another three select the smaller cache which does not support prefetching. The number of lanes selected is typically 8 or 16 since 32-lane configurations require significant area and also suffer from a significant clock frequency degradation. The VITERB benchmark being one of the least data-parallel applications benefits most from exploiting a high degree of chaining on a 1-lane soft vector processor. This configuration is certainly the most interesting as it differs the most from the general purpose and improves performance-per-area by 35.6%. The VITERB configuration has 2 banks and is the only one that benefits from enabling the APB parameter. The selected architecture is similar to a scalar processor except the vector instructions are issued up to two per cycle across the two ALUs, one multiplier, and the memory unit. Surprisingly, for this benchmark this is more efficient in terms of performance-per-area than a 2-lane configuration.

The FBITAL benchmark achieves 24.6% better performance-per-area than the general purpose configuration. This is gained largely by the half-sized crossbar and the reduced vector state from the decreased  $MVL$ . Further area savings is gained by disabling chaining in this configuration. The FILT3X3 benchmark selects the largest configuration with 4 banks,  $MVL=512$  and 16 homogeneous lanes achieving 7% improved performance-per-area over the general purpose. The benchmarks with little or no multiply operations are seen to employ heterogeneous lanes reducing the number of lanes with multipliers. This is seen in CONVEN, RGBCMYK, and IP\_CHECKSUM.

With the exception of VITERB the benchmarks are characteristically similar: streaming-

oriented across a large data set. With greater benchmark diversity we expect the improvements in selecting a per-application configuration to be significantly higher. Nonetheless, these improvements highlight the value in matching the soft vector processor architecture to the application.

## 7.4 Eliminating Functionality

All architectural parameters explored so far traded area and performance while preserving functionality. But if a soft processor need only execute one application, or the FPGA can be reconfigured between runs of different applications, one can create a highly-customized soft processor with only the functionality needed by the current application. In this section we target and automatically eliminate two key general purpose overheads: (i) the datapath width, since many applications do not require full 32-bit processing (we refer to this customization as *width reduction*); and (ii) the hardware support for instructions which do not exist in the application (we refer to this as *subsetting* or *instruction set subsetting*). We begin by analyzing the opportunity for customizing along these two axes. Note that both customizations reduce area without altering the cycle-behaviour of the vector processor.

### 7.4.1 Hardware Elimination Opportunities

The effectiveness of width reduction and instruction set subsetting are very application-dependent. Width reduction is effective when applications use less than the full 32-bit lane-width. Subsetting is effective if applications use only few vector instructions. Before implementing these customizations we predict their effectiveness by analyzing our benchmarks.

For width reduction, we inspect the source code and determine the maximum-sized vector element needed for each benchmark. This is done conservatively according to the variable types used in the C code and is then verified by executing the benchmark

Table 7.5: Hardware elimination opportunities across all benchmarks.

Benchmark	Largest Data Type Size	Percent of Supported VIRAM ISA used
AUTCOR	32 bits	9.6%
CONVEN	1 bit	5.9%
FBITAL	16 bits	14.1%
VITERB	16 bits	13.3%
RGBCMYK	8 bits	5.9%
RGBYIQ	16 bits	8.1%
IP_CHECKSUM	32 bits	8.1%
IMGBLEND	8 bits	7.4%
FILT3X3	8 bits	7.4%

in hardware on a VESPA configuration with reduced width. More aggressive width reduction can consider the data set and determine for example that despite using a 16-bit data type, the application requires only 11 bits. The BitValue compiler is an example of such a system [11]. In general we do not perform this aggressive customization except for the case of CONVEN which by inspection uses only 1-bit data elements and provides a best-case width-reduction result.

Table 7.5 shows the largest data type size used by each benchmark in the middle column. All benchmarks except AUTCOR and IP\_CHECKSUM use less than 32-bit data types hence providing ample opportunity for width reduction in the vector lanes. Three of the benchmarks, RGBCMYK, IMGBLEND and FILT3X3 use only 8-bit data types, while CONVEN uses only 1-bit binary values. These four benchmarks present the most opportunity for area savings through width reduction.

Table 7.5 shows the percentage of the total supported vector instruction set used by each benchmark. These values were determined by extracting the number of unique vector instructions that exist in a binary and dividing by the total number of vector instructions VESPA supports. Less than 10% of the vector instruction set is used in all benchmarks except for FBITAL and VITERB. For these two benchmarks 14.1% and 13.3% of the vector instruction set is used respectively. With all benchmarks using less than 15%, the opportunity for subsetting appears promising. These usages may not correlate

with the area savings achieved through subsetting since eliminating instruction variants may remove some multiplexer paths, but larger savings are achieved when whole functional units are removed. Because of this, the *specific* instructions used by the application can have a big impact on the area savings.

Overall, the values in the table motivate the pursuit of both of these customization techniques. Note that no benchmark was modified to aid or exaggerate the impact of these techniques. Certainly more aggressive customization can re-code benchmarks to use reduced widths and fewer instruction types, but our results are based on unmodified original versions of our benchmarks.

#### 7.4.2 Impact of Vector Datapath Width Reduction (W)

The width of each lane can be modified by simply changing the  $W$  parameter in the VESPA Verilog code which will automatically implement the corresponding width-reduced vector coprocessor. Although a 1-bit datapath can, with some hardware overhead, continue to support 32-bit values, VESPA does not insert this bit-serialization hardware overhead. Therefore a soft vector processor with lane width  $W$  will only correctly execute benchmarks if their computations do not exceed  $W$  bits. The area of a conventional hard vector processor cannot be reduced once it is fabricated, so designers opt instead to dynamically (with some area overhead) reclaim any unused vector lane datapath width to emulate an increased number of lanes, hence gaining performance. Our current benchmarks typically operate on a single data width, making support for dynamically configuring vector lane width and number of lanes uninteresting—however for a different set of applications this could be motivated.

Figure 7.13 shows the effect of width reduction on a 16-lane VESPA with full memory crossbar and 16KB data cache with 64B cache line size. Starting from a 1-bit vector lane width we double the width until reaching the full 32-bit configuration. The area is reduced to almost one-quarter in the 1-bit configuration with further reduction limited due to the control logic, vector state, and address generation which are unaffected by

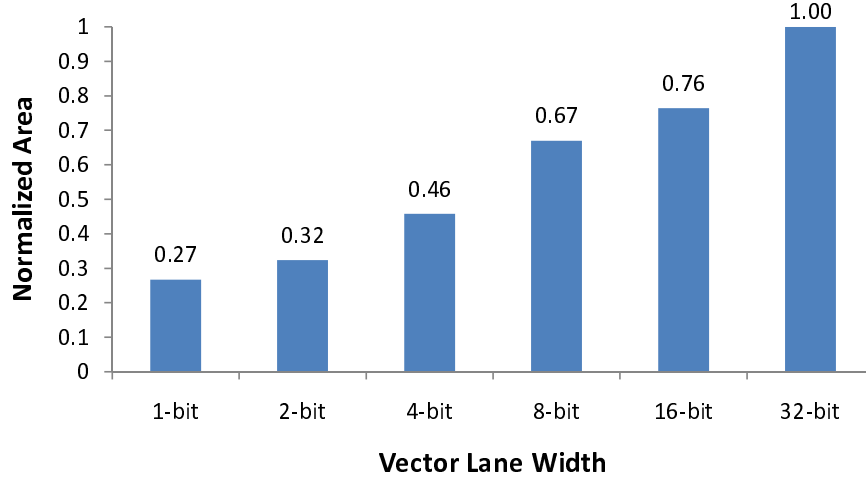


Figure 7.13: Area of vector coprocessors with different lane widths normalized against the full 32-bit configuration. All configurations have 16 lanes with full memory crossbar and 16KB data cache with 64B cache lines.

Table 7.6: Area after width reduction across benchmarks normalized to 32-bit width.

Benchmark	Largest Data Type Size	Normalized Area
AUTCOR	32 bits	1.00
CONVEN	1 bit	0.27
FBITAL	16 bits	0.76
VITERB	16 bits	0.76
RGBCMYK	8 bits	0.67
RGBYIQ	16 bits	0.76
IP_CHECKSUM	32 bits	1.00
IMGBLEND	8 bits	0.67
FILT3X3	8 bits	0.67
GEOMEAN		0.69

width reductions. A 2-bit width saves 68% area and is only slightly larger than the 1-bit configuration. Substantial area savings is possible with wider widths as well: a one-byte or 8-bit width eliminates 33% area, while a 16-bit width saves 24% of the area.

Table 7.6 lists the normalized area for each benchmark determined by matching the benchmark to a given width-reduced VESPA using Table 7.5. On average the area is reduced by 31% across our benchmarks including the two benchmarks which require 32-bit vector lane widths. These area savings decrease the area cost associated with each lane enabling low-cost lane scaling at the expense of reduced general purpose functionality.

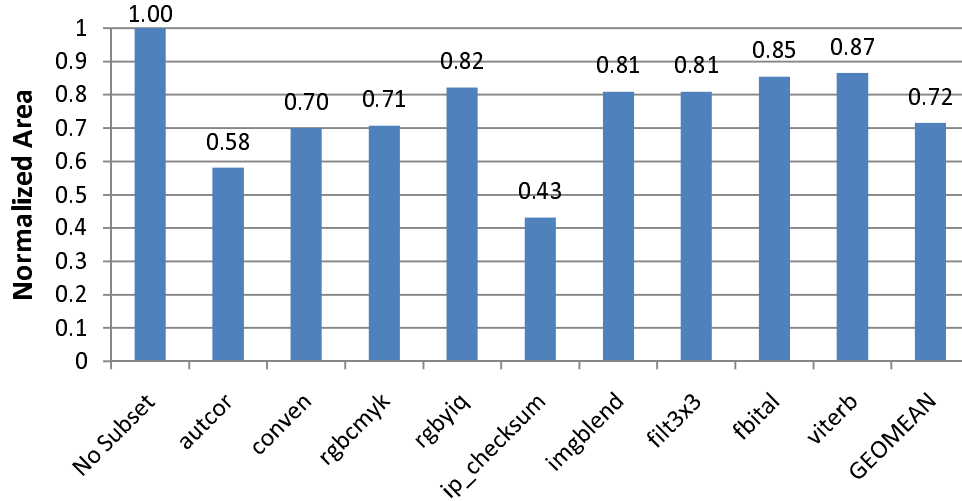


Figure 7.14: Area of the vector coprocessor after instruction set subsetting which eliminates hardware support for unused instructions. All configurations have 16 lanes with full memory crossbar and 16KB data cache with 64B cache lines. All area measurements are relative to the full un-subsetted VESPA.

### 7.4.3 Impact of Instruction Set Subsetting

In VESPA one can disable hardware support for any unused instructions by simply changing the opcode of a given instruction to the Verilog unknown value `x`. Doing so automatically eliminates control logic and datapath hardware for those instructions as discussed in Appendix C. If all the instructions that use a specific functional unit is removed, the whole functional unit is eliminated from all vector lanes. In the extreme case, disabling all vector instructions eliminates the entire vector coprocessor unit. To perform the reduction we developed a tool that parses an application binary and automatically disables unused instructions using the method described above. This is a conservative reduction since it depends on the compilers ability to remove dead code and is independent of the data set. In some cases a user may want to support only a specific path through their code, in which case a trace of the benchmark can reveal which instructions are never executed and can be disabled.

Figure 7.14 shows the area of the resulting subsetting vector coprocessors for each benchmark using a base VESPA configuration with 16 lanes, full memory crossbar, 16KB data cache, and 64B cache lines. Up to 57% of the area is reduced for IP\_CHECKSUM which

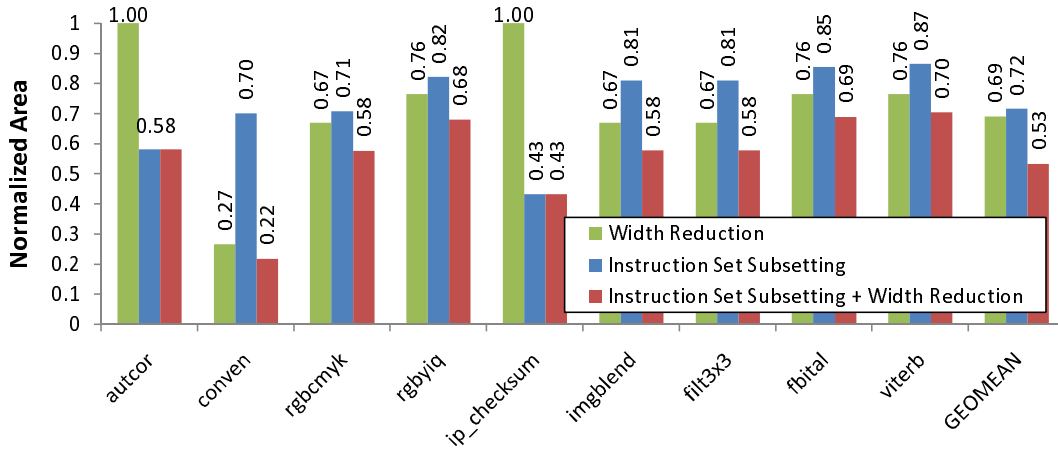


Figure 7.15: Area of the vector coprocessor after eliminating both unused lane-width and hardware support for unused instructions. All configurations have 16 lanes with full memory crossbar and 16KB data cache with 64B cache lines. All area measurements are relative to the full un-customized VESPA.

requires no multiplier functional unit and no support for stores which eliminates part of the memory crossbar. Similarly AUTCOR has no vector store instructions resulting in the second largest savings of 42% area despite using all functional units. The benchmarks CONVEN and RGBCMYK can eliminate the multiplier only resulting in 30% area savings while the remaining benchmarks cannot eliminate any whole functional unit. In those cases removing multiplexer inputs and support for instruction variations results in savings between 15-20% area. Across all our benchmarks a geometric mean of 28% area savings is achieved.

#### 7.4.4 Impact of Combining Width Reduction and Instruction Set Subsetting

We can additionally customize both the vector width and the supported instruction set of VESPA for a given application, thereby creating highly area-reduced VESPA processors with identical performance to a full VESPA processor. Since these customizations overlap, we expect that the savings will not be perfectly additive: for example, the savings from reducing the width of a hardware adder from 32-bits to 8-bits will disappear if that adder is eliminated by instruction set subsetting.

Figure 7.15 shows the area savings of combining both the width reduction and the

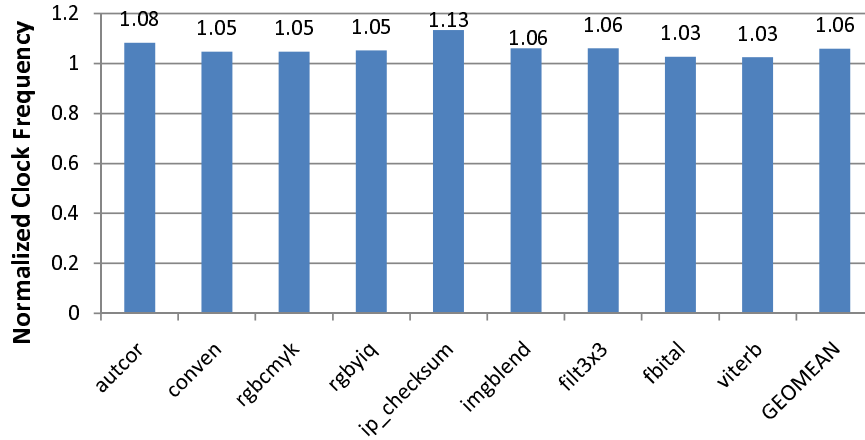


Figure 7.16: Normalized clock frequency of VESPA after eliminating both unused lane-width and hardware support for unused instructions. All configurations have 16 lanes with full memory crossbar and 16KB data cache with 64B cache lines. All clock frequency measurements are relative to the full un-customized VESPA.

instruction set subsetting. For comparison, on the same figure are the individual results from width reduction and instruction set subsetting. The CONVEN benchmark can have 78% of the VESPA vector coprocessor area eliminated through subsetting and reducing the datapath width to 1 bit. Except for the cases where width-reduction is not possible, the combined approach provides additional area savings over either technique alone. Compared to the average 31% from width reduction and 28% from subsetting, combining the two produces average area savings of 47%. This is an enormous overall area savings, allowing FPGA designers to scale their soft vector processors to 16 lanes with almost half the area cost of a full general-purpose VESPA.

Performing either of these hardware elimination customizations often has the beneficial side-effect of raising the clock frequency. We measure the impact on clock frequency after applying both instruction set subsetting and width reduction on the same 16-lane VESPA which has a clock frequency of 117 MHz and has full memory crossbar and 16KB data cache with 64B line size. Figure 7.16 depicts the clock frequency gains achieved for that VESPA customized to each application. As expected, the benchmarks which enabled the most area reduction also achieved the highest clock frequency gains. IP\_CHECKSUM achieves a 13% clock frequency gain and AUTCOR achieves an 8% gain. The remaining

benchmarks experience between 3% and 6% clock frequency improvements for an overall average of 6% faster clock than without subsetting and width reduction.

## 7.5 Summary

The reprogrammable fabric of FPGAs allows designers to choose an exact-fit processor solution. In the case of soft vector processors the most powerful parameter is the number of vector lanes which can be chosen depending on the amount of data level parallelism in an application. But this decision can also be influenced by other architectural parameters presented in this chapter which can change the area costs and speed improvements of adding more lanes.

We implemented heterogeneous lanes allowing the designer to reduce the number of lanes which support multiplication, as well as the number of lanes connected to the memory crossbar. With this ability, a designer can conserve FPGA multiply-accumulate blocks for applications with few multiplication and shift operations, and also reduce the size of the memory crossbar for applications with low demand of the memory system.

An FPGA-specific implementation of chaining was added to VESPA without requiring the large many-ported register files typically used. By interleaving across register file banks chaining can dispatch as many instructions as there are banks. We scale the banks up to 4 and observe significant performance improvements over no chaining. In addition by replicating the ALU within each lane we increase the likelihood of dispatching multiple vector instructions hence further increasing performance albeit at a substantial area cost.

The resulting design space of VESPA was explored after pruning it to 768 useful design points. The design space spanned 28x in area and 24x in cycle count (18x in wall clock time). Using VESPA's many architectural parameters this broad space was effectively filled in allowing precise selection of the desired area/performance. Also, significant improvements were observed when selecting a per-application configuration over the fastest or best performance-per-area over all our benchmarks, despite the similar

characteristics in these benchmarks.

Finally, we examined the area savings in removing unneeded datapath width for benchmarks that do not require full 32-bit processing. Lanes were shrunk to as small as 1-bit achieving a size almost one-fourth the original vector coprocessor area. We also implemented and evaluated our infrastructure for automatically parsing an application binary and removing all control and datapath hardware for vector instructions that do not appear in the binary. In the best case this instruction set subsetting can eliminate more than half the vector coprocessor area. Combining both techniques yields area savings as high as 78% and on average 47%.

## Chapter 8

# Soft Vector Processors vs Manual FPGA Hardware Design

The aim of this thesis is to enable easier creation of computation engines using software development instead of through more difficult hardware design. This is done by offering FPGA designers the option of scaling the performance of data parallel computations using a soft vector processor. The previous chapter showed that a broad space of VESPA configurations exists, but deciding on any of these configurations intelligently requires analysis of the costs and benefits of using a soft vector processor instead of manually designing FPGA hardware. While it is difficult to measure the ease of use benefit, it is possible to quantify the concrete aspects of performance and area. In this chapter we answer the question of *how does the area and performance of a soft vector processor compare to hardware?* With this information an FPGA designer can more accurately assess the costs and benefits of either implementation, including a scalar soft processor implementation, and select the implementation that best meets the needs of the system. Moreover, this data enables us to benchmark the progress of this research in having vector-extended soft processors compete with manual hardware design.

Previous works [27, 58] studied the benefits of FPGA hardware versus hard processors without considering soft processors. Soft vector processors were compared against

automatically generated hardware from the Altera C2H behavioural synthesis tool and found to achieve better scalability for 16-way parallelism and beyond [75]. Our comparison differs by comparing soft vector processors to custom-made FPGA hardware which is the most likely alternative to a soft processor implementation.

We compare the area and performance of the following three implementations of our benchmarks created via different design entry methods: (i) out-of-the-box `C` code executed on the MIPS-based SPREE scalar soft processor; (ii) hand-vectorized assembly language executed on many variations of our VESPA soft vector processor; and (iii) hardware designed manually in Verilog at the register transfer level. This comparison was initially evaluated on the TM4 platform [73] but in this thesis we use the newer DE3 board. While our DE3-based infrastructure is well equipped for evaluating the first scalar and vector processors, evaluating hardware requires manual design of hardware circuits from a `C` benchmark. To design and evaluate such a circuit with the same realism used to evaluate the processors would require many weeks or months for each benchmark. We hence simplify the hardware design process as described in the next section.

## 8.1 Designing Custom Hardware Circuits

We created custom FPGA hardware by manually converting each benchmark into a Verilog hardware circuit. Two factors heavily influence the implementation of this hardware circuit: (i) the assumed system-level design constraints require certain levels of performance as well as communication with specific peripherals; and (ii) the idealized assumptions we made to simplify and reduce the design time for each hardware circuit. Both of these are described below.

### 8.1.1 System-Level Design Constraints

For any given application, there are many hardware design variations ranging from area-optimized 1-bit datapaths to extremely parallel high-performance implementations. In

this work we focus on performance and implement the latter. Similarly, the peripherals used in the design will greatly influence its implementation. For example, a circuit that receives its data from on-chip SRAM may be designed significantly different than a circuit relying on serial RS-232 communication for its data. To fairly compare the hardware circuits with the processor implementations, we use similar memories for the data storage in both. Specifically we apply the following constraints on the hardware system to match those in the processors:

1. **Memory Width** – There is only one 128-bit wide path to memory, hence we assume a typical 64-pin (128 bits per clock) double data rate DRAM module.
2. **Memory Usage** – Input/output data starts/ends in memory. Internal storage can be used for any partial or temporary results, but the final result must be written to memory.
3. **No Value Optimizations** – All input data is assumed to be unknown at design-time—i.e., we perform no value-specific or value-range-specific optimizations.

We expect that without these constraints, the performance of the hardware circuits could be increased more than that of the processors. However to experimentally evaluate this would require re-engineering of the SPREE and VESPA soft processors and modification of the benchmarks. To avoid this added effort we apply these constraints to the hardware and as a result constrain the hardware design with conservative design assumptions.

### 8.1.2 Simplifying Hardware Design Optimistically

The design of custom FPGA hardware requires months of effort to plan, implement, and verify. Indeed, the complications associated with this effort motivate the introduction of soft vector processors to reduce the amount of hardware design required in a digital system. Rather than embracing these complications and pursuing full and complete hard-

ware implementations for each benchmark, we make the following optimistic assumptions to make this comparison measurement tractable in the time available.

1. **Benchmark Selection** – Hardware implementations were designed for six out of the nine benchmarks—FBITAL, VITERB, and FILT3X3 were excluded because of their relative complexity which would have resulted in extremely difficult hardware implementations. The six remaining benchmarks are very streaming-oriented resulting in simpler datapath designs. A key side-effect of this simplification is that these benchmarks can readily take advantage of parallel hardware circuits. This makes the simplification optimistic for the hardware since benchmarks with more complicated control would perform more similar to a processor.
2. **Datapath Only** – Any control logic or hardware for sending requests to/from the memory controller is assumed to have negligible size and ideal performance in both clock frequency and cycle count. In other words, only the datapath of the circuits are designed assuming input and output data streams are already entering and exiting the circuit. This assumption is optimistic in general but more reasonable for our benchmarks which access mostly contiguous arrays which can be tracked with a single counter and streamed at the highest memory bandwidth.
3. **No Datapath Stalls** – The datapath is fully pipelined, requires no stalls, and assumes a continuous flow of data, and hence does not implement stalling/buffering logic needed to handle data flow interruptions caused by DRAM refreshing for example. This is also optimistic but in the context of our streaming benchmarks with very predictable memory accesses, many data stalls can be avoided or hidden.
4. **Memory Alignment** – Data is assumed to be aligned in memory to the nearest 128-bit boundary, eliminating the need for shifting and alignment logic. This provides a significant area advantage for some benchmarks which would otherwise require a memory crossbar similar to that in VESPA.

5. **Memory Speed** – We do not let the speed of the memory limit the performance of the hardware circuits. In other words, we allow the 128-bit words to be transmitted at the full clock rate of the hardware circuit despite the fact that this clock rate is faster than the DDR2 DIMM used on the DE3 platform for the soft processors.

In summary, we build only the datapath of the circuit for the most streaming-oriented benchmarks under optimistic assumptions about the control logic and transfer of data. The memory being modelled is effectively an on-chip memory with a single 128-bit wide port. This assumption is a valid approximation since the latency of an off-chip memory could be amortized over the large contiguous access patterns in the benchmarks. Nonetheless, our idealizations imply that 100% of the memory bandwidth is utilized by the hardware circuit, while our consultations with industry revealed that typical FPGA system designers have difficulty achieving 50% utilization [9]. Hence, our simple benchmarks and simplifying assumptions have significantly idealized our hardware results meaning this study can be interpreted as an upper-bound on the advantages of custom hardware circuits.

As an example, consider the `IP_CHECKSUM` benchmark which simply sums all the 16-bit elements in an array. The hardware circuit used to implement this benchmark is shown in Figure 8.1. Since the array is stored contiguously in memory we can assume 8 16-bit words arrive from the 128-bit memory every clock cycle. Because addition is commutative we can separately accumulate the 8 words each in their own register. After the entire array has been processed we can reduce the 8 sums via an adder tree into a single 32-bit scalar sum. The circuit shown is easy to build since it neglects the cycle-to-cycle behaviour of control logic and data arrival, yet it captures the most significant part of the overall area.

Although not quantified, we can qualitatively discuss the components missing from the circuit and approximate their contribution to overall area. Missing from the figure is a counter which stores and increments the address currently being accessed in the array. Similarly absent is another counter for tracking the total progress and signalling when

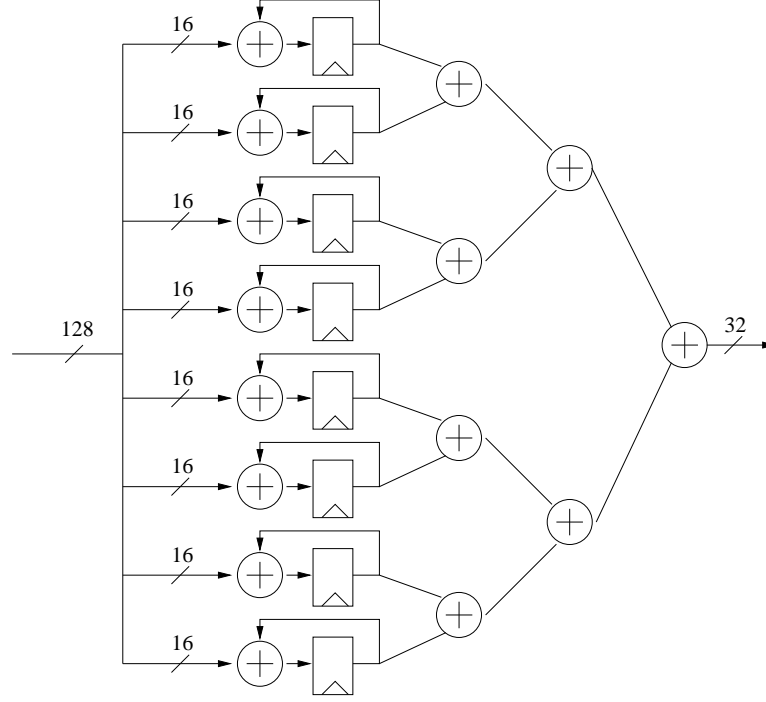


Figure 8.1: Hardware circuit implemented for IP\_CHECKSUM.

the final accumulation is valid. Also not included are enable signals for disabling the accumulation of data not part of the array—for example the first word of the array may not be aligned to the boundary of the 128-bit DRAM word. This disabling logic would be very small, especially compared to the vector memory crossbar required to map words to vector lanes. In total the area of these missing components would still be small compared to the 15 adders in the circuit.

## 8.2 Evaluating Hardware Circuits

While the evaluation of the scalar and vector soft processors is identical to that described in Chapter 3 (with the area excluding the memory controller and host communication hardware), the evaluation of the hardware circuits requires a slightly modified methodology due to their simplified and incomplete nature. For example, with an incomplete hardware design, performance can only be modelled rather than evaluated in a real system as is done for VESPA. The details of the measurement methodology used and the

performance modelling are discussed below.

### 8.2.1 Area Measurement

The hardware circuits are synthesized for the Stratix III FPGA on our DE3 platform using the same method for measuring actual silicon area of the design in equivalent ALMs as discussed in Chapter 3. Only the datapath is synthesized assuming, as mentioned previously, that control logic and memory request logic for communicating with the memory can be implemented with negligible area.

### 8.2.2 Clock Frequency Measurement

The clock frequency of the hardware circuits is measured through a full synthesis onto the FPGA over multiple seeds in the manner described in Chapter 3.

### 8.2.3 Cycle Count Measurement

Cycle count performance is modelled by considering the transfer of the data set through the pipelined datapath, which performs the computation as the data flows through the pipeline. As previously mentioned it is assumed that 128 bits are transferred on every clock cycle at the clock speed of the hardware circuit which is faster than the DIMM on the DE3. Therefore, to transfer the 40960 bytes of input data for the IP\_CHECKSUM benchmark requires 2560 clock cycles. Then, to transfer the 40 bytes of output data requires 3 cycles. The 4-cycle latency through the pipeline is also added to the cycle count yielding a total of  $2560 + 3 + 4 = 2567$  clock cycles for the IP\_CHECKSUM benchmark. In general the equation for calculating cycle performance of a streaming benchmark is given by

$$N_{cycles} = InputBytes/16 + OutputBytes/16 + pipeline\_latency \quad (8.1)$$

where *InputBytes* are the number of bytes in the input data set, *OutputBytes* are the number of bytes in the output data set, and *pipeline\_latency* is the number of stages in

the pipeline. All computations are performed in a pipelined fashion in parallel with the transfer of data, which is measured in the first two terms in the equation. For example, the circuit for IP\_CHECKSUM is computing the checksum across some data values at the same time that later data is being fetched into the datapath. As discussed earlier, we assume memory latency can be hidden because of the sequential memory accesses in our benchmarks. As a consequence, this makes our results equivalent to being executed using 128-bit wide on-chip block RAMs for memory.

#### 8.2.4 Area-Delay Product

For a given digital system, there may be a heavier emphasis on area than performance, or vice-versa. However, it is important to have an understanding of the overall performance-per-area of candidate designs motivating us to measure *area-delay product* as is traditionally done for digital circuits. We use the silicon area measured in equivalent ALMs for area and the wall-clock-time of benchmark execution as the delay. The wall-clock-time is measured by multiplying the cycle counts with the minimum clock period reported by the CAD tools.

### 8.3 Implementing Hardware Circuits

The six selected benchmarks were implemented in Verilog under the constraints and optimistic simplifications discussed earlier. Each circuit was tested in simulation using test vectors to ensure the correct compute elements exist in the datapath.

Table 8.1 lists the FPGA resources used, clock rates, and cycle counts for each benchmark circuit. The number of ALMs is relatively small compared to VESPA, especially for CONVEN and IP\_CHECKSUM. Some of this is due to our assumptions about the negligible area consumed by control logic and memory request logic.

The table also shows the extraordinarily high clock frequencies achieved by the hardware circuits. Clock rates range between 274-476 MHz, all faster than the 266 MHz of

Table 8.1: Hardware circuit area and performance.

Benchmark	ALMs	DSPs (18-bit)	M9Ks	Clock (MHz)	Cycles
AUTCOR	592	32	1	323	1057
CONVEN	46	0	0	476	226
RGBCMYK	527	0	0	447	237784
RGBYIQ	706	108	0	274	144741
IP_CHECKSUM	158	0	0	457	2567
IMGBLEND	302	32	0	443	14414

our DDR2 DIMM on the DE3 proving that the hardware is further advantaged by having memory bandwidth modelled faster than what is available to the scalar and vector soft processors on the DE3 platform. These clock frequencies are significantly faster than what we expect in a typical system—as a point of comparison the Altera Nios II soft processor can be clocked at only 250 MHz. Nonetheless we use these measured clock frequencies in our analysis hence presenting an upper bound on the performance of the hardware circuits.

## 8.4 Comparing to Hardware

Once the area, cycle performance, and clock frequency of each hardware circuit is measured, we can compare them against that achieved in software using either a scalar soft processor or a soft vector processor. We measure the area and wall clock time for the scalar SPREE core described in Chapter 5, Section 5.3.1, and across the pareto optimal VESPA designs from Chapter 7, Section 7.3. We compare how much larger these implementations are relative to the hardware, referred to as the *hardware area advantage*, and how much slower they are in terms of wall clock time, referred to as the *hardware speed advantage*.

### 8.4.1 Software vs Hardware: Area

Table 8.2 shows the hardware area advantage over the scalar SPREE soft processor and the pareto optimal VESPA configurations. This is measured using the equation in

Table 8.2: Area advantage for hardware over various processors

Processor									Clock	Area ( $A_{processor}/A_{hw}$ )						
DD (KB)	DW (B)	DPV	APB	B	MVL	L	M	X		AUTCOR	CONVEN	RGB- CMYK	RGB- YIQ	IP-CH- ECKSUM	IMG- BLEND	GEO MEAN
8	16	0			Scalar				143	2.9	69.5	6.1	1.4	20.2	4.3	7.3
8	16	0	0	1	4	1	1	1	134	4.6	109.5	9.6	2.3	31.9	6.7	11.5
8	16	0	0	1	8	2	1	1	132	5.2	122.1	10.7	2.5	35.5	7.5	12.9
8	16	0	0	1	8	2	1	2	132	5.3	124.0	10.8	2.6	36.1	7.6	13.1
8	16	0	0	1	8	2	2	2	131	5.4	127.1	11.1	2.6	37.0	7.8	13.4
8	16	0	0	2	8	2	2	1	127	5.9	139.3	12.2	2.9	40.6	8.5	14.7
8	16	0	0	2	8	2	2	2	125	6.0	141.1	12.3	2.9	41.1	8.7	14.9
8	16	0	0	1	16	4	2	2	129	6.3	148.9	13.0	3.1	43.3	9.1	15.7
8	16	0	0	1	16	4	2	4	127	6.5	152.2	13.3	3.2	44.3	9.3	16.0
8	16	0	0	1	16	4	4	2	128	6.5	152.7	13.3	3.2	44.5	9.4	16.1
8	16	0	0	1	16	4	4	4	128	6.6	156.8	13.7	3.3	45.7	9.6	16.5
8	16	0	0	2	16	4	4	2	126	7.4	174.9	15.3	3.6	50.9	10.7	18.4
8	16	0	0	1	128	4	4	4	125	7.7	181.9	15.9	3.8	53.0	11.2	19.2
8	16	0	0	2	16	4	4	4	122	7.7	182.7	16.0	3.8	53.2	11.2	19.3
8	16	0	0	2	128	4	4	2	123	8.1	191.7	16.7	4.0	55.8	11.8	20.2
32	64	0	0	1	16	4	2	4	129	8.5	199.6	17.4	4.1	58.1	12.2	21.0
32	64	8VL	0	1	16	4	2	4	129	8.5	199.8	17.4	4.1	58.2	12.3	21.1
8	16	0	0	1	32	8	4	4	123	8.5	199.8	17.4	4.1	58.2	12.3	21.1
8	16	0	0	2	128	4	4	4	121	8.5	199.9	17.4	4.1	58.2	12.3	21.1
8	16	0	0	1	32	8	8	4	124	8.8	207.8	18.1	4.3	60.5	12.7	21.9
32	64	7	0	1	16	4	4	2	128	8.9	211.0	18.4	4.4	61.4	12.9	22.2
32	64	7	0	1	16	4	4	4	128	9.2	217.8	19.0	4.5	63.4	13.4	22.9
32	64	7	0	2	16	4	4	2	124	9.9	234.3	20.5	4.9	68.2	14.4	24.7
32	64	7	0	2	16	4	4	4	121	10.2	241.3	21.1	5.0	70.2	14.8	25.4
32	64	7	0	2	128	4	4	2	123	10.7	251.9	22.0	5.2	73.3	15.4	26.5
32	64	8VL	0	2	128	4	4	2	124	10.7	253.5	22.1	5.3	73.8	15.5	26.7
32	64	7	0	2	128	4	4	4	121	10.9	258.0	22.5	5.4	75.1	15.8	27.2
32	64	8VL	0	2	128	4	4	4	121	11.1	261.0	22.8	5.4	76.0	16.0	27.5
32	64	8VL	1	2	128	4	4	4	121	11.6	273.1	23.8	5.7	79.5	16.7	28.8
32	64	8VL	0	1	32	8	8	4	123	12.5	295.6	25.8	6.1	86.1	18.1	31.2
32	64	7	0	1	32	8	8	4	123	12.6	297.8	26.0	6.2	86.7	18.3	31.4
32	64	7	0	1	32	8	8	8	125	12.9	303.4	26.5	6.3	88.3	18.6	32.0
32	64	8VL	0	1	128	8	8	8	124	13.6	321.8	28.1	6.7	93.7	19.7	33.9
32	64	7	0	2	128	8	8	4	117	14.2	334.3	29.2	6.9	97.3	20.5	35.2
32	64	8VL	0	2	128	8	8	4	119	14.3	336.7	29.4	7.0	98.0	20.6	35.5
32	64	7	0	2	128	8	8	8	118	14.7	347.5	30.3	7.2	101.2	21.3	36.6
32	64	8VL	0	2	128	8	8	8	118	15.2	359.6	31.4	7.5	104.7	22.1	37.9
32	64	7	1	2	128	8	8	8	119	16.0	376.6	32.9	7.8	109.6	23.1	39.7
32	64	8VL	1	2	128	8	8	8	119	16.4	385.7	33.7	8.0	112.3	23.7	40.7
32	64	8VL	0	2	128	16	8	8	112	19.9	469.9	41.0	9.7	136.8	28.8	49.5
32	64	8VL	0	1	64	16	16	8	116	20.2	477.1	41.6	9.9	138.9	29.3	50.3
32	64	8VL	0	1	128	16	16	8	114	20.3	479.8	41.9	10.0	139.7	29.4	50.6
32	64	8VL	0	2	128	16	8	16	111	20.9	493.7	43.1	10.2	143.7	30.3	52.0
32	64	8VL	0	1	64	16	16	16	114	21.2	499.5	43.6	10.4	145.4	30.6	52.6
32	64	8VL	0	1	128	16	16	16	115	21.4	504.1	44.0	10.5	146.8	30.9	53.1
32	64	8VL	0	2	128	16	16	8	109	23.8	562.0	49.1	11.7	163.6	34.5	59.2
32	64	7	0	2	128	16	16	16	111	24.9	587.7	51.3	12.2	171.1	36.0	61.9
32	64	7	1	2	128	16	16	16	111	27.1	640.3	55.9	13.3	186.4	39.3	67.5
32	64	8VL	1	2	128	16	16	16	111	27.7	653.2	57.0	13.5	190.2	40.1	68.8
32	64	7	0	1	128	32	32	32	96	36.9	870.9	76.0	18.1	253.6	53.4	91.8
32	64	8VL	0	2	512	32	16	32	99	38.8	914.6	79.8	19.0	266.3	56.1	96.4
32	64	7	0	1	512	32	32	32	99	39.7	935.7	81.7	19.4	272.4	57.4	98.6
32	64	8VL	0	1	512	32	32	32	99	39.7	935.7	81.7	19.4	272.4	57.4	98.6
32	64	8VL	0	2	128	32	32	32	94	43.0	1014.1	88.5	21.0	295.2	62.2	106.9
32	64	7	0	2	128	32	32	32	91	43.2	1019.0	88.9	21.1	296.7	62.5	107.4
32	64	8VL	0	2	512	32	32	32	92	44.8	1058.0	92.3	21.9	308.0	64.9	111.5
32	64	8VL	1	2	512	32	32	32	96	49.9	1177.2	102.7	24.4	342.7	72.2	124.1

Table 8.3: Speed advantage for hardware over various processors.

Processor									Clock	Wall Clock Time ( $T_{processor}/T_{hw}$ )						
DD (KB)	DW (B)	DPV	APB	B	MVL	L	M	X	(MHz)	AUTCOR	CONVEN	RGB- CMYK	RGB- YIQ	IP_CH- ECKSUM	IMG- BLEND	GEO MEAN
8	16	0			Scalar				143	491.4	2140.3	312.0	621.3	197.6	378.1	<b>497.9</b>
8	16	0	0	1	4	1	1	1	134	287.0	277.9	233.8	222.4	135.3	259.7	<b>229.4</b>
8	16	0	0	1	8	2	1	1	132	257.8	204.5	173.1	177.3	95.5	218.9	<b>179.8</b>
8	16	0	0	1	8	2	1	2	132	220.6	205.3	173.4	144.4	95.3	193.2	<b>166.0</b>
8	16	0	0	1	8	2	2	2	131	151.6	158.5	141.7	131.6	96.0	159.6	<b>137.8</b>
8	16	0	0	2	8	2	2	1	127	165.7	161.8	137.4	128.6	89.3	152.9	<b>136.5</b>
8	16	0	0	2	8	2	2	2	125	149.3	165.3	140.2	111.6	91.1	142.8	<b>130.9</b>
8	16	0	0	1	16	4	2	2	129	134.4	116.6	115.2	118.0	78.8	129.9	<b>113.9</b>
8	16	0	0	1	16	4	2	4	127	117.2	118.4	117.0	102.6	80.0	118.8	<b>108.0</b>
8	16	0	0	1	16	4	4	2	128	102.3	97.5	113.3	107.9	75.1	125.2	<b>102.3</b>
8	16	0	0	1	16	4	4	4	128	82.7	97.4	113.2	90.6	75.0	111.0	<b>94.0</b>
8	16	0	0	2	16	4	4	2	126	89.1	98.6	114.9	91.8	72.7	108.0	<b>94.9</b>
8	16	0	0	1	128	4	4	4	125	81.8	85.5	123.0	93.4	78.5	104.0	<b>93.2</b>
8	16	0	0	2	16	4	4	4	122	81.8	101.8	118.7	81.6	75.1	103.8	<b>92.5</b>
8	16	0	0	2	128	4	4	2	123	81.0	74.2	115.9	91.9	73.0	100.2	<b>88.1</b>
32	64	0	0	1	16	4	2	4	129	115.0	105.2	80.7	74.4	44.9	89.5	<b>81.4</b>
32	64	8VL	0	1	16	4	2	4	129	115.2	103.2	79.5	69.6	42.9	89.7	<b>79.5</b>
8	16	0	0	1	32	8	4	4	123	77.0	80.5	114.8	82.2	73.3	100.9	<b>87.0</b>
8	16	0	0	2	128	4	4	4	121	64.9	75.6	117.9	80.5	74.2	93.8	<b>82.9</b>
8	16	0	0	1	32	8	8	4	124	58.7	67.8	100.4	74.7	72.3	90.8	<b>76.2</b>
32	64	7	0	1	16	4	4	2	128	96.7	73.5	51.0	70.2	26.5	68.6	<b>59.9</b>
32	64	7	0	1	16	4	4	4	128	77.6	73.6	51.1	53.2	26.5	54.9	<b>53.2</b>
32	64	7	0	2	16	4	4	2	124	85.0	75.4	47.8	54.5	23.6	50.7	<b>52.1</b>
32	64	7	0	2	16	4	4	4	121	77.1	77.4	49.1	42.7	24.3	44.8	<b>48.9</b>
32	64	7	0	2	128	4	4	2	123	75.1	50.1	44.8	52.8	22.1	48.1	<b>46.0</b>
32	64	8VL	0	2	128	4	4	2	124	74.1	48.8	44.2	51.8	20.8	47.0	<b>44.8</b>
32	64	7	0	2	128	4	4	4	121	60.1	51.1	45.5	40.2	22.4	41.6	<b>41.7</b>
32	64	8VL	0	2	128	4	4	4	121	60.0	50.3	45.5	39.7	21.4	41.0	<b>41.0</b>
32	64	8VL	1	2	128	4	4	4	121	60.0	49.8	45.2	38.2	21.4	41.0	<b>40.7</b>
32	64	8VL	0	1	32	8	8	4	123	53.4	44.4	30.3	37.9	15.1	40.1	<b>34.4</b>
32	64	7	0	1	32	8	8	4	123	53.4	43.7	29.6	37.9	15.0	36.8	<b>33.6</b>
32	64	7	0	1	32	8	8	8	125	42.8	42.8	29.1	28.5	14.8	29.1	<b>29.4</b>
32	64	8VL	0	1	128	8	8	8	124	41.5	35.7	29.5	28.1	15.2	27.9	<b>28.4</b>
32	64	7	0	2	128	8	8	4	117	43.4	33.1	26.8	29.1	12.8	26.6	<b>26.9</b>
32	64	8VL	0	2	128	8	8	4	119	42.5	32.0	26.0	27.9	12.0	25.5	<b>25.9</b>
32	64	7	0	2	128	8	8	8	118	34.3	32.8	26.5	21.8	12.6	22.6	<b>23.9</b>
32	64	8VL	0	2	128	8	8	8	118	34.3	32.3	26.3	21.3	12.1	22.1	<b>23.4</b>
32	64	7	1	2	128	8	8	8	119	34.2	32.5	26.4	21.0	12.6	22.6	<b>23.7</b>
32	64	8VL	1	2	128	8	8	8	119	34.0	31.8	25.8	20.4	12.1	21.9	<b>23.0</b>
32	64	8VL	0	2	128	16	8	8	112	35.3	32.1	24.8	20.1	11.2	21.1	<b>22.6</b>
32	64	8VL	0	1	64	16	16	8	116	32.1	29.5	18.7	20.9	10.1	20.7	<b>20.7</b>
32	64	8VL	0	1	128	16	16	8	114	31.8	26.4	19.5	22.0	9.9	20.5	<b>20.4</b>
32	64	8VL	0	2	128	16	8	16	111	31.8	32.6	25.0	17.5	11.4	19.8	<b>21.6</b>
32	64	8VL	0	1	64	16	16	16	114	27.7	30.4	19.2	16.6	10.4	17.4	<b>19.1</b>
32	64	8VL	0	1	128	16	16	16	115	26.1	26.1	19.3	17.0	9.8	16.5	<b>18.2</b>
32	64	8VL	0	2	128	16	16	8	109	28.3	26.5	18.2	17.2	8.3	15.8	<b>17.7</b>
32	64	7	0	2	128	16	16	16	111	23.0	26.6	18.2	13.0	9.4	13.9	<b>16.3</b>
32	64	7	1	2	128	16	16	16	111	23.0	26.6	18.0	12.6	9.4	14.8	<b>16.4</b>
32	64	8VL	1	2	128	16	16	16	111	22.9	25.9	17.5	12.9	8.1	13.5	<b>15.7</b>
32	64	7	0	1	128	32	32	32	96	22.0	25.3	15.7	11.9	9.5	12.7	<b>15.2</b>
32	64	8VL	0	2	512	32	16	32	99	23.7	24.2	18.3	11.5	10.6	12.0	<b>15.8</b>
32	64	7	0	1	512	32	32	32	99	21.9	21.2	16.3	12.3	11.4	11.7	<b>15.2</b>
32	64	8VL	0	1	512	32	32	32	99	21.9	21.0	15.6	12.0	10.3	10.6	<b>14.5</b>
32	64	8VL	0	2	128	32	32	32	94	21.9	25.7	18.3	12.5	7.7	10.4	<b>14.7</b>
32	64	7	0	2	128	32	32	32	91	22.6	26.7	16.1	10.4	9.0	11.1	<b>14.7</b>
32	64	8VL	0	2	512	32	32	32	92	20.4	21.6	15.2	10.1	10.0	9.1	<b>13.5</b>
32	64	8VL	1	2	512	32	32	32	96	19.7	21.0	14.5	9.5	9.5	8.8	<b>13.0</b>

the top row of the table which divides the processor area by the hardware area. The configurations are sorted by their areas with the smallest area designs at the top of the table and the largest at the bottom. Since no instruction set subsetting or width reduction is performed in this section (these customizations will be evaluated in Section 8.5), the area of the processors are the same for each benchmark, however the area of the hardware circuit that implements each benchmark varies significantly. The first row shows the hardware area advantage over the scalar processor varies between 1.4x for the RGBYIQ benchmark and 69.5x for CONVEN which is extremely small in hardware due to its 1-bit datapath.

The geometrically averaged mean across the benchmark indicates a scalar soft processor is 7.3x bigger than a hardware circuit on average. The second row shows that adding minimum support for vector extensions creates a VESPA processor which is 11.5x larger than hardware. Thus, both processors require significantly more area than a custom-built hardware circuit. This is partly due to the simplifying assumptions made resulting in incomplete hardware circuits, but is also due to the general purpose processing capabilities of the processors. Both processors can perform any 32-bit computation on data organized in any pattern in memory (without requiring alignment). The hardware however performs only a very specific task, and due to the simplicity in these benchmarks, this is often a very small task which leads to circuits with small areas. We would expect more complicated benchmarks to require significantly more area than these six, however certain overheads are specific to the processors and can be avoided in hardware: the caches for hiding memory latency, the register file shared by all functional units, and the instruction fetch and decode logic contribute to additional area not required in the hardware circuits. These area overheads can be amortized over the many vector lanes as is the case for the largest VESPA configuration which has 32 lanes and is 124.1x larger than the hardware circuits. However the lanes themselves contain significant overheads in supporting a variety of operations and fixed 32-bit precision. Both of these are eliminated in Section 8.5 using the instruction set subsetting and width reduction techniques

from the previous chapter.

#### 8.4.2 Software vs Hardware: Wall Clock Speed

Table 8.3 shows the wall clock speed advantage of the hardware over the processors. The slowest processors are at the top of the table and fastest at the bottom. Focusing on the first row of the table, we observe that the scalar processor executing out-of-the-box C code performs approximately 500x slower than hardware. The primary cause of the under-performance is failing to exploit the available data parallelism, except for the CONVEN benchmark which performs extraordinarily worse in software. This benchmark performs different array operations depending on the values in a small matrix. Each array operation requires load and store operations to fetch each array element and write it back to memory. In hardware the elements are only fetched once and stored internally in flip flops removing this memory access overhead as well as loop overheads resulting in a 2140x hardware speedup. The scalar processor is relatively more competitive with the very simple IP\_CHECKSUM benchmark performing 197.6x slower than hardware. Nonetheless the speed gap is shown to be very large between the hardware and scalar soft processor. It is hence not surprising that current commercial soft processors are used predominantly for system control tasks, while hardware design is necessary for most computational tasks on an FPGA.

The slowest VESPA configuration is on average 229.4x slower than hardware, while the fastest configuration can dramatically reduce this performance gap to just 13x as seen in the last row of Table 8.3. Though this is still a significant performance gap, it makes a soft vector processor far more likely to be used for implementing a non-critical data parallel compute task than a scalar soft processor. The performance certainly does not match that of hardware design, and the area cost is significant as seen in the previous section, but the ease of programming a soft vector processor versus designing custom hardware can make a soft vector processor an effective implementation vehicle for data parallel workloads. Thus, the addition of vector processor extensions to commercial soft

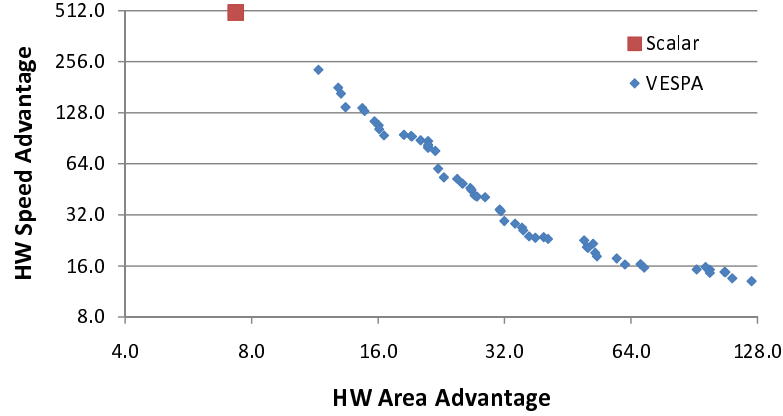


Figure 8.2: Area-performance design space of scalar soft processors and pareto-optimal VESPA processors normalized against hardware.

processors may well be justified.

Figure 8.2 graphs the area-performance design space of the scalar soft processor and VESPA configurations listed in the tables. The breadth of VESPA’s design space is depicted in the figure ranging from 11.5x-124.1x larger than hardware, and 229.4x-13x slower. This vast design space allows a designer to choose an area/speed tradeoff specific to their application, but ideally further improvements and customizations (seen in a subsequent section) will move the configurations closer to the origin and hence improve the overall competitiveness of soft vector processors versus hardware. In the next section the gap between the slowest VESPA and the scalar processor is discussed.

#### 8.4.2.1 Analysis of VESPA vs Scalar

Observing the first two rows of Table 8.3, we can compare the scalar processor with a VESPA processor that has only a single lane and identical cache organization. While the additional area of the 1-lane VESPA over the scalar is expected (because VESPA consists of a scalar augmented with vector extensions), the big performance benefit is not. The hand-vectorized assembly executed on the 1-lane VESPA gains more than twice the average performance over the scalar out-of-the-box C code on scalar SPREE. There is no data parallel execution on the single-lane version of VESPA, suggesting that the performance benefit is gained from a number of other advantages in VESPA:

1. **Amortization of loop control instructions.** The loop control instructions are executed far less often in VESPA than in the scalar.
2. **More register storage.** The large vector register file can store and manipulate arrays without having to access the cache or memory.
3. **More efficient pipelining.** VESPA executes batches of operations with no dependencies, meaning the pipeline can process these without stalling due to hazards.
4. **Instruction support.** VESPA has direct support for fixed-point operations, predication, and built-in min/max/absolute instructions from the VIRAM instruction set.
5. **Simultaneous execution across multiple pipelines.** In VESPA scalar operations are executed in the scalar pipeline, vector control operations are executed in the vector control pipeline, and vector operations in the vector pipeline. All three of these execute out-of-order with respect to each other.
6. **Assembly-level optimization.** Manual vectorization in assembly may have lead to optimizations beyond the C-compiled scalar output from GCC.

Determining the exact contribution of each advantage is beyond the scope of this work. We instead perform some qualitative analysis: Closer inspection of CONVEN revealed the cause of the 9x performance boost seen on the single lane VESPA to be the repeated operations performed on a single array. In VESPA the large vector register file can store large array chunks and manipulate them without storing and re-reading them from cache as the scalar processor must. The other benchmarks are less impacted because of their streaming and low-reuse nature. The loop overhead amortization gained by performing 64 loop iterations ( $MVL=64$ ) at once significantly impacts benchmarks with small loop bodies such as AUTCOR, CONVEN, IP\_CHECKSUM, and IMGBLEND. The more powerful VIRAM instruction set with fixed-point support further reduced the loop bodies of AUTCOR and RGBCMYK. Finally, the disassembled GCC output did not appear significantly

Table 8.4: Hardware advantages over fastest VESPA.

Benchmark	Clock	Iteration Parallelism	Cycles per Iteration
autcor	3.4x	0.5x	11.7x
conven	5.0x	0.5x	8.5x
rgbcmyk	4.7x	0.1875x	16.6x
rgbyiq	2.9x	0.1875x	17.8x
ip_checksum	4.8x	0.25x	8.0x
imgblend	4.6x	0.5x	3.8x
GEOMEAN	4.1x	0.32x	9.8x

more inefficient than the vectorized assembly for any of the benchmarks, leading us to infer that manual assembly optimization was not a significant advantage for the VESPA implementations.

#### 8.4.2.2 Analysis of VESPA vs Hardware

Our goal is to present a compelling case for soft vector processors as an FPGA implementation medium. The VESPA soft vector processor presented in this thesis was designed and optimized to meet this goal. Nonetheless further optimization of its architecture is certainly possible. In this section we more closely analyze the performance gap between soft vector processors and hardware to steer future optimizations in the architecture of soft vector processors.

By focussing only on loops we can decompose the reasons for the performance gap between VESPA and hardware into the following categories: (i) the clock frequency; (ii) the number of loop iterations executed concurrently called *iteration level parallelism*; and (iii) the number of cycles required to execute a single loop iteration. For each of these components, the hardware advantage over the fastest VESPA configuration (in the last row of Table 8.3) is shown in Table 8.4. The second column shows the hardware circuits have clock speeds between 2.9x and 5x faster than the best performing VESPA. Note this 4.1x average clock advantage is optimistic for the hardware circuits and can also be reduced through further circuit design effort in VESPA.

The third column of Table 8.4 shows that the iteration level parallelism exploited by

the hardware is less than or equal to that exploited by VESPA which is 32 for all benchmarks since there are 32 lanes in the chosen configuration. But in the hardware circuits we matched the parallelism to the memory bandwidth. For example, the IP\_CHECKSUM benchmark operates on a stream of 16-bit elements meaning in a given DRAM access only 8 elements can be retrieved from memory. The circuit is hence designed to have only 8-way parallelism. If the memory was widened further the hardware circuit would more effectively utilize the additional bandwidth than VESPA.

The last column gives the speedup of executing a single loop iteration in hardware over VESPA and is calculated from the measured overall speedups in the last row of Table 8.3 divided by the clock and iteration parallelism advantages. This component represents the cycle inefficiencies in the VESPA architecture much of which is inherent in any processor-style architecture. We list these inefficiencies below:

1. **Limited register ports** – Only a few data operands can be retrieved in a given clock cycle. This limits the number of instructions that can be ready for execution. Hardware design does not require a centralized register file and hence avoids this limitation.
2. **Limited functional units** – Only a few operations can be performed in a given clock cycle. In hardware a designer can instantiate as many dedicated processing elements as necessary.
3. **Limited cache access ports** – Only one cache line can be retrieved in a given clock cycle. In hardware a designer can distribute data into any organization that meets the needs of an application.
4. **Imperfect prefetching** – Ideally all memory latency can be hidden.

Overcoming the first two inefficiencies would allow many instruction to be simultaneously executed which more closely resembles the spatial computation performed by the hardware circuit. In addition, perfect prefetching and multiple cache ports would

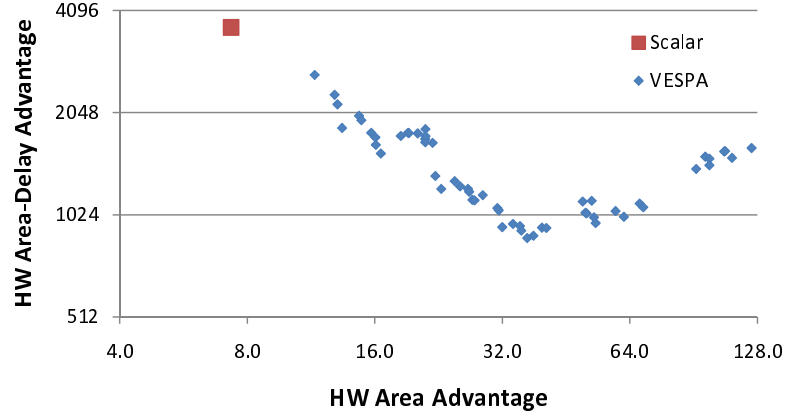


Figure 8.3: Area-delay product versus area of VESPA processors normalized against hardware.

allow large data sets to be accessed in ideally a single cycle without requiring the data to be contiguous in memory. In general resolving these limitations leads to high-latency components (such as register files and caches) and overall low clock frequency architectures due to the scaling limitations of crossbars, wiring, and the centralized register file. Future architectural improvements should leverage the compiler or the properties of the application itself to overcome these limitations without degrading clock frequency.

### 8.4.3 Software vs Hardware: Area-Delay

In addition to the area and performance gaps, it is also important to consider the gap in area-delay product compared to hardware design. A lower area-delay product implies the silicon area is being more efficiently used to produce increased performance. By measuring area-delay we aim to ascertain whether the addition of vector extensions can result in more efficient silicon usage, and for which configurations this is true.

Figure 8.3 shows the area-delay of the scalar and VESPA processors relative to that of hardware, averaged across the benchmark set, and plotted against area (for symmetry with previous graphs). The figure demonstrates that the addition of vector extensions results in lower (better) area-delay than the scalar processor alone which has a 3650x larger area-delay than hardware. All pareto-optimal VESPA configurations achieve lower area-delay product than the scalar. Recall that VESPA includes the same scalar SPREE processor, thus, despite the addition of the vector coprocessor, the area-delay product

is improved because of the large performance gains possible on the data-parallel benchmarks.

Starting from the smallest VESPA configuration in Figure 8.3, area-delay is decreased as more area (likely in the form of lanes) is added reaching a minimum area-delay that is 24% of that of the scalar processor. This VESPA configuration with the least area-delay product is still 874x worse than the hardware but is not the VESPA design with the highest performance. Instead it is the 8-lane, full memory crossbar vector processor with 2-way chaining, 32KB cache, 64B line size, and data prefetching of 7 cache lines. All configurations larger than this increase area-delay causing the “V” shape seen in the figure. The VESPA configurations with 16 or more lanes consume large amounts of silicon area without a proportionate increase in average wall clock performance. Reversing this trend would require higher clock rates and greater memory system performance to support scaling of this magnitude. Nonetheless these configurations more efficiently utilize silicon than the scalar processor alone.

## 8.5 Effect of Subsetting and Width Reduction

The pareto-optimal VESPA configurations previously discussed in this chapter used full 32-bit lanes with support for all vector instructions. This general purpose overhead disadvantages VESPA compared to hardware which implements only the functional units and bit-widths necessary for each application. VESPA can eliminate some of these overheads using the automatic instruction set subsetting and width reduction capabilities presented in Chapter 7, Section 7.4. We apply both techniques to the 56 pareto optimal configurations creating 312 customized soft vector processors (56 customized configurations for each of the six benchmarks) that can better compete with hardware, specifically by reducing area and mildly increasing clock frequency.

Figure 8.4 shows the average wall clock performance and area normalized to the hardware for: (i) the scalar soft processor, (ii) the pareto optimal VESPA configurations, and

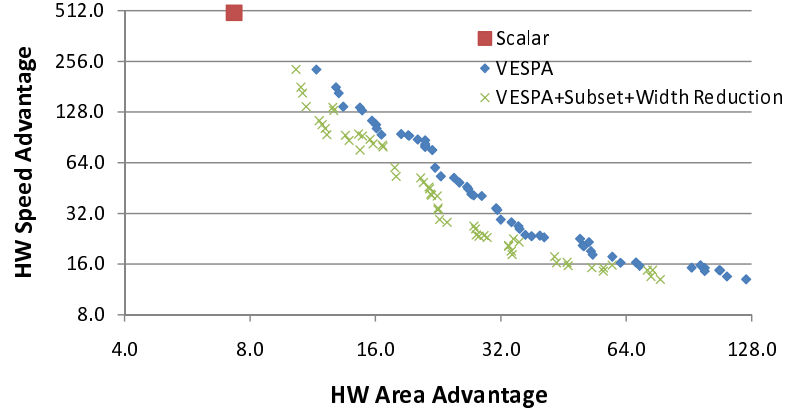


Figure 8.4: Area-performance design space of scalar and VESPA processors normalized against hardware. Also shown are the VESPA processors after applying instruction set subsetting and width reduction to match the application.

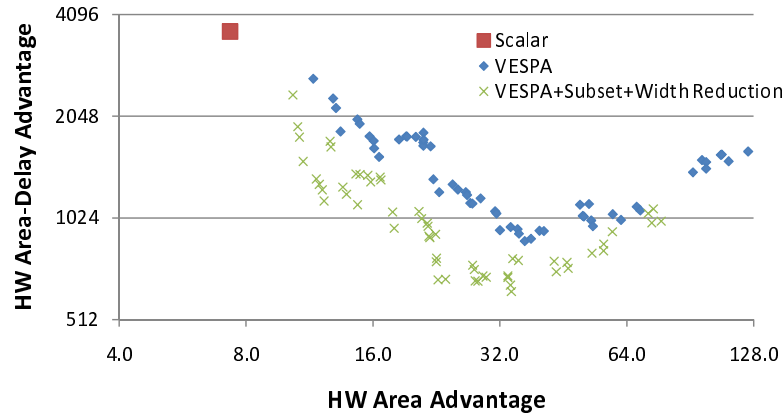


Figure 8.5: Area-delay product of scalar and VESPA processors normalized against hardware. Also shown are the VESPA processors after applying instruction set subsetting and width reduction to match the application.

(iii) the same VESPA configurations after applying both subsetting and width reduction. These customized configurations save between 10-43% area averaged across our benchmarks and hence are further left than the original pareto optimal VESPA configurations. For example, the largest configuration was originally 124x larger than hardware, but after applying subsetting and width reduction is only 77x larger. The area savings is more pronounced in this large configuration since the area of the scalar processor, instruction cache, and data cache is amortized. As general purpose overheads are removed, VESPA moves closer to the origin and hence is more competitive with hardware. The area savings similarly affects the area-delay product.

Figure 8.5 shows the area-delay versus area plot of the same three data series. The subsetting and width reduction customizations reduce area and hence area-delay resulting in VESPA configurations which are both further left and down than the original corresponding pareto optimal configurations. The lowest achievable area-delay is still 620x larger than hardware but is significantly smaller than the 874x area-delay without subsetting and width reduction. Interestingly, the configuration that achieves the 620x area-delay is not the same 8-lane VESPA discussed in the last section. Instead it is a 16-lane VESPA with no chaining, full memory crossbar, 32KB data cache, 64B line size, and prefetching of  $8VL$  cache lines. Thus, by reducing the area cost of adding more lanes we further enable many-lane configurations to efficiently trade area for performance.

## 8.6 Summary

This chapter described the manual hardware implementations of our benchmarks which we used to compare against VESPA and a scalar soft processor without vector extensions. The scalar was shown to be 500x slower than the hardware while VESPA can reduce this performance gap to 13x, although the area is increased from 7.3x to 124x. Nonetheless this area growth results in improved area-delay over the scalar soft processor. In the best case area-delay is reduced from 3650x to 874x larger than hardware. Furthermore subsetting and width reduction can be applied to save up to 43% area and reduce area-delay to 620x compared to hardware. While the gaps between VESPA and hardware remain large, they have been reduced considerably compared to the scalar soft processor. Further optimization of the VESPA architecture can continue to close the gap, however our idealized simplifications for the hardware circuits suggest these measurements likely upper bounds on the advantages of hardware design. As a result, soft vector processors are adequately motivated since an FPGA designer is more likely to implement a data parallel computation in software if hardware can at best outperform the soft processor by only 13x.

## Chapter 9

# Conclusions

FPGAs are increasingly used to implement complex digital systems, but the design of such systems is difficult due to the laborious hardware descriptions necessary for efficient FPGA implementation. A microprocessor can be used to more easily implement computation in a high-level programming language. Because of the performance overheads associated with a microprocessor it is limited to implementing system control and non-critical computation tasks. In fact, this microprocessor is often a *soft processor* implemented in the reprogrammable fabric hence inheriting both FPGA and processor overheads. The added overhead results in further inefficiencies in area/performance/power making soft processors useful for only the least critical computation tasks. Nonetheless, a soft processor is useful because it preserves the benefits of a single-chip solution without specializing the FPGA device and increasing its cost. By improving soft processors and offsetting these overheads, more computation can be designed in software and executed on a soft processor without the long hardware design times and without heavy area/performance/power penalties.

In this thesis, we improve soft processors by allowing their architecture to respond to characteristics in the application. Specifically, we focus on the amount of data level parallelism in an application, which is a property found in many embedded and multimedia applications. We propose that soft vector processors can be used to efficiently

scale performance for such applications, hence suggesting that current soft processors be augmented with vector extensions. This increased performance can be used to justify the implementation of more critical computation in a soft vector processor rather than using manual hardware design. As more computation is implemented with relative ease using sequential programming, we achieve our goal of simplifying FPGA design.

Through experimentation with real benchmarks and real hardware implementations, we validate the feasibility of soft vector processors hence making a compelling case for the inclusion of vector extensions in current soft processors. We consider the soft vector processor successful if it can take advantage of the FPGA reprogrammable fabric to: (i) scale performance when executing data parallel workloads; (ii) precisely control the area/performance tradeoff; and (iii) customize the functionality and area overheads to a given application. To this end we make the following contributions.

## 9.1 Contributions

1. **VESPA Infrastructure** – A proof-of-concept soft vector processor called VESPA was designed and implemented on real FPGA hardware, executing industry-standard embedded benchmarks from off-chip commodity DRAM. The VESPA processor, its ported GNU assembler, and instruction set simulator are valuable infrastructure components for enabling future research into soft vector processors.
2. **Performance Scalability** – VESPA was shown to scale up to 32 vector lanes on real FPGA hardware achieving up to 26.5x speedup over 1 lane using data parallel benchmarks from the industry-standard EEMBC suite. Much of this scaling was enabled through improvements to the memory system which were necessary to sustain performance scaling for many vector lanes.
3. **Architectural Parameters** – To precisely control the area and performance trade-off, many architectural parameters were implemented for modifying the compute architecture, interface, and memory system of the soft vector processor. In addition

to the cache configuration and prefetching strategy, VESPA also has a parameterized maximum vector length and number of lanes in the architecture. Beyond these, VESPA can be customized to the instruction mix allowing the designer to reduce the number of lanes with multiply functional units and access to the memory crossbar. Applications with low demand of the multiplier or memory can have area saved with minimal performance loss. Performance within each lane can be increased using the parameterized support for vector chaining. VESPA can simultaneously execute multiple chained vector instructions using a banked register file. All three VESPA functional units can potentially be active, and the number of ALUs can also be replicated to enable further scaling.

4. **Design Space Exploration** – To demonstrate that the architectural variations in a soft vector processor can be used to gain fine-grain control of area and performance, we explore the VESPA design space through 768 configurations. VESPA was shown to finely span a broad 28x range in area, 24x in cycle performance, and 18x in wall clock time due to the clock frequency degradation caused by instantiating many lanes. Of these 768 configurations, the 56 configurations found to be pareto optimal employed different combinations of all VESPA parameters, showing that each of these architectural variations can be useful to an FPGA designer. Moreover it was shown that performance-per-area gains can be achieved by choosing a configuration on a per-application basis.
5. **Customizing Functionality** – An important feature of soft processors is their ability to deliver exactly the functionality required by the application without added overheads. VESPA supports this through automatic subsetting of the instruction set by parsing the application binary and removing hardware support for unused instructions. Also, the width of the lanes can be reduced from the 32-bit default to match the precision required by an application down to 1-bit. The combination of these two customizations can dramatically reduce the area of the VESPA vector

coprocessor by up to 78%, on average 47%.

6. **VESPA Versus Hardware Comparison** – Although soft vector processors were shown to scale performance, span a broad design space, and customize their functionality, an FPGA designer must still consider that better area and performance can be achieved with manual hardware design. By quantifying the area and performance gaps between soft vector processors and hardware design we can better inform FPGA designers as well as benchmark the progress made with VESPA. A scalar soft processor was shown to perform 500x slower than hardware while the VESPA soft vector processor can reduce this performance gap to 13x. These measurements were made with idealized hardware implementations of our benchmarks and are hence upper bounds on the advantages of hardware design. In terms of area-delay product, scalar soft processors are 3650x worse than custom hardware design, while all pareto-optimal VESPA configurations improve on this. This suggests that the addition of vector extensions to a scalar soft processor makes it more efficient for data parallel workloads. The most efficient configuration reduces the 3650x area-delay gap to 874x without customization, and to 620x after unneeded instruction support and datapath width are removed.

In conclusion, the scalable performance provided by soft vector processors allows FPGA designers to meet their performance constraints without resorting to more difficult hardware design. This simplifies FPGA design since for a given digital system, the overall design time is reduced by leveraging the high-level programming languages and single-step debug infrastructure in software. Efficiency can be gained by performing fine-grain matching of the architecture of the soft vector processor to the needs of the application. Additionally, the soft vector processor can also be customized to support only the functionality required by the application to save area.

## 9.2 Future Work

Although VESPA was already used to thoroughly investigate the feasibility of soft vector processors, there are several new avenues of research enabled by this thesis.

**Improving the VESPA Architecture** – In terms of improving VESPA, the clock frequency and memory unit can be improved to make it significantly more powerful. The VESPA clock frequency is in the same range as the scalar SPREE processor it is based off of, which runs at 143 MHz, while the Altera Nios II can be clocked at 250 MHz on the same device. A faster clock rate may not translate to proportionally higher performance, but is necessary for designs with higher system clocks to avoid clock crossing delays. The memory system is pipelined but currently has one cycle start latency and one cycle end latency. These delays can be removed by better integrating the memory system into the VESPA pipeline or implementing a non-blocking cache. Either of these options would improve the impact of scaling across lanes and vector chaining. Alternatively, radically different vector architectures such as the CODE [34] vector processor could be implemented. Simultaneous with high-level architectural modifications, a generator tool could also consider low-level circuit optimizations which are imperative for supporting certain configurations. For example, much of the clock frequency degradation in the 32-lane VESPA could be eliminated with more careful re-engineering within the pipeline.

**Auto-Vectorizing Compiler Support** – The key attribute of VESPA over hardware design is its software interface making it easier to program and debug. In this thesis manual programming at the assembly-level was necessary to program VESPA. Although this is still very much easier than hardware design, ideally vectorization should be performed in the compiler from a high-level programming language. Successfully implementing this software toolchain would further promote the adoption of vector processing extensions in soft processors.

**Custom Instructions** – VESPA provides several methods of customizing the soft vector processor by *removing* hardware, but additional interesting research may be performed by *adding* new hardware to VESPA. An example of this is the option of adding a

custom functional unit to each lane which simultaneously exploits custom computation and data parallelism. Another example similar to Yu *et. al.* [75] is to include lane-local scratchpad memories, or dedicated instructions for reduction operations. Other more generically useful operations can be explored and included in VESPA.

**Architecture Selection Heuristics** – The expansive VESPA design space motivates exciting research into the automatic configuration of a soft vector processor. This thesis showed that choosing a per-application configuration can result in significantly more efficient soft vector processors, but searching this configuration space with tens of thousands of possible configurations is infeasible for FPGA designers under tight time-to-market constraints. Tools for automatically selecting a configuration given an application would enable designers to take advantage of the many architectural parameters without evaluating each configuration. One possible such method is to include in-hardware profiling to extract characteristics of the program behaviour and use heuristics for mapping these to a vector architecture configuration.

**System-Level Tradeoffs** – Soft vector processors are effective for data parallel code, but other processor architectures may be required for better exploiting other code characteristics. The integration of VESPA with a SPREE processor allows it to be included in the SPREE framework enabling simultaneous exploration of vector and scalar soft processor architectures. Such a framework allows system-level optimizations to be performed to best match the needs of the overall FPGA system.

**High Performance Computing** – VESPA makes a significant impact for current embedded FPGA system designers, but FPGAs are also useful in other computing domains such as in high-performance computing (HPC). VESPA can be used in this domain to provide scientists with a familiar vector processor interface reminiscent of previous vector supercomputers. The addition of floating point instructions is necessary for many HPC applications, but most importantly, these systems would need to provide scaling far beyond 32 lanes. Research in such an architecture and its memory system provides opportunity for interesting innovations as it likely spans multiple FPGA devices.

## Appendix A

# Measured Model Parameters

In chapter 4 we modelled a perfect memory system by extrapolating a model based on a few input parameters measured from the program behaviour. Specifically, the input parameters were: (i) the frequency of load instruction; (ii) the load miss rates on various sized direct-mapped data caches with 16B line size; (iii) the frequency of store instructions; and (iv) the store miss rates on various sized direct-mapped data caches with 16B line size.

These input parameters were measured across 46 EEMBC benchmarks using the MINT simulator. MINT was augmented with counters for tracking the number of total instructions, load instructions, and store instructions. These measurements were used to calculate the frequency of loads and stores in the instruction stream. MINT was also augmented with a model of a direct-mapped cache with 16B line size and parameterized depth. This model was used to count hits and misses in the data cache and derive the load and store miss rates for caches ranging from 256B to 1MB. The tables below list the values collected for loads and stores respectively.

Table A.1: Load frequency and miss rates across cache size for EEMBC benchmarks.

	Load Frequency	Load Miss Rate for Given Cache Size						
		256B	1KB	4KB	16KB	64KB	256KB	1MB
a2time01	0.036	0.140	0.022	0.003	0.000	0.000	0.000	0.000
aifftr01	0.186	0.867	0.857	0.561	0.029	0.002	0.000	0.000
aiffr01	0.201	0.266	0.158	0.137	0.000	0.000	0.000	0.000
aiifft01	0.189	0.893	0.883	0.578	0.028	0.002	0.000	0.000
basefp01	0.061	0.029	0.010	0.001	0.000	0.000	0.000	0.000
bitmnp01	0.051	0.109	0.052	0.008	0.000	0.000	0.000	0.000
cacheb01	0.206	0.269	0.107	0.053	0.027	0.000	0.000	0.000
canrdr01	0.124	0.430	0.103	0.031	0.001	0.000	0.000	0.000
idctrn01	0.171	0.258	0.075	0.030	0.000	0.000	0.000	0.000
iirflt01	0.040	0.213	0.108	0.071	0.000	0.000	0.000	0.000
matrix01	0.090	0.055	0.034	0.023	0.003	0.000	0.000	0.000
puwmod01	0.151	0.170	0.032	0.002	0.000	0.000	0.000	0.000
rspeed01	0.171	0.106	0.041	0.008	0.000	0.000	0.000	0.000
tblook01	0.099	0.076	0.034	0.003	0.001	0.000	0.000	0.000
bezier01fixed	0.046	0.044	0.036	0.034	0.010	0.000	0.000	0.000
dither01	0.130	0.282	0.200	0.021	0.014	0.002	0.000	0.000
rotate01	0.058	0.513	0.308	0.161	0.030	0.000	0.000	0.000
text01	0.157	0.379	0.156	0.099	0.041	0.000	0.000	0.000
autcor00data_2	0.200	0.063	0.063	0.000	0.000	0.000	0.000	0.000
conven00data_1	0.158	0.067	0.021	0.000	0.000	0.000	0.000	0.000
fbital00data_2	0.061	0.238	0.164	0.031	0.031	0.000	0.000	0.000
fft00data_3	0.130	0.780	0.076	0.002	0.000	0.000	0.000	0.000
viterb00data_2	0.162	0.075	0.018	0.016	0.000	0.000	0.000	0.000
ip_pktcheckb4m	0.191	0.146	0.117	0.109	0.107	0.093	0.040	0.012
ip_reassembly	0.264	0.383	0.265	0.190	0.156	0.143	0.127	0.074
nat	0.160	0.356	0.256	0.225	0.179	0.177	0.158	0.000
ospfv2	0.187	0.728	0.508	0.063	0.020	0.000	0.000	0.000
qos	0.233	0.240	0.002	0.001	0.000	0.000	0.000	0.000
routelookup	0.244	0.377	0.219	0.044	0.008	0.000	0.000	0.000
tcpbulk	0.133	0.201	0.181	0.120	0.075	0.013	0.000	0.000
tcpjumbo	0.180	0.172	0.169	0.168	0.103	0.022	0.000	0.000
tcpmixed	0.089	0.253	0.178	0.132	0.081	0.022	0.000	0.000
aes	0.143	0.274	0.121	0.000	0.000	0.000	0.000	0.000
cjpegv2data5	0.182	0.362	0.284	0.095	0.030	0.017	0.011	0.008
des	0.204	0.776	0.463	0.004	0.003	0.000	0.000	0.000
djpegv2data6	0.178	0.420	0.259	0.104	0.034	0.015	0.008	0.003
huffde	0.078	0.681	0.521	0.215	0.042	0.014	0.000	0.000
mp2decoddata1	0.169	0.157	0.073	0.033	0.014	0.010	0.009	0.005
mp2enfixdata1	0.222	0.174	0.084	0.010	0.004	0.003	0.003	0.002
mp3playerfixeddata2	0.221	0.373	0.174	0.086	0.023	0.009	0.006	0.006
mp4decodedata4	0.144	0.211	0.096	0.060	0.032	0.026	0.015	0.004
mp4encodedata3	0.217	0.260	0.113	0.037	0.013	0.009	0.006	0.002
rgbcmykv2data5	0.103	0.082	0.067	0.064	0.063	0.063	0.063	0.063
rgbhpgv2data5	0.232	0.115	0.031	0.009	0.007	0.006	0.006	0.001
rgbyiqv2data5	0.038	0.271	0.063	0.063	0.063	0.063	0.063	0.063
rsa	0.115	0.231	0.070	0.013	0.005	0.005	0.000	0.000
AVERAGE	0.148	0.295	0.171	0.081	0.028	0.016	0.011	0.005

Table A.2: Store frequency and miss rates across cache size for EEMBC benchmarks.

	Store Frequency	Store Miss Rate for Given Cache Size						
		256B	1KB	4KB	16KB	64KB	256KB	1MB
a2time01	0.144	0.022	0.006	0.000	0.000	0.000	0.000	0.000
aifftr01	0.135	0.350	0.340	0.225	0.024	0.000	0.000	0.000
aiffr01	0.085	0.093	0.010	0.003	0.000	0.000	0.000	0.000
aiifft01	0.138	0.348	0.338	0.214	0.026	0.000	0.000	0.000
basefp01	0.060	0.041	0.003	0.001	0.000	0.000	0.000	0.000
bitmnp01	0.103	0.053	0.045	0.017	0.000	0.000	0.000	0.000
cacheb01	0.188	0.214	0.116	0.031	0.008	0.000	0.000	0.000
canrdr01	0.163	0.123	0.035	0.007	0.000	0.000	0.000	0.000
idctrn01	0.109	0.125	0.047	0.031	0.000	0.000	0.000	0.000
iirfft01	0.154	0.046	0.004	0.001	0.000	0.000	0.000	0.000
matrix01	0.082	0.034	0.016	0.012	0.001	0.000	0.000	0.000
puwmod01	0.191	0.191	0.044	0.001	0.000	0.000	0.000	0.000
rspeed01	0.144	0.112	0.044	0.002	0.000	0.000	0.000	0.000
tblook01	0.081	0.053	0.020	0.002	0.000	0.000	0.000	0.000
bezier01fixed	0.019	0.016	0.004	0.001	0.000	0.000	0.000	0.000
dither01	0.029	0.801	0.751	0.039	0.018	0.008	0.000	0.000
rotate01	0.032	0.044	0.043	0.042	0.016	0.000	0.000	0.000
text01	0.097	0.219	0.088	0.061	0.039	0.000	0.000	0.000
autcor00data_2	0.000	1.000	1.000	0.941	0.941	0.000	0.000	0.000
conven00data_1	0.076	0.053	0.018	0.000	0.000	0.000	0.000	0.000
fbital00data_2	0.033	0.179	0.088	0.058	0.058	0.000	0.000	0.000
fft00data_3	0.084	0.391	0.031	0.004	0.000	0.000	0.000	0.000
viterb00data_2	0.118	0.086	0.016	0.009	0.000	0.000	0.000	0.000
ip_pktcheckb4m	0.075	0.132	0.034	0.008	0.002	0.001	0.000	0.000
ip_reassembly	0.177	0.255	0.215	0.188	0.176	0.171	0.158	0.111
nat	0.110	0.266	0.204	0.174	0.169	0.167	0.160	0.000
ospfv2	0.011	0.329	0.260	0.177	0.050	0.001	0.001	0.001
qos	0.089	0.127	0.002	0.001	0.000	0.000	0.000	0.000
routelookup	0.000	0.778	0.778	0.778	0.556	0.556	0.556	0.556
tcpbulk	0.174	0.248	0.242	0.231	0.099	0.052	0.000	0.000
tcpjumbo	0.093	0.249	0.246	0.244	0.163	0.043	0.000	0.000
tcpmixed	0.249	0.247	0.238	0.227	0.068	0.028	0.000	0.000
aes	0.051	0.099	0.049	0.000	0.000	0.000	0.000	0.000
cjpegv2data5	0.101	0.206	0.083	0.065	0.036	0.023	0.012	0.007
des	0.012	0.166	0.140	0.030	0.022	0.000	0.000	0.000
djpegv2data6	0.103	0.272	0.136	0.089	0.050	0.028	0.018	0.014
huffde	0.037	0.342	0.197	0.148	0.126	0.113	0.000	0.000
mp2decoddata1	0.103	0.113	0.053	0.034	0.010	0.007	0.007	0.004
mp2enfixdata1	0.026	0.106	0.050	0.019	0.012	0.011	0.010	0.010
mp3playerfixeddata2	0.048	0.197	0.095	0.062	0.034	0.009	0.007	0.006
mp4decodedata4	0.104	0.191	0.097	0.071	0.051	0.047	0.046	0.015
mp4encodedata3	0.050	0.251	0.119	0.047	0.035	0.032	0.030	0.019
rgbcmykv2data5	0.138	0.076	0.066	0.063	0.063	0.063	0.063	0.063
rgbhpgv2data5	0.023	0.647	0.079	0.068	0.065	0.064	0.064	0.006
rgbyiqv2data5	0.038	0.271	0.062	0.062	0.062	0.062	0.062	0.062
rsa	0.072	0.076	0.035	0.008	0.003	0.003	0.000	0.000
AVERAGE	0.090	0.223	0.143	0.098	0.065	0.032	0.026	0.019

## Appendix B

# Raw VESPA Data on DE3 Platform

Table B.1: Area of VESPA system **without** the vector coprocessor. Data cache is 4KB deep with 16B line size.

Resource	Number Consumed
ALMs	4181
M9Ks	37
M144Ks	0
18-bit DSPs	6

Table B.2: Area of VESPA system **without** the vector coprocessor. Data cache is 16KB deep with 64B line size.

Resource	Number Consumed
ALMs	4925
M9Ks	59
M144Ks	0
18-bit DSPs	6

Table B.3: System area of pareto optimal VESPA configurations.

DD	DW	DPV	APB	B	MVL	L	M	X	ALMs	M9Ks	M144Ks	18-bit DSPs
8KB	16B	0	0	1	4	1	1	1	5556	46	0	10
8KB	16B	0	0	1	8	2	1	1	6043	48	0	10
8KB	16B	0	0	1	8	2	1	2	6075	48	0	14
8KB	16B	0	0	1	8	2	2	2	6218	48	0	14
8KB	16B	0	0	2	8	2	2	1	6566	54	0	10
8KB	16B	0	0	2	8	2	2	2	6591	54	0	14
8KB	16B	0	0	1	16	4	2	2	7041	52	0	14
8KB	16B	0	0	1	16	4	2	4	7083	52	0	22
8KB	16B	0	0	1	16	4	4	2	7216	52	0	14
8KB	16B	0	0	1	16	4	4	4	7294	52	0	22
8KB	16B	0	0	2	16	4	4	2	7787	62	0	14
8KB	16B	0	0	1	128	4	4	4	7362	76	0	22
8KB	16B	0	0	2	16	4	4	4	8034	62	0	22
8KB	16B	0	0	2	128	4	4	2	7836	78	0	14
32KB	64B	0	0	1	16	4	2	4	8268	74	0	22
32KB	64B	8*VL	0	1	16	4	2	4	8261	74	0	23
8KB	16B	0	0	1	32	8	4	4	8910	60	0	22
8KB	16B	0	0	2	128	4	4	4	8100	78	0	22
8KB	16B	0	0	1	32	8	8	4	9278	60	0	22
32KB	64B	7	0	1	16	4	4	2	8903	74	0	14
32KB	64B	7	0	1	16	4	4	4	9102	74	0	22
32KB	64B	7	0	2	16	4	4	2	9525	84	0	14
32KB	64B	7	0	2	16	4	4	4	9732	84	0	22
32KB	64B	7	0	2	128	4	4	2	9608	100	0	14
32KB	64B	8*VL	0	2	128	4	4	2	9670	100	0	15
32KB	64B	7	0	2	128	4	4	4	9780	100	0	22
32KB	64B	8*VL	0	2	128	4	4	4	9904	100	0	23
32KB	64B	8*VL	1	2	128	4	4	4	10458	100	0	23
32KB	64B	8*VL	0	1	32	8	8	4	12309	82	0	23
32KB	64B	7	0	1	32	8	8	4	12421	82	0	22
32KB	64B	7	0	1	32	8	8	8	12458	82	0	38
32KB	64B	8*VL	0	1	128	8	8	8	12565	98	0	39
32KB	64B	7	0	2	128	8	8	4	13286	100	0	22
32KB	64B	8*VL	0	2	128	8	8	4	13383	100	0	23
32KB	64B	7	0	2	128	8	8	8	13672	100	0	38
32KB	64B	8*VL	0	2	128	8	8	8	14212	100	0	39
32KB	64B	7	1	2	128	8	8	8	15008	100	0	38
32KB	64B	8*VL	1	2	128	8	8	8	15416	100	0	39
32KB	64B	8*VL	0	2	128	16	8	8	17727	132	0	47
32KB	64B	8*VL	0	1	64	16	16	8	19598	98	0	47
32KB	64B	8*VL	0	1	128	16	16	8	19722	98	0	47
32KB	64B	8*VL	0	2	128	16	8	16	18375	132	0	79
32KB	64B	8*VL	0	1	64	16	16	16	20179	98	0	79
32KB	64B	8*VL	0	1	128	16	16	16	20392	98	0	79
32KB	64B	8*VL	0	2	128	16	16	8	21966	132	0	47
32KB	64B	7	0	2	128	16	16	16	22716	132	0	78
32KB	64B	7	1	2	128	16	16	16	25135	132	0	78
32KB	64B	8*VL	1	2	128	16	16	16	25713	132	0	79
32KB	64B	7	0	1	128	32	32	32	34489	130	0	174
32KB	64B	8*VL	0	2	512	32	16	32	33499	196	0	175
32KB	64B	7	0	1	512	32	32	32	34483	196	0	174
32KB	64B	8*VL	0	1	512	32	32	32	34471	196	0	175
32KB	64B	8*VL	0	2	128	32	32	32	38077	196	0	175
32KB	64B	7	0	2	128	32	32	32	38317	196	0	174
32KB	64B	8*VL	0	2	512	32	32	32	40097	196	0	175
32KB	64B	8*VL	1	2	512	32	32	32	45578	196	0	175

Table B.4: Performance of pareto optimal VESPA configurations.

Cycle Count																		
DD	DW	DPV	APB	B	MVL	L	M	X	Clock (MHz)	autocor	conven	rgbcmnyk	rgbyiq	ip-checksum	imgblend	flt3x3	fbital	viterb
8KB	16B	0	0	1	4	1	1	1	133.512	125376	17610	16608477	15683277	101257	1127965	2754216	358070	88624
8KB	16B	0	0	1	8	2	1	1	131.969	111321	12809	12150345	12359199	70685	939993	2008741	241874	112514
8KB	16B	0	0	1	8	2	1	2	131.745	95124	12836	12150357	10048857	70432	828369	1627390	225221	109469
8KB	16B	0	0	1	8	2	2	2	130.573	64791	9821	9839409	9078561	70271	677856	1432396	191954	82679
8KB	16B	0	0	2	8	2	2	1	127.009	68856	9755	9286014	8625714	63628	631669	1361568	179462	75842
8KB	16B	0	0	2	8	2	2	2	124.528	60852	9767	9286029	7338447	63605	578674	1053985	162839	74102
8KB	16B	0	0	1	16	4	2	2	129.191	56826	7149	7915923	8051466	57092	546178	1128954	134345	114677
8KB	16B	0	0	1	16	4	2	4	127.201	48768	7145	7915959	6894789	57091	491812	939159	126029	111779
8KB	16B	0	0	1	16	4	4	2	127.666	42726	5909	7697256	7277271	53794	519910	1014177	117710	98573
8KB	16B	0	0	1	16	4	4	4	127.811	34599	5906	7697339	6118071	53779	461620	822412	109390	95660
8KB	16B	0	0	2	16	4	4	2	125.901	36726	5891	7693395	6107049	51331	442597	791253	103154	90050
8KB	16B	0	0	1	128	4	4	4	125.344	33567	5087	8199347	6183678	55201	423969	682878	114434	96707
8KB	16B	0	0	2	16	4	4	4	121.88	32625	5891	7693476	5250533	51313	411571	632970	94842	87803
8KB	16B	0	0	2	128	4	4	2	122.655	32526	4319	7561532	5951457	50227	400074	653641	102716	90560
32KB	64B	0	0	1	16	4	2	4	129.386	48681	6459	5552233	5084771	32539	376620	862715	123639	89571
32KB	64B	8*VL	0	1	16	4	2	4	129.097	48681	6324	5457808	4747281	31058	376599	830558	123573	87756
8KB	16B	0	0	1	32	8	4	4	122.814	30945	4691	7500240	5333505	50476	403099	625785	79058	85253
8KB	16B	0	0	2	128	4	4	4	120.618	25623	4328	7562738	5129880	50187	368176	492534	94373	88272
8KB	16B	0	0	1	32	8	8	4	124.444	23910	4004	6646479	4911531	50478	367785	569163	78023	79841
32KB	64B	7	0	1	16	4	4	2	128.338	40629	4479	3484108	4759241	19034	286549	799001	115213	65421
32KB	64B	7	0	1	16	4	4	4	128.181	32556	4479	3484123	3604040	19027	229014	608222	106911	62760
32KB	64B	7	0	2	16	4	4	2	124.491	34632	4452	3162848	3587222	16503	205206	575041	100662	56688
32KB	64B	7	0	2	16	4	4	4	121.078	30564	4449	3162824	2731442	16487	176546	416918	92346	54774
32KB	64B	7	0	2	128	4	4	2	122.874	30207	2922	2926906	3426292	15212	192377	500289	100179	57738
32KB	64B	8*VL	0	2	128	4	4	2	124.401	30165	2883	2925245	3405185	14495	190233	498256	100179	57630
32KB	64B	7	0	2	128	4	4	4	120.99	23799	2934	2926873	2568510	15195	163642	338884	91860	55716
32KB	64B	8*VL	0	2	128	4	4	4	120.914	23760	2886	2925266	2536361	14483	161480	336776	91860	55623
32KB	64B	8*VL	1	2	128	4	4	4	120.979	23760	2862	2908483	2440244	14489	161515	336733	79239	53430
32KB	64B	8*VL	0	1	32	8	8	4	123.435	21579	2601	1991161	2469339	10485	161083	445229	71067	46443
32KB	64B	7	0	1	32	8	8	4	123.206	21537	2556	1939750	2468366	10376	147367	402355	71040	45711

Continued on next page ...

Continued on next page ...

Table B.5: Performance of pareto optimal VESPA configurations (cont'd).

Cycle Count																
DD	DW	DPV	APB	B	M	V	L	M	X	Clock (MHz)						
								autcor	conven	rgbcm	myk	rgbyiq	imgblend	flt3x3	fbital	viterb
32KB 64B	7	0	1	32	8	8	8	17544	2544	1939669	1889822	10384	118704	308331	66882	44885
32KB 64B 8*VL	0	1	128	8	8	8	8	16896	2103	1950742	1844327	10583	112937	271252	69186	44712
32KB 64B 7	0	2	128	8	8	4	8	16626	1836	1666588	1794917	8378	101376	258218	63546	43467
32KB 64B 8*VL	0	2	128	8	8	8	4	16599	1809	1649200	1755779	8048	99122	256711	63543	43416
32KB 64B 7	0	2	128	8	8	8	8	13290	1842	1666540	1365983	8351	87052	177391	59379	42681
32KB 64B 8*VL	0	2	128	8	8	8	8	13251	1806	1649200	1323693	8029	84761	175766	59388	42582
32KB 64B 7	1	2	128	8	8	8	8	13281	1827	1661881	1318280	8372	87060	177331	52998	41775
32KB 64B 8*VL	1	2	128	8	8	8	8	13251	1794	1632122	1281143	8048	84776	175745	52998	41691
32KB 64B 8*VL	0	2	128	16	8	8	8	12897	1701	1471887	1186151	7007	76584	165004	49428	40752
32KB 64B 8*VL	0	1	64	16	16	8	8	12234	1629	1160999	1286483	6622	78240	193657	49380	38655
32KB 64B 8*VL	0	1	128	16	16	8	8	11865	1428	1183943	1324460	6333	76235	189433	50130	38265
32KB 64B 8*VL	0	2	128	16	8	16	8	11538	1713	1471987	1025345	7111	71424	127225	47358	40338
32KB 64B 8*VL	0	1	64	16	16	16	8	10287	1638	1161370	997511	6629	64176	145729	47303	38219
32KB 64B 8*VL	0	1	128	16	16	16	8	9840	1428	1183981	1035968	6356	61842	141815	48054	37845
32KB 64B 8*VL	0	2	128	16	16	8	8	10086	1371	1052614	990512	5083	56070	134456	45393	38121
32KB 64B 7	0	2	128	16	16	16	8	8364	1407	1078405	763593	5850	50232	98573	43323	37830
32KB 64B 7	1	2	128	16	16	16	8	8355	1401	1065568	742232	5869	53324	98540	40074	37743
32KB 64B 8*VL	1	2	128	16	16	16	8	8337	1368	1035611	756419	5068	48893	94654	40068	37607
32KB 64B 7	0	1	128	32	32	32	8	6951	1158	803440	604454	5165	39757	82480	38391	37164
32KB 64B 8*VL	0	2	512	32	16	32	8	7722	1140	968581	606074	5896	38828	64750	38784	37392
32KB 64B 7	0	1	512	32	32	32	8	7095	996	860407	641773	6338	37752	72856	39348	36840
32KB 64B 8*VL	0	1	512	32	32	32	8	7062	984	819688	622727	5708	33953	72966	39372	36879
32KB 64B 8*VL	0	2	128	32	32	32	8	6718	1143	910417	619962	4026	31614	63493	36513	37095
32KB 64B 7	0	2	128	32	32	32	8	6744	1153	779770	498854	4582	32909	60284	36513	37149
32KB 64B 8*VL	0	2	512	32	32	32	8	6171	948	746737	492193	5160	27223	49078	36990	36834
32KB 64B 8*VL	1	2	512	32	32	32	8	6177	957	741493	480515	5098	27573	49076	35352	36792

Table B.6: System area of pareto optimal VESPA configurations after instruction subsetting and width reduction for AUTCOR.

DD	DW	DPV	APB	B	MVL	L	M	X	ALMs	M9Ks	M144Ks	18-bit DSPs
8KB	16B	0	0	1	4	1	1	1	5172	46	0	10
8KB	16B	0	0	1	8	2	1	1	5425	48	0	10
8KB	16B	0	0	1	8	2	1	2	5379	48	0	14
8KB	16B	0	0	1	8	2	2	2	5485	48	0	14
8KB	16B	0	0	2	8	2	2	1	6329	54	0	10
8KB	16B	0	0	2	8	2	2	2	6440	54	0	14
8KB	16B	0	0	1	16	4	2	2	5984	52	0	14
8KB	16B	0	0	1	16	4	2	4	6138	52	0	22
8KB	16B	0	0	1	16	4	4	2	6063	52	0	14
8KB	16B	0	0	1	16	4	4	4	6087	52	0	22
8KB	16B	0	0	2	16	4	4	2	7548	62	0	14
8KB	16B	0	0	1	128	4	4	4	6197	76	0	22
8KB	16B	0	0	2	16	4	4	4	7749	62	0	22
8KB	16B	0	0	2	128	4	4	2	7646	78	0	14
32KB	64B	0	0	1	16	4	2	4	6913	74	0	22
32KB	64B	8*VL	0	1	16	4	2	4	6916	74	0	22
8KB	16B	0	0	1	32	8	4	4	7125	60	0	22
8KB	16B	0	0	2	128	4	4	4	7784	78	0	22
8KB	16B	0	0	1	32	8	8	4	7319	60	0	22
32KB	64B	7	0	1	16	4	4	2	7135	74	0	14
32KB	64B	7	0	1	16	4	4	4	7207	74	0	22
32KB	64B	7	0	2	16	4	4	2	9371	84	0	14
32KB	64B	7	0	2	16	4	4	4	9548	84	0	22
32KB	64B	7	0	2	128	4	4	2	9345	100	0	14
32KB	64B	8*VL	0	2	128	4	4	2	9397	100	0	15
32KB	64B	7	0	2	128	4	4	4	9496	100	0	22
32KB	64B	8*VL	0	2	128	4	4	4	9641	100	0	23
32KB	64B	8*VL	1	2	128	4	4	4	10233	100	0	23
32KB	64B	8*VL	0	1	32	8	8	4	8988	82	0	22
32KB	64B	7	0	1	32	8	8	4	9096	82	0	22
32KB	64B	7	0	1	32	8	8	8	8956	82	0	38
32KB	64B	8*VL	0	1	128	8	8	8	9137	98	0	38
32KB	64B	7	0	2	128	8	8	4	13006	100	0	22
32KB	64B	8*VL	0	2	128	8	8	4	13007	100	0	23
32KB	64B	7	0	2	128	8	8	8	13352	100	0	38
32KB	64B	8*VL	0	2	128	8	8	8	13531	100	0	39
32KB	64B	7	1	2	128	8	8	8	14572	100	0	38
32KB	64B	8*VL	1	2	128	8	8	8	14593	100	0	39
32KB	64B	8*VL	0	2	128	16	8	8	17035	132	0	39
32KB	64B	8*VL	0	1	64	16	16	8	12456	98	0	38
32KB	64B	8*VL	0	1	128	16	16	8	12481	98	0	38
32KB	64B	8*VL	0	2	128	16	8	16	17837	132	0	71
32KB	64B	8*VL	0	1	64	16	16	16	12779	98	0	70
32KB	64B	8*VL	0	1	128	16	16	16	12754	98	0	70
32KB	64B	8*VL	0	2	128	16	16	8	22321	132	0	39
32KB	64B	7	0	2	128	16	16	16	21901	132	0	70
32KB	64B	7	1	2	128	16	16	16	25152	132	0	70
32KB	64B	8*VL	1	2	128	16	16	16	24363	132	0	71
32KB	64B	7	0	1	128	32	32	32	20555	130	0	134
32KB	64B	8*VL	0	2	512	32	16	32	31633	196	0	135
32KB	64B	7	0	1	512	32	32	32	20744	196	0	134
32KB	64B	8*VL	0	1	512	32	32	32	21034	196	0	134
32KB	64B	8*VL	0	2	128	32	32	32	39621	196	0	135
32KB	64B	7	0	2	128	32	32	32	36944	196	0	134
32KB	64B	8*VL	0	2	512	32	32	32	37234	196	0	135
32KB	64B	8*VL	1	2	512	32	32	32	43321	196	0	135

Table B.7: System area of pareto optimal VESPA configurations after instruction subsetting and width reduction for CONVEN.

DD	DW	DPV	APB	B	MVL	L	M	X	ALMs	M9Ks	M144Ks	18-bit DSPs
8KB	16B	0	0	1	4	1	1	1	4900	46	0	6
8KB	16B	0	0	1	8	2	1	1	4885	46	0	6
8KB	16B	0	0	1	8	2	1	2	4967	46	0	6
8KB	16B	0	0	1	8	2	2	2	4952	46	0	6
8KB	16B	0	0	2	8	2	2	1	5257	50	0	6
8KB	16B	0	0	2	8	2	2	2	5292	50	0	6
8KB	16B	0	0	1	16	4	2	2	5135	46	0	6
8KB	16B	0	0	1	16	4	2	4	5125	46	0	6
8KB	16B	0	0	1	16	4	4	2	5193	46	0	6
8KB	16B	0	0	1	16	4	4	4	5243	46	0	6
8KB	16B	0	0	2	16	4	4	2	5528	50	0	6
8KB	16B	0	0	1	128	4	4	4	5273	52	0	6
8KB	16B	0	0	2	16	4	4	4	5607	50	0	6
8KB	16B	0	0	2	128	4	4	2	5618	54	0	6
32KB	64B	0	0	1	16	4	2	4	5912	68	0	6
32KB	64B	8*VL	0	1	16	4	2	4	6007	68	0	7
8KB	16B	0	0	1	32	8	4	4	5498	48	0	6
8KB	16B	0	0	2	128	4	4	4	5617	54	0	6
8KB	16B	0	0	1	32	8	8	4	5494	48	0	6
32KB	64B	7	0	1	16	4	4	2	6107	68	0	6
32KB	64B	7	0	1	16	4	4	4	6120	68	0	6
32KB	64B	7	0	2	16	4	4	2	6458	72	0	6
32KB	64B	7	0	2	16	4	4	4	6552	72	0	6
32KB	64B	7	0	2	128	4	4	2	6603	76	0	6
32KB	64B	8*VL	0	2	128	4	4	2	6586	76	0	7
32KB	64B	7	0	2	128	4	4	4	6551	76	0	6
32KB	64B	8*VL	0	2	128	4	4	4	6601	76	0	7
32KB	64B	8*VL	1	2	128	4	4	4	6606	76	0	7
32KB	64B	8*VL	0	1	32	8	8	4	6751	70	0	7
32KB	64B	7	0	1	32	8	8	4	6676	70	0	6
32KB	64B	7	0	1	32	8	8	8	6737	70	0	6
32KB	64B	8*VL	0	1	128	8	8	8	6766	74	0	7
32KB	64B	7	0	2	128	8	8	4	7328	76	0	6
32KB	64B	8*VL	0	2	128	8	8	4	7355	76	0	7
32KB	64B	7	0	2	128	8	8	8	7282	76	0	6
32KB	64B	8*VL	0	2	128	8	8	8	7291	76	0	7
32KB	64B	7	1	2	128	8	8	8	7419	76	0	6
32KB	64B	8*VL	1	2	128	8	8	8	7438	76	0	7
32KB	64B	8*VL	0	2	128	16	8	8	8179	84	0	15
32KB	64B	8*VL	0	1	64	16	16	8	8101	74	0	15
32KB	64B	8*VL	0	1	128	16	16	8	8054	74	0	15
32KB	64B	8*VL	0	2	128	16	8	16	8266	84	0	15
32KB	64B	8*VL	0	1	64	16	16	16	8082	74	0	15
32KB	64B	8*VL	0	1	128	16	16	16	8103	74	0	15
32KB	64B	8*VL	0	2	128	16	16	8	8975	84	0	15
32KB	64B	7	0	2	128	16	16	16	8909	84	0	14
32KB	64B	7	1	2	128	16	16	16	9173	84	0	14
32KB	64B	8*VL	1	2	128	16	16	16	9236	84	0	15
32KB	64B	7	0	1	128	32	32	32	11032	82	0	46
32KB	64B	8*VL	0	2	512	32	16	32	11146	100	0	47
32KB	64B	7	0	1	512	32	32	32	10876	100	0	46
32KB	64B	8*VL	0	1	512	32	32	32	10676	100	0	47
32KB	64B	8*VL	0	2	128	32	32	32	12470	100	0	47
32KB	64B	7	0	2	128	32	32	32	12516	100	0	46
32KB	64B	8*VL	0	2	512	32	32	32	12639	100	0	47
32KB	64B	8*VL	1	2	512	32	32	32	12863	100	0	47

Table B.8: System area of pareto optimal VESPA configurations after instruction subsetting and width reduction for RGBCMYK.

DD	DW	DPV	APB	B	MVL	L	M	X	ALMs	M9Ks	M144Ks	18-bit DSPs
8KB	16B	0	0	1	4	1	1	1	5072	46	0	6
8KB	16B	0	0	1	8	2	1	1	5105	46	0	6
8KB	16B	0	0	1	8	2	1	2	5127	46	0	6
8KB	16B	0	0	1	8	2	2	2	5264	46	0	6
8KB	16B	0	0	2	8	2	2	1	5761	50	0	7
8KB	16B	0	0	2	8	2	2	2	5603	50	0	8
8KB	16B	0	0	1	16	4	2	2	5413	46	0	6
8KB	16B	0	0	1	16	4	2	4	5497	46	0	6
8KB	16B	0	0	1	16	4	4	2	5588	46	0	6
8KB	16B	0	0	1	16	4	4	4	5656	46	0	6
8KB	16B	0	0	2	16	4	4	2	6240	50	0	8
8KB	16B	0	0	1	128	4	4	4	5701	52	0	6
8KB	16B	0	0	2	16	4	4	4	6296	50	0	10
8KB	16B	0	0	2	128	4	4	2	6295	54	0	8
32KB	64B	0	0	1	16	4	2	4	6672	68	0	6
32KB	64B	8*VL	0	1	16	4	2	4	6660	68	0	7
8KB	16B	0	0	1	32	8	4	4	5994	48	0	6
8KB	16B	0	0	2	128	4	4	4	6340	54	0	10
8KB	16B	0	0	1	32	8	8	4	6469	48	0	6
32KB	64B	7	0	1	16	4	4	2	7403	68	0	6
32KB	64B	7	0	1	16	4	4	4	7458	68	0	6
32KB	64B	7	0	2	16	4	4	2	7878	72	0	8
32KB	64B	7	0	2	16	4	4	4	7924	72	0	10
32KB	64B	7	0	2	128	4	4	2	8018	76	0	8
32KB	64B	8*VL	0	2	128	4	4	2	8050	76	0	9
32KB	64B	7	0	2	128	4	4	4	7922	76	0	10
32KB	64B	8*VL	0	2	128	4	4	4	8102	76	0	11
32KB	64B	8*VL	1	2	128	4	4	4	8241	76	0	11
32KB	64B	8*VL	0	1	32	8	8	4	9493	70	0	7
32KB	64B	7	0	1	32	8	8	4	9434	70	0	6
32KB	64B	7	0	1	32	8	8	8	9473	70	0	6
32KB	64B	8*VL	0	1	128	8	8	8	9553	74	0	7
32KB	64B	7	0	2	128	8	8	4	10754	76	0	10
32KB	64B	8*VL	0	2	128	8	8	4	10729	76	0	11
32KB	64B	7	0	2	128	8	8	8	10477	76	0	14
32KB	64B	8*VL	0	2	128	8	8	8	10670	76	0	15
32KB	64B	7	1	2	128	8	8	8	10748	76	0	14
32KB	64B	8*VL	1	2	128	8	8	8	11152	76	0	15
32KB	64B	8*VL	0	2	128	16	8	8	12005	84	0	23
32KB	64B	8*VL	0	1	64	16	16	8	14619	74	0	15
32KB	64B	8*VL	0	1	128	16	16	8	14677	74	0	15
32KB	64B	8*VL	0	2	128	16	8	16	12064	84	0	31
32KB	64B	8*VL	0	1	64	16	16	16	14545	74	0	15
32KB	64B	8*VL	0	1	128	16	16	16	14627	74	0	15
32KB	64B	8*VL	0	2	128	16	16	8	16942	84	0	23
32KB	64B	7	0	2	128	16	16	16	16245	84	0	30
32KB	64B	7	1	2	128	16	16	16	16934	84	0	30
32KB	64B	8*VL	1	2	128	16	16	16	17635	84	0	31
32KB	64B	7	0	1	128	32	32	32	22141	82	0	46
32KB	64B	8*VL	0	2	512	32	16	32	20361	100	0	79
32KB	64B	7	0	1	512	32	32	32	22012	100	0	46
32KB	64B	8*VL	0	1	512	32	32	32	21898	100	0	47
32KB	64B	8*VL	0	2	128	32	32	32	27560	100	0	79
32KB	64B	7	0	2	128	32	32	32	25509	100	0	78
32KB	64B	8*VL	0	2	512	32	32	32	27573	100	0	79
32KB	64B	8*VL	1	2	512	32	32	32	28766	100	0	79

Table B.9: System area of pareto optimal VESPA configurations after instruction subsetting and width reduction for RGBYIQ.

DD	DW	DPV	APB	B	MVL	L	M	X	ALMs	M9Ks	M144Ks	18-bit DSPs
8KB	16B	0	0	1	4	1	1	1	5145	46	0	8
8KB	16B	0	0	1	8	2	1	1	5201	46	0	8
8KB	16B	0	0	1	8	2	1	2	5178	46	0	10
8KB	16B	0	0	1	8	2	2	2	5381	46	0	10
8KB	16B	0	0	2	8	2	2	1	5919	50	0	8
8KB	16B	0	0	2	8	2	2	2	5935	50	0	10
8KB	16B	0	0	1	16	4	2	2	5631	48	0	10
8KB	16B	0	0	1	16	4	2	4	5719	48	0	14
8KB	16B	0	0	1	16	4	4	2	5865	48	0	10
8KB	16B	0	0	1	16	4	4	4	5917	48	0	14
8KB	16B	0	0	2	16	4	4	2	6687	54	0	10
8KB	16B	0	0	1	128	4	4	4	6012	60	0	14
8KB	16B	0	0	2	16	4	4	4	6835	54	0	14
8KB	16B	0	0	2	128	4	4	2	6819	62	0	10
32KB	64B	0	0	1	16	4	2	4	6999	70	0	14
32KB	64B	8*VL	0	1	16	4	2	4	6964	70	0	15
8KB	16B	0	0	1	32	8	4	4	6453	52	0	14
8KB	16B	0	0	2	128	4	4	4	6790	62	0	14
8KB	16B	0	0	1	32	8	8	4	6848	52	0	14
32KB	64B	7	0	1	16	4	4	2	7597	70	0	10
32KB	64B	7	0	1	16	4	4	4	7627	70	0	14
32KB	64B	7	0	2	16	4	4	2	8370	76	0	10
32KB	64B	7	0	2	16	4	4	4	8407	76	0	14
32KB	64B	7	0	2	128	4	4	2	8408	84	0	10
32KB	64B	8*VL	0	2	128	4	4	2	8358	84	0	11
32KB	64B	7	0	2	128	4	4	4	8440	84	0	14
32KB	64B	8*VL	0	2	128	4	4	4	8551	84	0	15
32KB	64B	8*VL	1	2	128	4	4	4	8836	84	0	15
32KB	64B	8*VL	0	1	32	8	8	4	9862	74	0	15
32KB	64B	7	0	1	32	8	8	4	9930	74	0	14
32KB	64B	7	0	1	32	8	8	8	10044	74	0	22
32KB	64B	8*VL	0	1	128	8	8	8	9974	82	0	23
32KB	64B	7	0	2	128	8	8	4	11284	84	0	14
32KB	64B	8*VL	0	2	128	8	8	4	11458	84	0	15
32KB	64B	7	0	2	128	8	8	8	11541	84	0	22
32KB	64B	8*VL	0	2	128	8	8	8	11780	84	0	23
32KB	64B	7	1	2	128	8	8	8	12168	84	0	22
32KB	64B	8*VL	1	2	128	8	8	8	12442	84	0	23
32KB	64B	8*VL	0	2	128	16	8	8	13908	100	0	31
32KB	64B	8*VL	0	1	64	16	16	8	15379	82	0	31
32KB	64B	8*VL	0	1	128	16	16	8	15416	82	0	31
32KB	64B	8*VL	0	2	128	16	8	16	14174	100	0	47
32KB	64B	8*VL	0	1	64	16	16	16	15530	82	0	47
32KB	64B	8*VL	0	1	128	16	16	16	15499	82	0	47
32KB	64B	8*VL	0	2	128	16	16	8	18432	100	0	31
32KB	64B	7	0	2	128	16	16	16	18369	100	0	46
32KB	64B	7	1	2	128	16	16	16	20239	100	0	46
32KB	64B	8*VL	1	2	128	16	16	16	19879	100	0	47
32KB	64B	7	0	1	128	32	32	32	24181	98	0	110
32KB	64B	8*VL	0	2	512	32	16	32	24082	132	0	111
32KB	64B	7	0	1	512	32	32	32	24100	132	0	110
32KB	64B	8*VL	0	1	512	32	32	32	23758	132	0	111
32KB	64B	8*VL	0	2	128	32	32	32	31992	132	0	111
32KB	64B	7	0	2	128	32	32	32	30434	132	0	110
32KB	64B	8*VL	0	2	512	32	32	32	32241	132	0	111
32KB	64B	8*VL	1	2	512	32	32	32	32783	132	0	111

Table B.10: System area of pareto optimal VESPA configurations after instruction subsetting and width reduction for IP\_CHECKSUM.

DD	DW	DPV	APB	B	MVL	L	M	X	ALMs	M9Ks	M144Ks	18-bit DSPs
8KB	16B	0	0	1	4	1	1	1	4932	46	0	6
8KB	16B	0	0	1	8	2	1	1	5096	48	0	6
8KB	16B	0	0	1	8	2	1	2	5196	48	0	6
8KB	16B	0	0	1	8	2	2	2	5203	48	0	6
8KB	16B	0	0	2	8	2	2	1	6378	54	0	10
8KB	16B	0	0	2	8	2	2	2	6382	54	0	14
8KB	16B	0	0	1	16	4	2	2	5615	52	0	6
8KB	16B	0	0	1	16	4	2	4	5549	52	0	6
8KB	16B	0	0	1	16	4	4	2	5674	52	0	6
8KB	16B	0	0	1	16	4	4	4	5658	52	0	6
8KB	16B	0	0	2	16	4	4	2	7529	62	0	14
8KB	16B	0	0	1	128	4	4	4	5724	76	0	6
8KB	16B	0	0	2	16	4	4	4	7706	62	0	22
8KB	16B	0	0	2	128	4	4	2	7619	78	0	14
32KB	64B	0	0	1	16	4	2	4	6483	74	0	6
32KB	64B	8*VL	0	1	16	4	2	4	6471	74	0	6
8KB	16B	0	0	1	32	8	4	4	6294	60	0	6
8KB	16B	0	0	2	128	4	4	4	7769	78	0	22
8KB	16B	0	0	1	32	8	8	4	6599	60	0	6
32KB	64B	7	0	1	16	4	4	2	6799	74	0	6
32KB	64B	7	0	1	16	4	4	4	6762	74	0	6
32KB	64B	7	0	2	16	4	4	2	9345	84	0	14
32KB	64B	7	0	2	16	4	4	4	9494	84	0	22
32KB	64B	7	0	2	128	4	4	2	9380	100	0	14
32KB	64B	8*VL	0	2	128	4	4	2	9454	100	0	15
32KB	64B	7	0	2	128	4	4	4	9534	100	0	22
32KB	64B	8*VL	0	2	128	4	4	4	9583	100	0	23
32KB	64B	8*VL	1	2	128	4	4	4	10190	100	0	23
32KB	64B	8*VL	0	1	32	8	8	4	8185	82	0	6
32KB	64B	7	0	1	32	8	8	4	8219	82	0	6
32KB	64B	7	0	1	32	8	8	8	8216	82	0	6
32KB	64B	8*VL	0	1	128	8	8	8	8165	98	0	6
32KB	64B	7	0	2	128	8	8	4	12923	100	0	22
32KB	64B	8*VL	0	2	128	8	8	4	12934	100	0	23
32KB	64B	7	0	2	128	8	8	8	13497	100	0	38
32KB	64B	8*VL	0	2	128	8	8	8	13393	100	0	39
32KB	64B	7	1	2	128	8	8	8	14486	100	0	38
32KB	64B	8*VL	1	2	128	8	8	8	15054	100	0	39
32KB	64B	8*VL	0	2	128	16	8	8	17058	132	0	39
32KB	64B	8*VL	0	1	64	16	16	8	10895	98	0	6
32KB	64B	8*VL	0	1	128	16	16	8	11030	98	0	6
32KB	64B	8*VL	0	2	128	16	8	16	18028	132	0	71
32KB	64B	8*VL	0	1	64	16	16	16	10808	98	0	6
32KB	64B	8*VL	0	1	128	16	16	16	11018	98	0	6
32KB	64B	8*VL	0	2	128	16	16	8	20952	132	0	39
32KB	64B	7	0	2	128	16	16	16	22525	132	0	70
32KB	64B	7	1	2	128	16	16	16	24445	132	0	70
32KB	64B	8*VL	1	2	128	16	16	16	24351	132	0	71
32KB	64B	7	0	1	128	32	32	32	16854	130	0	6
32KB	64B	8*VL	0	2	512	32	16	32	31153	196	0	135
32KB	64B	7	0	1	512	32	32	32	17031	196	0	6
32KB	64B	8*VL	0	1	512	32	32	32	16911	196	0	6
32KB	64B	8*VL	0	2	128	32	32	32	37247	196	0	135
32KB	64B	7	0	2	128	32	32	32	39438	196	0	134
32KB	64B	8*VL	0	2	512	32	32	32	39597	196	0	135
32KB	64B	8*VL	1	2	512	32	32	32	42765	196	0	135

Table B.11: System area of pareto optimal VESPA configurations after instruction subsetting and width reduction for IMGBLEND.

DD	DW	DPV	APB	B	MVL	L	M	X	ALMs	M9Ks	M144Ks	18-bit DSPs
8KB	16B	0	0	1	4	1	1	1	4991	46	0	7
8KB	16B	0	0	1	8	2	1	1	5102	46	0	7
8KB	16B	0	0	1	8	2	1	2	5116	46	0	8
8KB	16B	0	0	1	8	2	2	2	5185	46	0	8
8KB	16B	0	0	2	8	2	2	1	5652	50	0	7
8KB	16B	0	0	2	8	2	2	2	5645	50	0	8
8KB	16B	0	0	1	16	4	2	2	5475	46	0	8
8KB	16B	0	0	1	16	4	2	4	5491	46	0	10
8KB	16B	0	0	1	16	4	4	2	5676	46	0	8
8KB	16B	0	0	1	16	4	4	4	5627	46	0	10
8KB	16B	0	0	2	16	4	4	2	6147	50	0	8
8KB	16B	0	0	1	128	4	4	4	5633	52	0	10
8KB	16B	0	0	2	16	4	4	4	6191	50	0	10
8KB	16B	0	0	2	128	4	4	2	6216	54	0	8
32KB	64B	0	0	1	16	4	2	4	6581	68	0	10
32KB	64B	8*VL	0	1	16	4	2	4	6671	68	0	10
8KB	16B	0	0	1	32	8	4	4	6058	48	0	10
8KB	16B	0	0	2	128	4	4	4	6270	54	0	10
8KB	16B	0	0	1	32	8	8	4	6545	48	0	10
32KB	64B	7	0	1	16	4	4	2	7356	68	0	8
32KB	64B	7	0	1	16	4	4	4	7386	68	0	10
32KB	64B	7	0	2	16	4	4	2	7794	72	0	8
32KB	64B	7	0	2	16	4	4	4	7904	72	0	10
32KB	64B	7	0	2	128	4	4	2	7925	76	0	8
32KB	64B	8*VL	0	2	128	4	4	2	7945	76	0	9
32KB	64B	7	0	2	128	4	4	4	7927	76	0	10
32KB	64B	8*VL	0	2	128	4	4	4	7855	76	0	11
32KB	64B	8*VL	1	2	128	4	4	4	8119	76	0	11
32KB	64B	8*VL	0	1	32	8	8	4	9485	70	0	10
32KB	64B	7	0	1	32	8	8	4	9406	70	0	10
32KB	64B	7	0	1	32	8	8	8	9486	70	0	14
32KB	64B	8*VL	0	1	128	8	8	8	9520	74	0	14
32KB	64B	7	0	2	128	8	8	4	10245	76	0	10
32KB	64B	8*VL	0	2	128	8	8	4	10546	76	0	11
32KB	64B	7	0	2	128	8	8	8	10322	76	0	14
32KB	64B	8*VL	0	2	128	8	8	8	10621	76	0	15
32KB	64B	7	1	2	128	8	8	8	10559	76	0	14
32KB	64B	8*VL	1	2	128	8	8	8	10950	76	0	15
32KB	64B	8*VL	0	2	128	16	8	8	11751	84	0	15
32KB	64B	8*VL	0	1	64	16	16	8	14513	74	0	14
32KB	64B	8*VL	0	1	128	16	16	8	14397	74	0	14
32KB	64B	8*VL	0	2	128	16	8	16	11933	84	0	23
32KB	64B	8*VL	0	1	64	16	16	16	14559	74	0	22
32KB	64B	8*VL	0	1	128	16	16	16	14752	74	0	22
32KB	64B	8*VL	0	2	128	16	16	8	15952	84	0	15
32KB	64B	7	0	2	128	16	16	16	15867	84	0	22
32KB	64B	7	1	2	128	16	16	16	16632	84	0	22
32KB	64B	8*VL	1	2	128	16	16	16	16800	84	0	23
32KB	64B	7	0	1	128	32	32	32	22180	82	0	38
32KB	64B	8*VL	0	2	512	32	16	32	19231	100	0	39
32KB	64B	7	0	1	512	32	32	32	22179	100	0	38
32KB	64B	8*VL	0	1	512	32	32	32	22064	100	0	38
32KB	64B	8*VL	0	2	128	32	32	32	26417	100	0	39
32KB	64B	7	0	2	128	32	32	32	24604	100	0	38
32KB	64B	8*VL	0	2	512	32	32	32	24790	100	0	39
32KB	64B	8*VL	1	2	512	32	32	32	25952	100	0	39

Table B.12: System area of pareto optimal VESPA configurations after instruction subsetting and width reduction for FILT3x3.

DD	DW	DPV	APB	B	MVL	L	M	X	ALMs	M9Ks	M144Ks	18-bit DSPs
8KB	16B	0	0	1	4	1	1	1	4991	46	0	7
8KB	16B	0	0	1	8	2	1	1	5102	46	0	7
8KB	16B	0	0	1	8	2	1	2	5116	46	0	8
8KB	16B	0	0	1	8	2	2	2	5185	46	0	8
8KB	16B	0	0	2	8	2	2	1	5652	50	0	7
8KB	16B	0	0	2	8	2	2	2	5645	50	0	8
8KB	16B	0	0	1	16	4	2	2	5475	46	0	8
8KB	16B	0	0	1	16	4	2	4	5491	46	0	10
8KB	16B	0	0	1	16	4	4	2	5676	46	0	8
8KB	16B	0	0	1	16	4	4	4	5627	46	0	10
8KB	16B	0	0	2	16	4	4	2	6147	50	0	8
8KB	16B	0	0	1	128	4	4	4	5633	52	0	10
8KB	16B	0	0	2	16	4	4	4	6191	50	0	10
8KB	16B	0	0	2	128	4	4	2	6216	54	0	8
32KB	64B	0	0	1	16	4	2	4	6581	68	0	10
32KB	64B	8*VL	0	1	16	4	2	4	6671	68	0	10
8KB	16B	0	0	1	32	8	4	4	6058	48	0	10
8KB	16B	0	0	2	128	4	4	4	6270	54	0	10
8KB	16B	0	0	1	32	8	8	4	6545	48	0	10
32KB	64B	7	0	1	16	4	4	2	7356	68	0	8
32KB	64B	7	0	1	16	4	4	4	7386	68	0	10
32KB	64B	7	0	2	16	4	4	2	7794	72	0	8
32KB	64B	7	0	2	16	4	4	4	7904	72	0	10
32KB	64B	7	0	2	128	4	4	2	7925	76	0	8
32KB	64B	8*VL	0	2	128	4	4	2	7945	76	0	9
32KB	64B	7	0	2	128	4	4	4	7927	76	0	10
32KB	64B	8*VL	0	2	128	4	4	4	7855	76	0	11
32KB	64B	8*VL	1	2	128	4	4	4	8119	76	0	11
32KB	64B	8*VL	0	1	32	8	8	4	9485	70	0	10
32KB	64B	7	0	1	32	8	8	4	9406	70	0	10
32KB	64B	7	0	1	32	8	8	8	9486	70	0	14
32KB	64B	8*VL	0	1	128	8	8	8	9520	74	0	14
32KB	64B	7	0	2	128	8	8	4	10245	76	0	10
32KB	64B	8*VL	0	2	128	8	8	4	10546	76	0	11
32KB	64B	7	0	2	128	8	8	8	10322	76	0	14
32KB	64B	8*VL	0	2	128	8	8	8	10621	76	0	15
32KB	64B	7	1	2	128	8	8	8	10559	76	0	14
32KB	64B	8*VL	1	2	128	8	8	8	10950	76	0	15
32KB	64B	8*VL	0	2	128	16	8	8	11751	84	0	15
32KB	64B	8*VL	0	1	64	16	16	8	14513	74	0	14
32KB	64B	8*VL	0	1	128	16	16	8	14397	74	0	14
32KB	64B	8*VL	0	2	128	16	8	16	11933	84	0	23
32KB	64B	8*VL	0	1	64	16	16	16	14559	74	0	22
32KB	64B	8*VL	0	1	128	16	16	16	14752	74	0	22
32KB	64B	8*VL	0	2	128	16	16	8	15952	84	0	15
32KB	64B	7	0	2	128	16	16	16	15867	84	0	22
32KB	64B	7	1	2	128	16	16	16	16632	84	0	22
32KB	64B	8*VL	1	2	128	16	16	16	16800	84	0	23
32KB	64B	7	0	1	128	32	32	32	22180	82	0	38
32KB	64B	8*VL	0	2	512	32	16	32	19231	100	0	39
32KB	64B	7	0	1	512	32	32	32	22179	100	0	38
32KB	64B	8*VL	0	1	512	32	32	32	22064	100	0	38
32KB	64B	8*VL	0	2	128	32	32	32	26417	100	0	39
32KB	64B	7	0	2	128	32	32	32	24604	100	0	38
32KB	64B	8*VL	0	2	512	32	32	32	24790	100	0	39
32KB	64B	8*VL	1	2	512	32	32	32	25952	100	0	39

Table B.13: System area of pareto optimal VESPA configurations after instruction subsetting and width reduction for FBITAL.

DD	DW	DPV	APB	B	MVL	L	M	X	ALMs	M9Ks	M144Ks	18-bit DSPs
8KB	16B	0	0	1	4	1	1	1	5251	46	0	8
8KB	16B	0	0	1	8	2	1	1	5305	46	0	8
8KB	16B	0	0	1	8	2	1	2	5290	46	0	10
8KB	16B	0	0	1	8	2	2	2	5530	46	0	10
8KB	16B	0	0	2	8	2	2	1	5930	50	0	8
8KB	16B	0	0	2	8	2	2	2	5974	50	0	10
8KB	16B	0	0	1	16	4	2	2	5768	48	0	10
8KB	16B	0	0	1	16	4	2	4	5860	48	0	14
8KB	16B	0	0	1	16	4	4	2	6066	48	0	10
8KB	16B	0	0	1	16	4	4	4	6013	48	0	14
8KB	16B	0	0	2	16	4	4	2	6662	54	0	10
8KB	16B	0	0	1	128	4	4	4	6139	60	0	14
8KB	16B	0	0	2	16	4	4	4	6729	54	0	14
8KB	16B	0	0	2	128	4	4	2	6716	62	0	10
32KB	64B	0	0	1	16	4	2	4	6968	70	0	14
32KB	64B	8*VL	0	1	16	4	2	4	7123	70	0	14
8KB	16B	0	0	1	32	8	4	4	6640	52	0	14
8KB	16B	0	0	2	128	4	4	4	6882	62	0	14
8KB	16B	0	0	1	32	8	8	4	7150	52	0	14
32KB	64B	7	0	1	16	4	4	2	7716	70	0	10
32KB	64B	7	0	1	16	4	4	4	7726	70	0	14
32KB	64B	7	0	2	16	4	4	2	8416	76	0	10
32KB	64B	7	0	2	16	4	4	4	8428	76	0	14
32KB	64B	7	0	2	128	4	4	2	8315	84	0	10
32KB	64B	8*VL	0	2	128	4	4	2	8539	84	0	11
32KB	64B	7	0	2	128	4	4	4	8574	84	0	14
32KB	64B	8*VL	0	2	128	4	4	4	8504	84	0	15
32KB	64B	8*VL	1	2	128	4	4	4	8919	84	0	15
32KB	64B	8*VL	0	1	32	8	8	4	10157	74	0	14
32KB	64B	7	0	1	32	8	8	4	10172	74	0	14
32KB	64B	7	0	1	32	8	8	8	10199	74	0	22
32KB	64B	8*VL	0	1	128	8	8	8	10364	82	0	22
32KB	64B	7	0	2	128	8	8	4	11435	84	0	14
32KB	64B	8*VL	0	2	128	8	8	4	11572	84	0	15
32KB	64B	7	0	2	128	8	8	8	11380	84	0	22
32KB	64B	8*VL	0	2	128	8	8	8	11459	84	0	23
32KB	64B	7	1	2	128	8	8	8	12286	84	0	22
32KB	64B	8*VL	1	2	128	8	8	8	11852	84	0	23
32KB	64B	8*VL	0	2	128	16	8	8	13566	100	0	23
32KB	64B	8*VL	0	1	64	16	16	8	15925	82	0	22
32KB	64B	8*VL	0	1	128	16	16	8	15854	82	0	22
32KB	64B	8*VL	0	2	128	16	8	16	13851	100	0	39
32KB	64B	8*VL	0	1	64	16	16	16	16040	82	0	38
32KB	64B	8*VL	0	1	128	16	16	16	16085	82	0	38
32KB	64B	8*VL	0	2	128	16	16	8	17587	100	0	23
32KB	64B	7	0	2	128	16	16	16	18060	100	0	38
32KB	64B	7	1	2	128	16	16	16	18909	100	0	38
32KB	64B	8*VL	1	2	128	16	16	16	18923	100	0	39
32KB	64B	7	0	1	128	32	32	32	25095	98	0	70
32KB	64B	8*VL	0	2	512	32	16	32	22773	132	0	71
32KB	64B	7	0	1	512	32	32	32	25278	132	0	70
32KB	64B	8*VL	0	1	512	32	32	32	25288	132	0	70
32KB	64B	8*VL	0	2	128	32	32	32	30822	132	0	71
32KB	64B	7	0	2	128	32	32	32	30714	132	0	70
32KB	64B	8*VL	0	2	512	32	32	32	31040	132	0	71
32KB	64B	8*VL	1	2	512	32	32	32	33409	132	0	71

Table B.14: System area of pareto optimal VESPA configurations after instruction subsetting and width reduction for VITERB.

DD	DW	DPV	APB	B	MVL	L	M	X	ALMs	M9Ks	M144Ks	18-bit DSPs
8KB	16B	0	0	1	4	1	1	1	5149	46	0	8
8KB	16B	0	0	1	8	2	1	1	5314	46	0	8
8KB	16B	0	0	1	8	2	1	2	5377	46	0	10
8KB	16B	0	0	1	8	2	2	2	5416	46	0	10
8KB	16B	0	0	2	8	2	2	1	5903	50	0	8
8KB	16B	0	0	2	8	2	2	2	5885	50	0	10
8KB	16B	0	0	1	16	4	2	2	5750	48	0	10
8KB	16B	0	0	1	16	4	2	4	5833	48	0	14
8KB	16B	0	0	1	16	4	4	2	6005	48	0	10
8KB	16B	0	0	1	16	4	4	4	6088	48	0	14
8KB	16B	0	0	2	16	4	4	2	6714	54	0	10
8KB	16B	0	0	1	128	4	4	4	6126	60	0	14
8KB	16B	0	0	2	16	4	4	4	6767	54	0	14
8KB	16B	0	0	2	128	4	4	2	6805	62	0	10
32KB	64B	0	0	1	16	4	2	4	7078	70	0	14
32KB	64B	8*VL	0	1	16	4	2	4	6908	70	0	15
8KB	16B	0	0	1	32	8	4	4	6656	52	0	14
8KB	16B	0	0	2	128	4	4	4	6849	62	0	14
8KB	16B	0	0	1	32	8	8	4	7231	52	0	14
32KB	64B	7	0	1	16	4	4	2	7733	70	0	10
32KB	64B	7	0	1	16	4	4	4	7769	70	0	14
32KB	64B	7	0	2	16	4	4	2	8404	76	0	10
32KB	64B	7	0	2	16	4	4	4	8446	76	0	14
32KB	64B	7	0	2	128	4	4	2	8510	84	0	10
32KB	64B	8*VL	0	2	128	4	4	2	8350	84	0	11
32KB	64B	7	0	2	128	4	4	4	8504	84	0	14
32KB	64B	8*VL	0	2	128	4	4	4	8478	84	0	15
32KB	64B	8*VL	1	2	128	4	4	4	8881	84	0	15
32KB	64B	8*VL	0	1	32	8	8	4	10142	74	0	15
32KB	64B	7	0	1	32	8	8	4	10151	74	0	14
32KB	64B	7	0	1	32	8	8	8	10095	74	0	22
32KB	64B	8*VL	0	1	128	8	8	8	10271	82	0	23
32KB	64B	7	0	2	128	8	8	4	11447	84	0	14
32KB	64B	8*VL	0	2	128	8	8	4	11358	84	0	15
32KB	64B	7	0	2	128	8	8	8	11422	84	0	22
32KB	64B	8*VL	0	2	128	8	8	8	11695	84	0	23
32KB	64B	7	1	2	128	8	8	8	11964	84	0	22
32KB	64B	8*VL	1	2	128	8	8	8	12296	84	0	23
32KB	64B	8*VL	0	2	128	16	8	8	13867	100	0	31
32KB	64B	8*VL	0	1	64	16	16	8	15784	82	0	31
32KB	64B	8*VL	0	1	128	16	16	8	15814	82	0	31
32KB	64B	8*VL	0	2	128	16	8	16	14167	100	0	47
32KB	64B	8*VL	0	1	64	16	16	16	16119	82	0	47
32KB	64B	8*VL	0	1	128	16	16	16	16032	82	0	47
32KB	64B	8*VL	0	2	128	16	16	8	17666	100	0	31
32KB	64B	7	0	2	128	16	16	16	17966	100	0	46
32KB	64B	7	1	2	128	16	16	16	19147	100	0	46
32KB	64B	8*VL	1	2	128	16	16	16	19982	100	0	47
32KB	64B	7	0	1	128	32	32	32	24991	98	0	110
32KB	64B	8*VL	0	2	512	32	16	32	23890	132	0	111
32KB	64B	7	0	1	512	32	32	32	25096	132	0	110
32KB	64B	8*VL	0	1	512	32	32	32	25891	132	0	111
32KB	64B	8*VL	0	2	128	32	32	32	31784	132	0	111
32KB	64B	7	0	2	128	32	32	32	31810	132	0	110
32KB	64B	8*VL	0	2	512	32	32	32	32233	132	0	111
32KB	64B	8*VL	1	2	512	32	32	32	34351	132	0	111

## Appendix C

# Instruction Disabling Using Verilog

Instruction subsetting is supported by automatically disabling instructions directly in Verilog as opposed to building higher-level tools that generate the Verilog of the subsetting processor. In this appendix we briefly describe the mechanism for enabling this in Verilog.

Similar to C, Verilog supports case statements which compare multiple values to a single variable and perform the operations associated with the value that matches the current value of the variable. Verilog also supports two special non-integer values: **z** for high-impedance values and **x** for unknown values. To support the desired matching or ignoring of these special values (treat as don't care), three case statement variants exist.

1. **case** – Matches both **z** and **x**
2. **casez** – Don't care for **z**, matches **x**
3. **casex** – Don't care for both **z** and **x**

A real hardware circuit can never produce the value **x**—it is symbolic. Therefore any requests to match **x** will be optimized away by the FPGA synthesis tools. We can use this behaviour to eliminate hardware for a given instruction as described below using Listing C.1 as an example.

First, use a **case** or **casez** statement to examine the current instruction opcode and compare it against the different opcode values. Then, each instruction should enable key

Listing C.1: Example Verilog case statement for decoding instructions and accompanying multiplexer for selecting results between adder and multiplier.

```
parameter OP_ADD='h3f5
parameter OP_MUL='h3c7

always@*
begin
    sel=0;
    case(instr_opcode)
        OP_ADD: sel=0;
        OP_MUL: sel=1;
    endcase
end

assign result= (sel) ? mul_result : add_result;
```

control signals upon being matched with the current instruction. In the example shown a multiplexer selects the result from either the adder or multiplier functional units and makes this selection based on the current opcode. To disable the multiply instruction a user need only insert a single `x` into its opcode value. In the example shown we can change `'h3c7` to `'hxxx`. As a result of this, the synthesis tools will recognize that the value `OP_MUL` can never match the current opcode and ignore any signals being set within the `OP_MUL` case statement clause. The synthesis tool will then discern that the multiplexer `sel` signal is never set to 1 and will eliminate that input to the multiplexer as well as the multiplier feeding it since it longer has any fan-out.

The reader should notice that the reason the `sel` signal never takes the value 1 after disabling the multiply is because its default assignment is set to 0 as seen in the `sel=0` statement beneath the `begin` keyword. This illuminates a key consideration for performing instruction subsetting using this method: default values of control signals should be assigned to match the values of the instructions that are least likely to be subsetting in any application and/or least costly to support in hardware. In the example above, the `sel` signal is set to 0 by default to match the add instruction. Addition instructions are more likely to be used within an application than a multiply. They are also much cheaper to implement in the FPGA fabric. With this default setting, the hardware for supporting add instructions could never be fully eliminated by the synthesis

tool, however since this is unlikely to occur and would only save a moderate amount of area we accept this limitation. VESPA has this same limitation for adds as well as loads. The only way to fully eliminate the hardware associated for these instructions is to eliminate the complete coprocessor.

# Bibliography

- [1] “Intelligent ram (iram): the industrial setting, applications, and architectures,” in *ICCD '97: Proceedings of the 1997 International Conference on Computer Design (ICCD '97)*. Washington, DC, USA: IEEE Computer Society, 1997, p. 2.
- [2] “Actel ARM Cortex-M1,” <http://www.actel.com/products/mpu/cortexm1/default.aspx>, Actel Corporation.
- [3] T. Allen, “Altera Corporation,” Private Communication, 2009.
- [4] “Excalibur,” <http://www.altera.com/products/devices/arm/arm-index.html>, Altera.
- [5] “Nios II,” <http://www.altera.com/products/ip/processors/nios2>, Altera.
- [6] K. Asanovic, J. Beck, B. Irissou, B. Kingsbury, and N. Morgan, “The TO Vector Microprocessor,” *Hot Chips*, vol. 7, pp. 187–196, 1995.
- [7] K. Asanovic, “Vector Microprocessors,” Ph.D. dissertation, University of California-Berkeley, 1998.
- [8] J. Ball, “Altera Corporation,” Private Communication, 2005.
- [9] —, “Altera Corporation,” Private Communication, 2009.
- [10] D. Besedin, “Platform benchmarking with RightMark memory analyzer,” <http://www.digit-life.com>, 2004.

- [11] M. Budiu and S. C. Goldstein, “Bitvalue inference: Detecting and exploiting narrow bitwidth computations,” in *In Proceedings of the EuroPar 2000 European Conference on Parallel Computing*. Springer Verlag, 2000, pp. 969–979.
- [12] R. Carli, “Flexible MIPS Soft Processor Architecture,” Massachusetts Institute of Technology, Tech. Rep. MIT-CSAIL-TR-2008-036, 2008. [Online]. Available: <http://hdl.handle.net/1721.1/41874>
- [13] R. Cliff, “Altera Corporation,” Private Communication, 2005.
- [14] G. C. Collections, “Auto-vectorization in GCC,” <http://gcc.gnu.org/projects/tree-ssa/vectorization.html>, 2009.
- [15] R. Dimond, O. Mencer, and W. Luk, “Application-specific customisation of multi-threaded soft processors,” *Computers and Digital Techniques, IEE Proceedings -*, vol. 153, no. 3, pp. 173–180, May 2006.
- [16] —, “CUSTARD - A Customisable Threaded FPGA Soft Processor and Tools ,” in *International Conference on Field Programmable Logic (FPL)*, August 2005.
- [17] B. A. Draper, A. P. W. Böhm, J. Hammes, W. A. Najjar, J. R. Beveridge, C. Ross, M. Chawathe, M. Desai, and J. Bins, “Compiling sa-c programs to fpgas: Performance results,” in *ICVS '01: Proceedings of the Second International Workshop on Computer Vision Systems*. London, UK: Springer-Verlag, 2001, pp. 220–235.
- [18] “The Embedded Microprocessor Benchmark Consortium,” <http://www.eembc.org>, EEMBC.
- [19] J. Fender, J. Rose, and D. R. Galloway, “The transmogrifier-4: An fpga-based hardware development system with multi-gigabyte memory capacity and high host and memory bandwidth.” in *IEEE International Conference on Field Programmable Technology*, 2005, pp. 301–302.

- [20] M. Flynn and P. Hung, "Microprocessor design issues: thoughts on the road ahead," *Micro, IEEE*, vol. 25, no. 3, pp. 16–31, May-June 2005.
- [21] B. Fort, D. Capalija, Z. G. Vranesic, and S. D. Brown, "A multithreaded soft processor for soc area reduction," in *FCCM '06: Proceedings of the 14th Annual IEEE Symposium on Field-Programmable Custom Computing Machines*. Washington, DC, USA: IEEE Computer Society, 2006, pp. 131–142.
- [22] J. W. C. Fu and J. H. Patel, "Data prefetching in multiprocessor vector cache memories," *SIGARCH Comput. Archit. News*, vol. 19, no. 3, pp. 54–63, 1991.
- [23] "LEON SPARC," <http://www.gaisler.com>, Gaisler Research.
- [24] J. Gebis and D. Patterson, "Embracing and Extending 20th-Century Instruction Set Architectures," *Computer*, vol. 40, no. 4, pp. 68–75, 2007.
- [25] M. B. Gokhale, J. M. Stone, J. Arnold, and M. Kalinowski, "Stream-oriented fpga computing in the streams-c high level language," in *FCCM '00: Proceedings of the 2000 IEEE Symposium on Field-Programmable Custom Computing Machines*. Washington, DC, USA: IEEE Computer Society, 2000. [Online]. Available: <http://portal.acm.org/citation.cfm?id=795916>
- [26] J. Gray, "Designing a simple fpga-optimized risc cpu and system-on-a-chip," 2000. [Online]. Available: [citeseer.ist.psu.edu/article/gray00designing.html](http://citeseer.ist.psu.edu/article/gray00designing.html)
- [27] Z. Guo, W. Najjar, F. Vahid, and K. Vissers, "A quantitative analysis of the speedup factors of fpgas over processors," in *Symposium on Field programmable gate arrays*. New York, NY, USA: ACM, 2004, pp. 162–170.
- [28] J. L. Hennessy and D. A. Patterson, *Computer Architecture; A Quantitative Approach*. San Francisco, CA, USA: Morgan Kaufmann Publishers Inc., 1992.
- [29] "Intel Core i7," <http://www.intel.com/products/processor/corei7/>, Intel Corporation.

- [30] A. Jones, D. Bagchi, S. Pal, X. Tang, A. Choudhary, and P. Banerjee, “Pact hdl: a c compiler targeting asics and fpgas with power and performance optimizations,” in *CASES '02: Proceedings of the 2002 international conference on Compilers, architecture, and synthesis for embedded systems*. New York, NY, USA: ACM, 2002, pp. 188–197.
- [31] A. K. Jones, R. Hoare, D. Kusic, J. Fazekas, and J. Foster, “An fpga-based vliw processor with custom hardware execution,” in *FPGA '05: Proceedings of the 2005 ACM/SIGDA 13th international symposium on Field-programmable gate arrays*. New York, NY, USA: ACM, 2005, pp. 107–117.
- [32] C. Kozyrakis and D. Patterson, “Vector vs. superscalar and VLIW architectures for embedded multimedia benchmarks,” *IEEE/ACM International Symposium on Microarchitecture, 2002.(MICRO-35).*, pp. 283–293, 2002.
- [33] —, “Scalable, vector processors for embedded systems,” *Micro, IEEE*, vol. 23, no. 6, pp. 36–45, 2003.
- [34] C. Kozyrakis, “Scalable Vector Media Processors for Embedded Systems,” Ph.D. dissertation, University of California-Berkeley, 2002.
- [35] C. Kozyrakis and D. Patterson, “Overcoming the limitations of conventional vector processors,” *SIGARCH Comput. Archit. News*, vol. 31, no. 2, pp. 399–409, 2003.
- [36] I. Kuon, “Measuring and Navigating the Gap Between FPGAs and ASICs,” Ph.D. dissertation, University of Toronto, 2008.
- [37] M. Labrecque and J. G. Steffan, “Improving pipelined soft processors with multi-threading,” in *Proc. of FPL '07*, Amsterdam, Netherlands, August 2007, pp. 210–215.
- [38] M. Labrecque, P. Yiannacouras, and J. G. Steffan, “Scaling Soft Processor Systems,” in *IEEE Symposium on Field-Programmable Custom Computing Machines (FCCM'08).*, Palo Alto, CA, April 2008.

- [39] “Lattice Micro32,” <http://www.latticesemi.com/products/intellectualproperty/ipcores/mico32/in>  
Lattice Semiconductor Corporation.
- [40] D. Lau, O. Pritchard, and P. Molson, “Automated generation of hardware accelerators with direct memory access from ansi/iso standard c functions.” in *FCCM*, 2006, pp. 45–56.
- [41] A. Lodi, M. Toma, and F. Campi, “A pipelined configurable gate array for embedded processors,” in *FPGA '03: Proceedings of the 2003 ACM/SIGDA eleventh international symposium on Field programmable gate arrays*. New York, NY, USA: ACM Press, 2003, pp. 21–30.
- [42] R. Lysecky and F. Vahid, “A study of the speedups and competitiveness of fpga soft processor cores using dynamic hardware/software partitioning,” in *DATE '05: Proceedings of the conference on Design, Automation and Test in Europe*. Washington, DC, USA: IEEE Computer Society, 2005, pp. 18–23.
- [43] S. McCloud, “Catapult c synthesis-based design flow: Speeding implementation and increasing flexibility,” in *White Paper, Mentor Graphics*, 2004.
- [44] K. Meier and A. Forin, “Hardware compilation from machine code with m2v,” *Field-Programmable Custom Computing Machines, Annual IEEE Symposium on*, vol. 0, pp. 293–295, 2008.
- [45] P. Metzgen, “A high performance 32-bit ALU for programmable logic,” in *Proceeding of the 2004 ACM/SIGDA 12th international symposium on Field programmable gate arrays*. ACM Press, 2004, pp. 61–70.
- [46] “MIPS,” <http://www.mips.com>, MIPS Technologies.
- [47] R. Moussali, N. Ghanem, and M. A. R. Saghir, “Supporting multithreading in configurable soft processor cores,” in *International Conference on Compilers, architecture, and synthesis for embedded systems*. New York, NY, USA: ACM, 2007, pp. 155–159.

- [48] R. Mukherjee, A. Jones, and P. Banerjee, “Handling data streams while compiling c programs onto hardware,” in *VLSI, 2004. Proceedings. IEEE Computer society Symposium on*, Feb. 2004, pp. 271–272.
- [49] J. Nurmi, *Processor Design: System-On-Chip Computing for ASICs and FPGAs*. Springer Publishing Company, Incorporated, 2007.
- [50] D. Nuzman and A. Zaks, “Outer-loop vectorization: revisited for short simd architectures,” in *PACT ’08: Proceedings of the 17th international conference on Parallel architectures and compilation techniques*. New York, NY, USA: ACM, 2008, pp. 2–11.
- [51] “SystemC,” <http://www.systemc.org>, OSCI.
- [52] D. Pellerin and S. Thibault, *Practical fpga programming in c*. Upper Saddle River, NJ, USA: Prentice Hall Press, 2005.
- [53] F. Plavec, Z. Vranesic, and S. Brown, “Towards compilation of streaming programs into fpga hardware,” in *Specification, Verification and Design Languages, 2008. FDL 2008. Forum on*, Sept. 2008, pp. 67–72.
- [54] A. Putnam, S. Eggers, D. Bennett, E. Dellinger, J. Mason, H. Styles, P. Sundararajan, and R. Wittig, “Performance and power of cache-based reconfigurable computing,” in *ISCA ’09: Proceedings of the 36th annual international symposium on Computer architecture*. New York, NY, USA: ACM, 2009, pp. 395–405.
- [55] K. Ravindran, N. Satish, Y. Jin, and K. Keutzer, “An fpga-based soft multiprocessor system for ipv4 packet forwarding,” Aug. 2005, pp. 487–492.
- [56] R. M. Russell, “The cray-1 computer system,” *Communications of the ACM*, vol. 21, no. 1, pp. 63–72, 1978.
- [57] M. A. R. Saghir, M. El-Majzoub, and P. Akl, “Datapath and isa customization for soft vliw processors,” Sept. 2006, pp. 1–10.

- [58] A. F. Scott Sirowy, “Where’s the Beef? Why FPGAs Are So Fast,” Microsoft Research, Tech. Rep. MSR-TR-2008-130, 2008.
- [59] C. Sullivan and S. Chapell, “Handel-c for coprocessing and co-design of field programmable system on chip,” in *JCRA*, 2002.
- [60] “Vector extensions to the mips-iv instruction set architecture (the v-iram architecture manual),” <http://iram.cs.berkeley.edu/isa.ps>, University of California-Berkeley.
- [61] “MiBench,” <http://www.eecs.umich.edu/mibench/>, University of Michigan.
- [62] D. Unnikrishnan, J. Zhao, and R. Tessier, “Application-Specific Customization and Scalability of Soft Multiprocessors,” in *IEEE Symposium on Field-Programmable Custom Computing Machines (FCCM’09)*., Napa, CA, April 2009.
- [63] S. P. Vanderwiel and D. J. Lilja, “Data prefetch mechanisms,” *ACM Comput. Surv.*, vol. 32, no. 2, pp. 174–199, 2000.
- [64] J. E. Veenstra and R. J. Fowler, “MINT: a front end for efficient simulation of shared-memory multiprocessors,” in *Proceedings of the Second International Workshop on Modeling, Analysis, and Simulation of Computer and Telecommunication Systems (MASCOTS ’94)*., Durham, NC, January 1994, pp. 201–207.
- [65] R. Wittig, “Xilinx Corporation,” Private Communication, 2005.
- [66] W. A. Wulf and S. A. McKee, “Hitting the memory wall: implications of the obvious,” *SIGARCH Comput. Archit. News*, vol. 23, no. 1, pp. 20–24, 1995.
- [67] “MicroBlaze,” <http://www.xilinx.com/microblaze>, Xilinx.
- [68] “Xilinx Virtex II Pro,” [http://www.xilinx.com/xlnx/xil\\_prodcataloglandingpage.jsp?title=Virtex-II+Pro+FPGAs](http://www.xilinx.com/xlnx/xil_prodcataloglandingpage.jsp?title=Virtex-II+Pro+FPGAs), Xilinx.
- [69] P. Yiannacouras, “The Microarchitecture of FPGA-Based Soft Processors,” Master’s thesis, University of Toronto, 2005,

<http://www.eecg.toronto.edu/~jayar/pubs/theses/Yiannacouras/PeterYiannacouras.pdf>.

- [70] P. Yiannacouras, J. Rose, and J. G. Steffan, “The Microarchitecture of FPGA Based Soft Processors,” in *CASES’05: International Conference on Compilers, Architecture and Synthesis for Embedded Systems*. ACM Press, 2005, pp. 202–212.
- [71] P. Yiannacouras, J. G. Steffan, and J. Rose, “Application-specific customization of soft processor microarchitecture,” in *FPGA’06: Proceedings of the International Symposium on Field Programmable Gate Arrays*. New York, NY, USA: ACM Press, 2006, pp. 201–210.
- [72] —, “Vespa: Portable, scalable, and flexible fpga-based vector processors,” in *CASES’08: International Conference on Compilers, Architecture and Synthesis for Embedded Systems*. ACM, 2008.
- [73] —, “Data parallel fpga workloads: Software versus hardware,” in *Proc. of FPL’09*, Grenoble, France, August 2009.
- [74] —, “Fine-grain performance scaling of soft vector processors,” in *CASES’09: International Conference on Compilers, Architecture and Synthesis for Embedded Systems*. ACM, 2009.
- [75] J. Yu, G. Lemieux, and C. Eagleston, “Vector processing as a soft-core cpu accelerator,” in *Symposium on Field programmable gate arrays*. New York, NY, USA: ACM, 2008, pp. 222–232.